UNIVERSITÀ DEGLI STUDI
DI MILANO

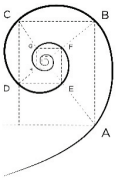

DOTTORATO DI MEDICINA MOLECOLARE E TRASLAZIONALE

CICLO XXXIII

Anno Accademico 2019/2020

TESI DI DOTTORATO DI RICERCA

BIO-10

LIPIDOMICS UNVEILS THE ROLE OF BIOACTIVE LIPIDS IN CELLULAR MODELS OF CYSTIC FIBROSIS

Dottorando:
Michele Vittorio **DEI CAS**
Matricola N°:
R11946

TUTORE: Prof. Michele SAMAJA

COTUTORE: Prof. Riccardo GHIDONI

COORDINATORE DEL DOTTORATO: Prof. Michele SAMAJA

To all those who failed my expectations

CONTENTS

ABSTRACT

Cystic fibrosis is a genetic disease affecting mainly the lungs, causing chronic inflammation and recurrent infections. The lipid accrual directly contributes to the persistent damage in the cystic fibrosis airways; thus, the deregulated lipid metabolism can be targeted with pharmacological treatment. Here, we aim at demonstrating, in an in vitro model of cystic fibrosis, the role of inflammatory and bioactive lipids in the disease pathophysiology and its modulation by myriocin, which inhibits sphingolipids synthesis. The blended use of both targeted and untargeted mass spectrometry techniques unveiled an atypical lipid composition in broncho-epithelial cystic fibrosis cells and the derived extracellular vesicles. The airways cells in cystic fibrosis accumulate lipids, exacerbating inflammation that can be partly reversed by myriocin therapy, which acts directly on sphingolipid synthesis and indirectly on the accrual of other lipid classes. The CFTR dysfunction leads to an increased metabolism of sphingolipids, which in turn is connected to the release of ceramide-enriched extracellular vesicles that export a pro-inflammatory signal to the recipient cells. The accumulation of lipids may be the result of dysfunctional lipid traffic in the cell and may be responsible for blocking the ER-Golgi network, overproduction of reactive oxygen species and uncontrolled inflammatory stimuli. We proposed new insights on the role of lipid metabolism in the development of cystic fibrosis pathogenesis by using a validated mass spectrometry lipidomics approach. To conclude, we hypothesize that the metabolism of sphingolipids may be an effective pharmacological target to help the reduction of the intrinsic inflammatory state in the airways.

RIASSUNTO

La fibrosi cistica è una malattia genetica che colpisce principalmente i polmoni, causando infiammazione cronica e infezioni ricorrenti. L'accumulo di lipidi nelle vie aeree in fibrosi cistica contribuisce direttamente a mantenere uno status infiammatorio cronico. Per questo il dismetabolismo lipidico può essere considerato un nuovo obiettivo farmacologico. In questo lavoro, ci siamo proposti di dimostrare in un modello cellulare il ruolo dei lipidi infiammatori e bioattivi nella fisiopatologia della fibrosi cistica e la sua modulazione attraverso l'inibizione della sintesi degli sfingolipidi. L'uso combinato di tecniche di spettrometria di massa sia mirate che non mirate ha rivelato nella malattia una composizione lipidica atipica nelle cellule bronco-epiteliali e delle derivanti vescicole extracellulari. Le cellule delle vie aeree nella fibrosi cistica accumulano lipidi che aggravano l'infiammazione. Questa può essere parzialmente ridotta dalla terapia con miriocina, che agisce direttamente sulla sintesi degli sfingolipidi e indirettamente sull'accumulo di altre classi lipidiche. La disfunzione del gene CFTR porta ad un aumento del metabolismo degli sfingolipidi, che a sua volta è collegato al rilascio di vescicole extracellulari arricchite di ceramidi che esportano un segnale pro-infiammatorio alle cellule circostanti. L'accumulo di lipidi può essere il risultato di un traffico disfunzionale di lipidi nella cellula, che a sua volta può essere responsabile del blocco del trasporto reticolo endoplasmatico-Golgi, di una iper-produzione di ROS e di stimoli infiammatori incontrollati. Abbiamo esplorato nuove prospettive sul metabolismo lipidico nello sviluppo della patogenesi della fibrosi cistica utilizzando un approccio lipidomico di spettrometria di massa per il rilevamento di possibili biomarcatori. Inoltre per concludere, ipotizziamo che il metabolismo degli sfingolipidi possa essere un obiettivo farmacologico efficace nel coadiuvare la riduzione dello status infiammatorio intrinseco delle vie aeree.

LIST OF ORIGINAL PAPERS

This thesis is based on the following paper, which in their edited versions are attached in the appendix.

1. Zulueta, A., Peli, V., Dei Cas, M., Colombo, M., Paroni, R., Falleni, M., ... & Ghidoni, R. (2019). Inflammatory role of extracellular sphingolipids in Cystic Fibrosis. *The International Journal of Biochemistry & Cell Biology*, 116, 105622.

2. Dei Cas, M.; Zulueta, A.; Mingione, A.; Caretti, A.; Ghidoni, R.; Signorelli, P.; Paroni, R. (2020). An Innovative Lipidomic Workflow to Investigate the Lipid Profile in a Cystic Fibrosis Cell Line. *Cells*, 9, 1197.

3. Mingione, A., Dei Cas, M., Bonezzi, F., Caretti, A., Piccoli, M., Anastasia, L., ... Signorelli, P. (2020). Inhbition of Sphingolipid Synthesis as a Phenotype-Modifying Therapy in Cystic Fibrosis. *Cell Physiol Biochem*, 54, 110-125.

I would like to acknowledge the publishers – Elsevier, S. Karger AG and MDPI – for allowing me to include the edited versions of the papers in my PhD thesis.

LIST OF ABBREVIATIONS

H	healthy phenotype
CF	cystic fibrosis
Cer	ceramides
DHCer	dihydroceramides
HexCer	glucosylceramides
LacCer	lactosylceramides
SM	sphingomyelins
GM3	gangliosides
Chol	free cholesterol
CE	cholesterol esters
LPE	lysophosphatidyletanolamines
PC	phosphatidylcholines
PG	phosphatidylglicerols
PI	phosphatidylinositoles
LPI	lysophosphatidylinositoles
PG	phosphatidylglicerols
LPG	lysophosphatidylglicerols
FA	free fatty acids
ACar	acylcarnitines
CL	cardiolipins
etherPL	ether-linked phospholipids
SFA	saturated fatty acids
MUFA	monounsaturated fatty acids
PUFA	polyunsaturated fatty acids

LIST OF TABLES

LIST OF FIGURES

RESEARCH INTEGRITY DECLARATION

Results reported in this work comply with the four fundamental principles of research integrity of The European Code of Conduct for Research Integrity (ALLEA, Berlin, 2018):

1. Reliability in ensuring the quality of research, reflected in the design, the methodology, the analysis and the use of resources;
2. Honesty in developing, undertaking, reviewing, reporting and communicating research in a transparent, fair, full and unbiased way;
3. Respect for colleagues, research participants, society, ecosystems, cultural heritage and the environment;
4. Accountability for the research from idea to publication, for its management and organization, for training, supervision and mentoring, and for its wider impacts.

1. INTRODUCTION

1. Cystic fibrosis

Cystic fibrosis (CF) is a multi-system disease affecting the lungs, the pancreas, the gastrointestinal tract, the liver, and the reproductive tract, caused by different mutations on the CFTR gene, which encodes for a sodium/chloride transmembrane channel [1]. CFTR is crucial for electrolytic balance but also affects inflammatory responses, ion transport, and cell signalling by modulating the gene expression.

The loss of CFTR physiological activity leads to electrolytic imbalances, in particular on bicarbonate/chloride balance, with the abnormal production and deposition of very thick and sticky mucus that can clog vessels and airways (Figure 1).

The classic symptoms of CF are respiratory insufficiency, chronic pulmonary infections, exocrine pancreatic insufficiency, gastrointestinal disturbances, metabolic alkalosis, and sterility [2,3]. Specifically, the lung disease is CF is always characterized by an exaggerated, sustained, and extended inflammatory response to bacteria, among which *Pseudomonas aeruginosa, Staphylococcus aureus, Haemophilus influenzae,* and *Stenotrophomonas maltophilia* [3,4].

1.2 Genetics

CF is an autosomal recessive disease and, currently, over 2000 variants of the CFTR gene have been reported (http:// genet.sickkids.on.ca) that can be classified as (1) CF-causing, (2) varied clinical consequence, (3) not-disease causing, and (4) unsure significance (https://cftr2.org).

The prevalence was estimated in about 1 in 25 babies born with a defective CFTR. However, only 1 in 2000–3000 (Europe) or at least 1 in 30000 newborns (America) bring both the incorrect alleles and are diagnosed with CF [4,5].

Different variants impact the amount and functionality of the CFTR protein with variable clinical consequences [2,6]. Boyle and De Boeck [6] classified the CFTR mutations into six classes reported here in Table.

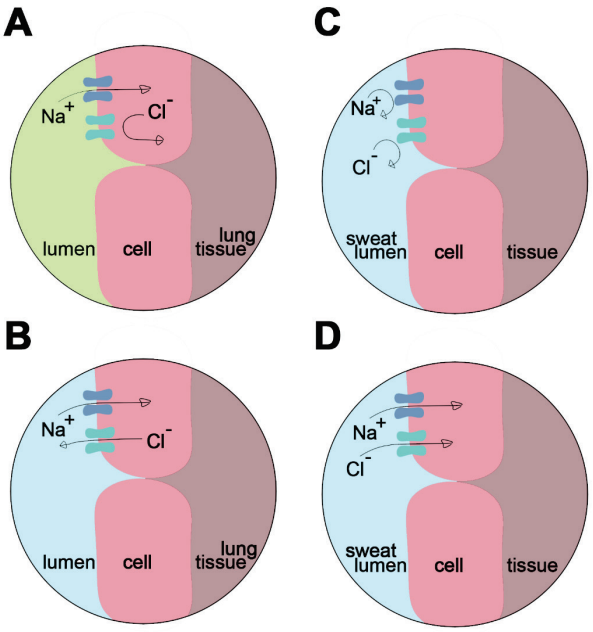

Figure 1.
Electrolytic alteration in CF due to mutations on CFTR channel in (A) broncho-epithelial cell and (C) sweat, used for diagnosis purpose in comparison with healthy (B) broncho-epithelial cell and (D) sweat

The most common mutation, about 70% of defective CFTR alleles in patients, is F508del, which consists of the deletion of three nucleotides causing the loss of phenylalanine at residue 508. Other frequent mutations are G542X (3.4%), G551D (2.4%), W1282X (2.1%) and 3905insT (2.1%) [1,2,6].

1.3 Diagnosis

Patients are typically diagnosed with CF as neonates or infants through genetic screening, family history, or symptomatic characteristics such as stunted growth, meconium ileus, rectal prolapse, malabsorption, cough, and persistent lung infections.

Diagnosis is based on the presence of two disease-causing CFTR mutations, along with a positive sweat test and compatible clinical features.

Sweat chloride levels are usually higher in CF than in healthy adult (Figure 1):

1. >60mmol/L, usually 90–110mmol/L, is clearly considered CF;
2. 40–60mmol/L is borderline;
3. <40 is considered normal even though it can occur in CF.

However, the diagnostic process can be more intricate, especially for milder or minimal phenotypes (5%). The initial diagnostic test findings are frequently

inconclusive in these patients: borderline concentration of sweat chloride and or less than 2 CF mutations found. Thus, specialized medical investigations are necessary in these cases, such as nasal potential difference measurements or intestinal current measurements [1,7].

Table 1. Classes of CFTR mutations according to the classification proposed by Boyle and De Boeck [6]

Class	CFTR alteration	Type of mutations	Relevant specific mutations
I	Complete absence of the CFTR protein that is not synthetized	Nonsense; frameshift; canonical splice	Gly542X Trp1282X Arg553X 621+1G→T
II	Complete absence of the CFTR protein that is prematurely destroyed in the ER	Missense; deletion	Phe508del Asn1303Lys Ile507del Arg560Thr
III	Impaired gating of the CFTR channel	Missense; substitution	Gly551Asp Gly178Arg Gly551Ser Ser549Asn
IV	Presence of CFTR protein but decreased channel conductance	Missense; substitution	Arg117His Arg347Pro Arg117Cys Arg334Trp
V	Reduced level of normal and functional CFTR proteins	Missense; Splicing defect	3849+10kbC→T 2789+5G→A 3120+1G→A 5T
VI	instability of the CFTR protein at the apical surface of the epithelial cells.	Missense; substitution	4326delTC Gln1412X 4279insA

1.4 Management

The primary aim of CF pharmacological care consists of the administration of various antibiotics to counteract chronic pulmonary sepsis and its complications, which account for much of the morbidity and mortality.

Choice of antibiotics is based on clinical features or by sputum culture results, and treatment should be for 14 days with either oral or IV antibiotics depending on the severity of infection [1,3,8].

The majority of patients with chronic *P.aeruginosa* infection are treated with colistin or tobramycin solution for inhalation. Prevention and eradication of *Staphylococcus aureus* infection should also be considered, even if the patient is asymptomatic. A minimum of 2 weeks of treatment in adults is deemed with either flucloxacillin, erythromycin, or clindamycin [9].

Some people with cystic fibrosis might receive treatment with immunomodulatory agents, such as corticosteroids, to reduce the intense neutrophil-dominated airway inflammation [3].

The guideline also provides recommendations on the use of the mucolytic agents (i.e., dornase alfa, hypertonic sodium chloride, and mannitol) and airway clearance procedures with anti-inflammatory treatment with corticosteroids [1].

2. Lipids

2.1 Structures

The scientific community still debates on what should be the correct definition for "lipid", however the two most accredited were here reported:

1. "lipids are fatty acids and their derivatives, and substances related biosynthetically or functionally to these compounds" [10]
2. "lipids are hydrophobic or amphipathic small molecules that may originate entirely or in part by carbanion-based condensations of thioesters (fatty acids, polyketides, etc.) and/or by carbocation-based condensations of isoprene units (prenols, sterols, etc.)" [11]

Lipids were categorized based on their chemically functional backbone into eight main classes: fatty acyls, plant-derived polyketides, glycerolipids, glycerophospholipids, sphingolipids, prenols, sterol, and saccharolipids (Figure 2). There can be hundreds to thousands of individual molecular species for each of these lipid classes, particularly for those lipids that combine fatty acyl groups such as glycerolipids, glycerophospholipids, and sphingolipids.

2.2 Functions

Lipids are involved in structural compartmentalization of cell membranes, energy storage, and cell-signalling that affect cellular functions, including apoptosis, proliferation, response to stress, and inflammation [12,13].

Firstly, lipids are considered the building blocks of membranes providing the fluid lipid bilayer within membrane proteins fold, organize, and function. Their structural role is the direct consequence of their biochemical and biophysical properties, either deformable or very stable [13,14]. Lipids also made it possible for the cells to isolate their internal components from the external environment and create separate organelles. Through cell compartmentalization, they increased biochemical efficiency by segregating chemical reactions and products to a specific location. Furthermore, lipids are essential for cell division, biological reproduction, and intracellular membrane trafficking [12].

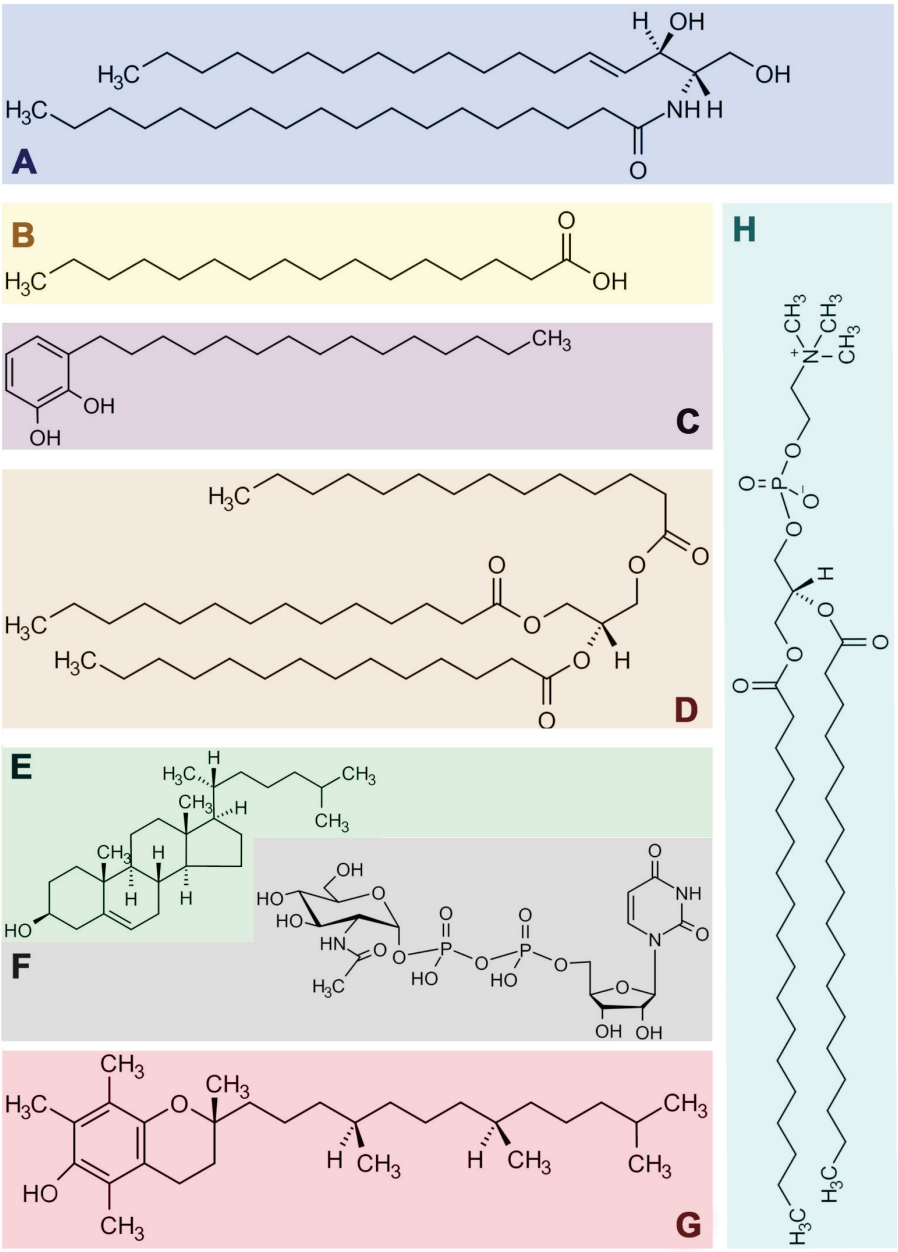

Figure 2. Exemplification of structures for each lipid category: (A) ceramide d18:1, 18:0, sphingolipids; (B) palmitic acid, fatty acyls; (C) alkyl catechol, polyketides; (D) trimyristin, acylglycerol; (E) cholesterol, sterol; (F) UDP-GlcNAc, saccharolipids; (G) alfa-tocopherol, prenols and (H) disteatorylglycerophoshocholine, glycerophospholipids.

The lipid composition in biological membranes strongly depends on the cell type and the subcellular location. Generally, in mammalian cells, the most abundant lipids are phosphatidylcholine, phosphatidylethanolamine and cholesterol, whereas some lipids are more abundant in specific organelles, such as cardiolipin in mitochondria.

To note, in cellular membranes lipids are distributed asymmetrically: glycolipids are located exclusively on the outer leaflet of plasma membranes, whereas phosphatidylserine is principally in the inner leaflet [15,16].

Secondly, lipids, packed in lipid droplets, are used for energy storage, principally as triacylglycerol and steryl esters. These adiposomes are necessary to store caloric resources and preserve membrane components such as fatty acid and sterol.

Finally, lipids can actively participate in signal transduction and molecular recognition processes acting as first and second messengers [12,17]. The degradation of amphipathic lipids makes structured signaling: the hydrophobic parts of the molecule can be transmitted within the membrane, whereas the polar head can be distributed through the cytosol. In addition, some membrane lipids can also recruit proteins from the cytosol, which in turn can act as secondary signalling or effector complexes [12].

2.3 Lipids in inflammatory responses

Lipids exert crucial physiological and pathological signalling activities in cells and tissues. Bioactive lipids are recognized as novel biomarkers that would contribute to innovative treatment methods, early intervention, and better patients' prognosis. In particular, a significant effort was made by decoding the role of lipid in mediating and resolving inflammation [16,18].

Inflammation is an immune response that develops after infections, cellular stress, or tissue insults and may be spontaneously depleted after the damage has been removed. Lipids and other preformed or newly synthesized mediators can be gathered to elicit specific inflammatory responses. In some cases, such as in autoimmune disorders, immune responses can evolve in the excessive and unregulated process leading to persistent inflammation, irreversible tissue damage, and chronic disease [19]. It is well known that endogenous bioactive lipids play a crucial role in inflammatory processes: they can initiate,

coordinate, resolve and confine inflammation by regulating hypervascular reactivity, pain, leukocyte trafficking, and clearance [20–23]. Based on their chemical composition or functional activity, bioactive lipids may be classified into various classes: eicosanoids, advanced pro-resolving mediators, lysoglycerophospholipids, sphingolipids, and endocannabinoids [22].

2.3.1 Eicosanoids

This bioactive lipid-family includes a wide range of 20-carbon derivatives such as arachidonic acid (AA), eicosapentaenoic acid (EPA), and docosahexaenoic acid (DHA). Eicosanoids are mainly derived from AA, which can be released from membrane phospholipids primarily by phospholipase A2 and secondary by phospholipase C. Eicosanoid biosynthesis is drove by three enzymes: 1) cyclooxygenase 1 and 2 (COX-1/2) generate prostanoid class consisting of prostaglandins (PGs), prostacyclines, and thromboxanes (TXs); 2) leukotriene (5/12/15-LOX) lipoxygenase (LTs), hydroxy-eicosatetraenoids, and lipoxins; and 3) P450 epoxygenase generates hydroxyeicosatetraenoic acids (HETEs) and epoxy-eicosatetraenoic acids (HETEs) [24,25].

Eicosanoids are classified into omega-6 and omega-3 families based on the unsaturation position in their precursors. The pro-inflammatory omega-6 family is derived from AA, while the anti-inflammatory omega-3 family is derived from EPA and DHA.

Eicosanoids are involved in inflammation and vascular tone, platelet aggregation, pain perception, ovulation, and embryonic development. In general, omega-6 eicosanoids are pro-inflammatory, while omega-3 eicosanoids can be anti-inflammatory and pro-resolving [26,27].

In particular, five mechanisms are related to PGs-induced inflammation: 1) expanding the release of pro-inflammatory cytokines [27,28]; 2) improving the innate immunity [29]; 3) activating the T-helper cells [30]; 4) supporting leukocyte enrolment [27]; and 5) stimulating the expression of pro-inflammatory genes such as NF-κB [31].

By acting as chemoattractants for neutrophils, macrophages, eosinophils, and TH17 lymphocytes, the primary roles of LTs in acute inflammation are to cause edema and promote a sustained inflammatory status. Vasoconstrictors and vasodilating agents are predominantly TXs and prostacyclines, respectively.

[20,22,32]. Epoxyeicosatrienoic acids (EETs) are synthesized from AA by cytochrome P450 epoxygenases. By blocking the activation of NF-kB, they regulate vasorelaxation, anti-inflammation and fibrinolysis. They can be converted to the less active dihydroxyeicosatrienoic acids (DHETs) by soluble epoxide hydrolase [33].

2.3.2 Sphingolipids

Sphingolipids chemically consist of an amino-alcohol backbone, that is sphingosine. They are synthesized by the de novo condensation of serine and acyl-CoA (Figure 3). They are involved in a multitude of pathophysiological functions [34], such as regulation of apoptosis [35,36], proliferation [37], differentiation [38], autophagy [39,40], invasiveness [41,42], modification of signaling cascade [43,44], and mediation of inflammatory responses by cytokines [45]. In particular, ceramide and sphingosine promote apoptosis via different pathways, which involve the catalytic activity of Bcl-2, protein kinase C, protein phosphatases 1-2, and proteases. In contrast with ceramide, which is predominantly pro-apoptotic [46], sphingosine-1-phosphate (S1P) is mainly an anti-apoptotic messenger [47] that can modulate mitogenesis, cell migration, cytoskeletal rearrangement, and angiogenesis [40,48]. The phosphate forms of sphingolipids are notably related to inflammation, where S1P acts on either COX-2 or NF-kB and ceramide-1P acts on phospholipases A2 [49,50].

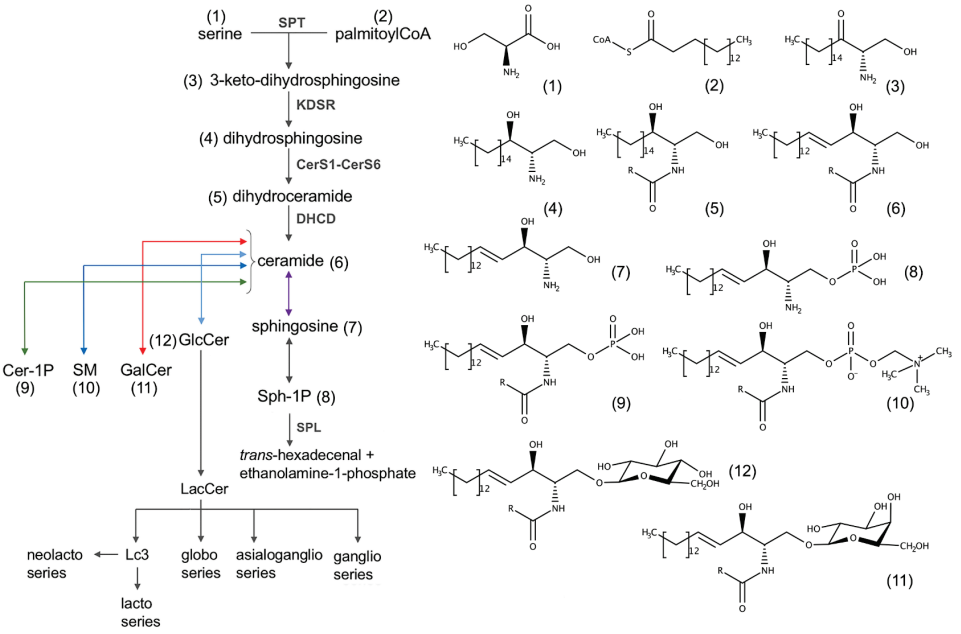

Figure 3. Sphingolipids metabolism and related chemical structures.

2.3.3 Endocannabinoids

Endocannabinoids comprise amides, esters or long-chain polyunsaturated fatty acid ethers capable of binding and activating the G-protein-coupled cannabinoid receptors (CB1 and CB2) in the same way as the tetrahydrocannabinol (THC), the main psychoactive principle of Cannabis sativa. These endogen lipid mediators share cannabimetic activity, but with different chemical structures from phytocannabinoids. The most studied molecules in this class are anandamide (AEA), 2-arachidonoylglycerol (2-AG), 2-AG-ether, O-arachidonoylethanolamine, arachidonoyldopamine, and palmitoylethanolamide (PEA). They modulate biological functions such as immunity, endocrine, and inflammatory responses [51,52]. In particular, AEA and PEA have anti-inflammatory properties [53,54], whereas 2-AG has both pro- and anti-inflammatory properties [55–57]. Alterations in the endocannabinoid system can cause a dysfunction in tissue homeostasis and chronic inflammatory status: in the concentration of endocannabinoids and the expression of their metabolic enzymes and receptors [58].

2.3.4 Lysoglycerophospholipids

Lysoglycerophospholipids contain glycerol backbones linked to two long fatty acid chains and a polar head comprising a phosphate modified with ethanolamine, choline, inositol, or serine [14]. Lysoglycerophospholipids are produced as intermediate in the phospholipid synthesis or derived from their catabolism, which consists in the hydrolitic removal of one fatty acid. This hydrolysis process affords lysophosphatidylcholines (LPC), lysophosphatidylinositols (LPI), lysophosphatidylethanolamines (LPE), lysophosphatidylserines (LPS), and lysophosphatidic acid (LPA). Lysophospholipids were demonstrated to modulate inflammatory cascade, and in the cellular compartment proliferation, survival and morphological changes [59,60]. LPC and LPA modulate the immune response by controlling the distribution, trafficking, and activation of immune cells [59,61]. Therefore, they have been linked with different inflammatory diseases such as diabetes, obesity [62], atherosclerosis, cancer [63], and rheumatoid arthritis (RA) [64].

3. Myriocin

Myriocin (Myr) is a natural product derived from sugar fermentation of thermophilic Ascomycetes, such as *Myriococcum Albomyces, Mycelia sterilia* and *Isaria sinclairii* [65,66]. Myriocin is a complex amino acid having three successive asymmetric centers and was later recognized as a potent immunosuppressant [67,68].

Myr exerts a powerful immunosuppressive activity, 10 to 100 times more potent than that of cyclosporin A, and exhibits a simple structure compared with other microbial immunosuppressive products. Several structural analogues are produced by other fungi, such as *Mycelia sterilia* ATC20349, *Isaria sinclarii*, although their biological activity is not fully characterized [69–71]. This led to the development of an *in vitro* synthesis procedure to obtain Myr and its derivatives [69,70,72]. Next, Myr was found to inactivate *in vivo* and *in vitro* serine-palmitoyl-transferase (Serine-Palmitoyl Transferase) (EC 2.3.1.50), the first and rate-limiting enzyme in the *de-novo* biosynthesis of sphingolipids [73] (Figure 4) and to exert potent biological activity on cell growth inhibition [74]. Since then, Myr has been widely used as a sphingolipids synthesis inhibitor, but Myr itself can significantly modulates inflammation,

induces autophagy, and lipid oxidation [75]. Myr is currently evaluated in pre-clinical studies for the treatment of different diseases, among which are retinitis pigmentosa [76,77], myocardial infarction [78–80], atherosclerosis [81], fatty liver disease [82], and cystic fibrosis [83–86].

In CF Myr administration: (1) activates some transcriptions of genes (i.e. TFEB, FOXOs) involved in regulating lipid metabolism, anti-inflammatory, anti-oxidants responses, and autophagy [87]; (2) decreases the overall lipid cell content [86] and (3) enhances mitochondrial lipid oxidation [75].

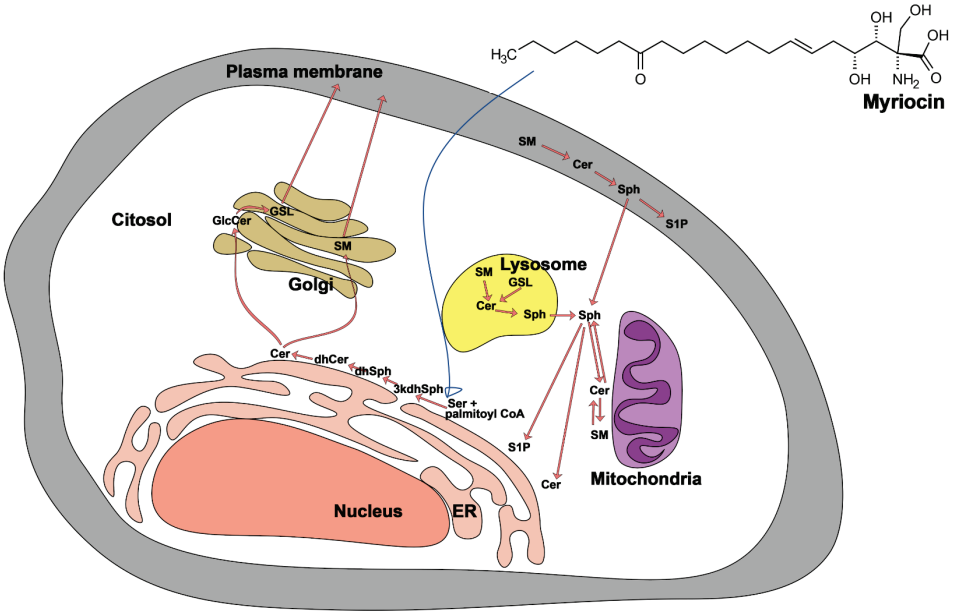

Figure 4. De-novo sphingolipids synthesis inhibition by Myriocin, which interfere with the first-rate enzyme that is serine-palmitoyl-transferase.

4. Lipidomic

Lipidomics is the most powerful quali-quantitative analytical tool to study lipids in biological specimens and their biochemical involvement in human diseases. The structure and the composition of lipids in cells and tissue can change in reaction to pathophysiological modifications: gene alterations, epigenetic changes, protein expression, and post-translational modifications. Thus, recognizing lipidomic biomarkers in various diseases may be relevant to diagnose purpose or test responses to therapies [88].

Lipid imbalances are also closely associated with several outbreak diseases, namely atherosclerosis and cardiovascular diseases [89,90], diabetes [91,92], metabolic syndromes [93,94], autoimmune syndromes [19], cancers [95–98], Alzheimer's disease [99,100], and infectious diseases [24,101].

Lipidomics has progressed tremendously in the last decade, but there are still challenges in extending a precise and comprehensive evaluation of the lipidome. Given their structural diversity, which also means different chemical properties, it is difficult to achieve a comprehensive lipid analysis method. Another difficulty lies in the wide-ranging concentrations of lipids in the same biological samples: from millimolar of cholesterol esters, triacylglycerols, and phospholipids to pico-femtomolar of ceramides and prostaglandins [102,103]. Liquid chromatography combined with mass spectrometry represents the most promising analytical technique to study the lipidome, as demonstrated by the latest scientific trends [102,104,105].

The whole human lipidome is a complex biological system, comprising 10 to 100 thousand different chemical entities, that can be covered by this large-scale technique. For instance, it has been reported between 150 and 700 different lipids could be present within the human plasma. The most represent classes are CE (47%), PC (18%), cholesterol (12%), TAG (9%), SM (5%), free fatty acids (4%) and LCP (2%) [103].

Lipids can be studied by two approaches: targeted or untargeted lipidomics (Figure 5). A high-sensitive analysis dedicated to identify and quantify specific classes of lipids is a targeted method. On the other hand, the non-targeted method, typically using high-resolution mass spectrometry, aims to objectively identify and semi-quantify all potential lipid species in the samples that give an overall lipid fingerprint [106–108]. Different tasks can be performed using this technique: (1) characterization, detection, and quantification of lipid species reported to be correlated with pathological events, and (2) identification of new prognostic or diagnostic biomarkers, compared to a control group, with high levels of precision and sensitivity. The identification in LC-MS untargeted lipidomics can be accomplished by three independent levels of selection: (1) the chromatographic separation, (2) mass-to-charge (m/z) ratio of the precursor ion, and then fragmented to gain (3) product ions (MS/MS).

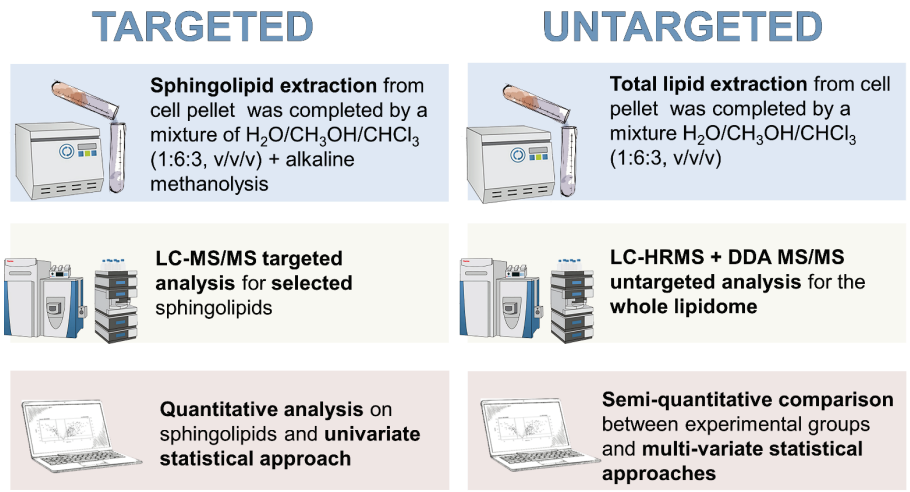

Figure 5. Workflow for targeted and untargeted lipidomics.

The strength of lipidomics is recognizing single species that reflect significant changes and providing an overview of an inherently complex process. Metabolites, and thus their concentrations, are constantly exposed to synthesis or degradation in this process. By highlighting important metabolic pathways and elucidating specific biological function, bioinformatics analysis is then aimed at understanding biological data [104]. It is possible to classify pathways and cell functions engaged in the studied condition or dysfunction by clustering metabolites that are at the same time involved in those changes. [109]. In this way, multivariate modelling methods were implemented to address limitations imposed by sample size and to unveil significant correlations in high-throughput data. Further validations are needed in large cohorts and clinical trials before achieving clinical approval of possible prognostic or diagnostic biomarkers, established using lipidomics [104].

5. Lipid abnormalities in Cystic fibrosis

Along with therapeutic strategies improvement and life expectancy increase, the number of comorbidities affecting CF patients is enlarging, including less-studied dyslipidemia. CTFR interaction with lipid metabolism and cell membranes is still poorly understood. Interaction with membrane lipids also tends to play a role in CFTR stabilization and function, in addition to other

protein-mediated regulation. Interactions between CFTR and cholesterol have been described and these interactions somehow control CFTR distribution and dynamics on the plasma membrane [110]. The apical aberrant CFTR (F508del) was demonstrated to be stabilized by blocking endocytosis, inhibiting proteasomal degradation, and depriving the membrane of cholesterol, which in turn affects the properties and composition of lipid rafts [111]. The lateral mobility of CFTR is reliant on cholesterol and consistent with cholesterol-rich lipid drafts confinement [112]. Even if little is known, some studies recognized in CF an altered fatty acid, cholesterol, and sphingolipid metabolism [113].

High triglycerides (TAG) and low LDL and cholesterol levels have been identified in the plasma of CF patients [114,115], as well as peripheral tissue fat accumulation [116–119], cholesterol malabsorption, and enhanced synthesis in the liver and in other tissues [120,121]. In particular, cystic fibrosis patients showed dyslipidemia with an increment in odd-chain and polyunsaturated fatty acids [122].

5.1 Fatty acids metabolism in cystic fibrosis

It is reported that in cftr-/cftr- mice and CF patients, fatty acids metabolism is altered with increased levels of n-6 PUFAs, such as arachidonic and linoleic acid, along with a reduction of DHA levels [123]. Relevantly, the biologic effects of fatty acids depend not only on their absolute levels but especially on the ratio of n–6 to n–3 fatty acids, which appeared to be altered and directly related to CFTR dysfunction as well [124]. The supplementation of n-3 PUFAs as a pharmacological treatment in CF is controversial even if it was demonstrated beneficial on several inflammatory diseases [123]. As a whole, an overall fatty acids imbalance was found in CF and principally interested more saturated species [125].

The potential causes of CF imbalance between high saturated fatty acids and low unsaturated fatty acids lipointoxication [123] were summarized as follows: (1) malabsorption of PUFAs due to systemic CFTR alteration such as Cystic Fibrosis-related Liver Disease (CFLD) and pancreatic insufficiency; (2) hypoxia, which prevents the oxygen-dependent desaturation steps needed to form unsaturated fatty acids from their saturated precursors; (3) an increased flux through the omega-6 pathway and (4) and increased activity of Phospholipase

A2. The increase in the activity of both the omega-6 pathway and Phospholipase A2 produce, in turn, an accumulation of pro-inflammatory arachidonic acid.
The inflammation and several clinical outcomes can be related to the irregular metabolism of omega-6 fatty acids, particularly in increased arachidonic acid level and linoleic acid deficiency. Some recent findings advocate inflammation as the primary cause followed by infection, further enhancing the release of arachidonic acid and inflammatory eicosanoids [126,127]. Moreover, lung transplantation can lead to an increase in the essential fatty acids profile, and it was attributed to (1) the presence of functional CFTR ; (2) the elimination of compromised and inflamed CF lungs; (2) the removal of excess fatty acids oxidation, and (4) the restoration in linoleic and arachidonic acids metabolism [128,129].

5.2 Cholesterol and lipoprotein in cystic fibrosis

CF patients with pancreatic insufficiency are more prompt to have reduced levels of total, LDL, and HDL cholesterol along with hypertriglyceridemia. In some cases, especially in those with pancreatic sufficiency, can also occur hypertriglyceridemia and hypercholesterolemia [130–134]. Decreased exogenous lipid absorption may be the explanation for lower lipid values observed in pancreatic insufficiency subjects. Along with chronic inflammation, this is also due to either inadequate intraluminal solubilization or diminished intestinal absorption of long-chain fatty acids [131].
In the same way, in a CF pediatric population, a high-fat diet along with an inadequate intake of saturated fat showed a decrease in the overall cholesterol, HDL and LDL concentrations and an increase in the TAG levels. The increment in TAG levels and in the ratio TAG / HDL was related in those patients to an elevated risk of cardiovascular diseases [135]. The explanation for hypertriglyceridemia can lie in systemic inflammation and an accumulation of carbohydrates that successively contribute to hepatic glycogen overload [134]. Unesterified cholesterol deposition in lung and trachea parts derived from CF patients was demonstrated and indicated as an underlying deficiency in cholesterol metabolism. Moreover, in both cultured CF cells [119,136] and nasal tissue excised from CFTR model mice was revealed an excess in plasma membrane cholesterol content. A disrupted intracellular cholesterol movement

could promote in turn, cholesterol synthesis, a hypothesis confirmed by the enhanced de novo cholesterol synthesis in cftr-/-mice in the lungs and liver [119].

Pancreatic insufficiency CF patients displayed lower cholesterol and phytosterol plasma levels and higher plasma lathosterol levels. The common cause that underlies to these abnormalities was found in reduced digestion and absorption of cholesterol itself. Different causes can contribute to altered synthesis and secretion of bile salts, intestinal inflammation, and decreased pancreatic secretion of cholesterol esterase [120,137].

Other evidence comes from lipid fraction of broncho-alveolar fluid that was reduced but displayed a fraction cholesterol esters concentrations, which are likely to play a role in inflammation processes [138].

5.3 Sphingolipids in cystic fibrosis

Sphingolipids and particularly the bioactive ceramide are recognised as one of the major regulators of inflammation in the initiation and propagation of severe lung complications associated with airway infection [75,139,140].

As well, the properties of cell membranes and the expansion of lipid rafts have also been correlated with ceramides[141].

The sensitivity of CF cells to apoptosis was examined to investigate the biological significance of the decline in ceramide expression. Ceramides acting as second messengers have also been involved in the activation of lung endothelial and epithelial cell apoptosis [142,143]. In this way, by lowering ceramide levels, the sensitivity of cells to apoptosis could be effectively reduced [141].

The distribution of ceramide, sphingomyelin, and sphingosine in the host reaction to infection leads to the delicate balance of anti-inflammatory activity and antimicrobial effectiveness. The disruption of ceramide metabolism in *P. aeruginosa* infection was associated with increased TNF receptor 1 expression, NFkB activation, and overproduction of proinflammatory cytokines [144].

The sphingolipid composition of CF airway epithelial cells is substantially altered with a rise in ceramide and decreased sphingosine in the luminal membrane of tracheal and bronchial epithelial cells. Moreover, sphingosine was demonstrated to be necessary for the killing of bacterial in the airways of cystic

fibrosis. Thus, the reduction of sphingosine, due to reduced activity of acid ceramidase, in CF epithelial airway cells was linked with increased infection sensitivity [145–148]. Ceramide, its precursors, isoprostanes, and lysolipids were also associated with neutrophilic inflammation in the airways of CF infants [149,150]. Different experiments also determined the imbalance in the chain length of ceramide and its implication in CF that is marked by abnormally low levels of ceramide C24:0 and high concentration of C16:0 [151,152].

However, not only ceramide but also its indirect catabolite sphingosine-1-phosphate (S1P) may be essential regulators in CF. S1P effect in pathophysiology is still difficult to decipher since it can control diverse or even opposing cellular effects, including those that counteract ceramide ones [153]. In cross-talk with other signalling pathways, in particular ceramides, S1P has significant effects on cell differentiation and proliferation, plays a role in tissue repair [153] and immunomodulation [154].A possible feedback relation was proposed between S1P and CFTR that is also capable of amplifies S1P signals. In pathological settings, this mechanism can additionally worsen the reduction of CFTR activity. Therefore, pharmacological strategies such as CFTR correction/potentiation can be enhanced by inhibiting S1P/AMPK signalling for greater effectiveness [155].The anomalous myeloid invasion and delayed resolution of mediated inflammation in CF lung pathology were correlated with decreased lung tissue S1P levels, which can be partly reversed by chronic treatment with an S1P lyase inhibitor. Specifically, the recovery of lung S1P levels leads to increased mucus deposition [156], low basal lung inflammation, amplified reaction to bleomycin, and *Pseudomonas aeruginosa* infection[157]. This infection of the lung epithelium was demonstrated to stimulate the nuclear localization of SPHK2, which results in turn to increased nuclear production of S1P. Besides, the secretion of pro-inflammatory cytokines, which followed the infection, was epigenetically regulated by nuclear S1P via histone deacetylases and interleukin-6 promoter H3 and H4 histone acetylation [158].

A clinical study investigated total and unbound S1P levels in lung-transplanted CF patients. CF patients had lower unbound S1P plasma, which differs depending on the CFTR mutation and gastrointestinal clinical implications [159].

2. AIMS OF THE STUDY

This thesis aimed to unveil the relationship between alteration in bioactive lipids metabolism and the inflammatory phenotype of cystic fibrosis.

Specifically:

1. To correlate the sphingolipid profile of extracellular vesicles (Evs) from lung mesenchymal stem cell (MSCs) and their immunomodulatory function in CF
2. To demonstrate a pervasive lipid dysmetabolism in both immortalized and primary cystic fibrosis bronchial epithelial cells
3. To evaluate the effect of Myriocin, a suicide inhibitor of the first enzyme in the de-novo sphingolipids biosynthesis, in the modulation of this imbalance

3. MATERIALS AND METHODS

3.1 Reagent and chemicals

Pure synthetic lipids standards were purchased from Avanti Polar Lipids (Alabaster, AL, USA). The chemicals acetonitrile, 2-propanol, methanol, chloroform, formic acid, ammonium acetate, and ammonium formate were LC-grade and purchased by Sigma-Aldrich (St. Louis, MO, USA). All aqueous solutions were prepared using purified water at a Milli-Q grade (Burlington, MA, USA).

The tool used to inhibit the cystic fibrosis transmembrane conductance regulator was the CFTR(inh)-172 from Sigma-Aldrich (St. Louis, MO, USA).

3.2 Human mesenchymal stem cells

Human lung mesenchymal stem cells (MSCs) were extracted from lung biopsies from seven patients undergoing lung surgery either for suspected lung tumor or bullous emphysema. Tissues were retrieved after the approval of the Ethical Committee of the ASST Santi Paolo e Carlo, Milano, Area A (n. 2211, 12/14/2016).

Each lung biopsy (about 1 cm^3), was divided with surgical scissors and maintained for ten days in DMEM medium containing 18% FBS, 1% penicillin/streptomycin at 37 °C and 5% CO_2. On the last day, adherent cells were cultured regularly with bFGF (5 ng/mL, Peprotech LTD, Israel) until passage seven. MSCs were treated with 10 μg/mL of CFTR(inh)-172 inhibitor for 48h obtaining an in vitro model of CF (CF-MSCs) [160]. In the same way, control MSCs (CTR-MSCs) were treated with the same amount of dimethyl sulfoxide.

3.3 Extracellular vesicles derived from human lung mesenchymal stem cells

After 48–72h the cultured media of both CTR-MSCs and CF-MSCs was subjected to ultracentrifugation to recover extracellular vesicles (EVs), as previously described [161]. The protocol consisted of a series of normal centrifugations (1000, 2000, and 3000 g for 15 min at 4 °C), followed by ultracentrifugation at 110,000 g (Beckman Coulter Optima L-90 K ultracentrifuge) for 75 min at 4 °C.

3.4 Cell culture

3.4.1 Immortalized cell model

Human bronchial epithelial cell line (IB3), derived from a CF patient (ΔF508/W1282X) provided by LGC Promochem (Teddington, UK), were grown in LHC-8 medium supplemented with 5% FBS, 1% penicillin/streptomycin at 37 °C, and 5% CO_2. Healthy (H) human lung bronchial epithelial cell line (16HBE14O, initially developed by Dieter C. Gruenert) were provided by Luis J. Galietta (Telethon Institute of Genetics and Medicine—TIGEM, Napoli, Italy). Originally HBE primary cells were grown in LHC-8, even though in the present study they were cultured as recommended (Merck Millipore SCC150 datasheet) in MEM Earle's salt supplemented with 5% FBS, 1% penicillin/streptomycin at 37 °C, and 5% CO_2. For cell lipidomics, 1×10^5 cells/100-mm plate in 5 mL medium were plated, harvested when confluence has reached 90%, washed in PBS, and pelleted.

3.4.2 Patient-derived primary cell lines

Primary broncho-epithelial cells from three CF patients and three healthy donors were obtained from the Fondazione Fibrosi Cistica facility (Verona, Italy). CF cells were selected for bearing homozygous or compound heterozygous ΔF508. About 250×10^4 cells were seeded on collagen-coated flasks and grown in proliferative conditions with LHC9/RPM1 for at least two weeks. For lipidomics, cells were harvested when confluence has reached 90%, washed in PBS, and pelleted.

3.5 In vitro pharmacological treatment

Myriocin (Myr) treatments were performed at a concentration of 50 μM overnight in 100 mm dishes plated at 1×10^5 cells/each. At least triplicate samples for each experiment were performed.

3.6 Protein quantification

For normalization purpose, a small aliquot of the cell lysate was preserved for total protein quantification by following the manufacturer (Bio-Rad, Hercules, CA, US) instruction for the Bradford dye-binding method. The resultant blue colour was measured at 595 nm following a 5 min room temperature

incubation and compared to a standard curve of bovine serum albumin (BSA) in the range of 1-20 μg/mL.

3.7 Untargeted lipidomics

3.7.1 Total lipids extraction

Lipid extraction was completed by a modified version of the Bligh & Dyer method [86]. Cells (about 1×10^6) were reconstituted in 100 μL of water + 0.1% proteases inhibitor cocktail (Roche, Basel, Switzerland) and extracted with 850 μL of a methanol/chloroform mixture (2:1, v/v). The samples were sonicated for 30 min, and the organic phase was evaporated under a stream of nitrogen. The residues were dissolved in 100 μL of isopropanol/acetonitrile (2:1, v/v), centrifuged for 10 min at 13,400 RPM, and withdrawn in a glass vial.

3.7.2 Sphingolipid extraction

For the targeted sphingolipid analysis, cell pellets were incubated overnight in an oscillator bath at 48 °C after the addition of 100 μL of water and 850 μL of methanol/chloroform mixture (2:1, v/v). Then, alkaline methanolysis was carried out by incubation at 37 °C for 2 h with 75 μL of potassium hydroxide 1 M in methanol to improve their recovery. Samples were evaporated after neutralization with 75 μL of 1 M acetic acid in methanol. The residues were dissolved in 100 μL of methanol, centrifuged at 13,400 RPM for 10 minutes, and transferred in a glass vial.

3.7.3 LC-MS/MS Untargeted method

The LC-MS/MS consisted of a Shimadzu UPLC coupled with a Triple TOF 6600 Sciex (Concord, ON, CA) equipped with Turbo Spray IonDrive. All samples were analyzed in duplicate in both positive and negative mode with electrospray ionization. The instrument parameters were: CUR 35, GS1 55, GS2 65, capillary voltage 5.5 kV, and source temperature 350 °C. Spectra were contemporarily acquired by both full-mass scan from 200–1500 m/z (100 ms accumulation time) and data-dependent acquisition from 50–1500 m/z (40 ms accumulation time, top 18 spectra per cycle 0.8 s). Declustering potential and the collision energy were fixed to 50 eV and 35 ± 15 eV, respectively.

The chromatographic separation on an Acquity BEH C18 column 1.7 µm, 2.1 × 50 mm (Waters, Franklin, MA, USA), equipped with a precolumn [162], was realized gradually mixing mobile phase A, water/acetonitrile (60:40) and, mobile phase B, 2-propanol/acetonitrile (90:10), both containing 10-mM ammonium acetate and 0.1% of formic acid. The flow rate was 0.4 mL/min, and the column temperature was 45 °C. The elution gradient was set as below: 0–2 min (45% B), 2–12 min (45%–97% B), 12–17 min (97% B), 17–17.10 min (97%–45% B), and 17.10–21 min (45% B).

Additionally, another chromatographic separation was reached on an Acquity CSH C18 column 1.7 µm, 2.1 × 100 mm (Waters, Franklin, MA, USA) equipped with a precolumn by using, as mobile phase A, water/acetonitrile (60:40) and, as mobile phase B, 2-propanol/acetonitrile (90:10), both containing 10-mM ammonium acetate and 0.1% of formic acid. The flow rate was 0.4 mL/min, and the column temperature was 45 °C. The elution gradient (%B) was set as below: 0–2.0 min (40%), 2.0–2.5 min (40%–50%), 2.5–12.5 min (50%–55%), 12.5–13.0 min (55%–70%), 13.0–19.0 min (70%–99%), 19.0–24.0 min (99%), and 24.0–24.2 (99%–40%) and kept constant until 30 min. Five microliters of clear supernatant were directly injected in the LC-MS/MS.

3.7.4 Lipidomic data processing for the untargeted studies

The correct identification and relative quantification were attained using MS-DIAL (version 4.0) software [163–165]. Data raw files were aligned and retention time corrected. For the lipid identification, the experimental spectra were matched with those in the LipidBlast library [166], setting a total identification score >70% for both accurate mass and MS/MS fragmentation (Table 2).

Prevalent adducts were previously investigated in our experimental conditions, and thus, the identification was restricted only to them. MS and MS/MS tolerance for peak profile were set to 0.01 and 0.05 Da, respectively. Data were then filtered for blank sample signals. During the batch, a quality control pooled sample (QC, a combination of all samples in the batch) was injected every four samples to assess the instrumental variability. Lipids with a coefficient of variation (CV%) in the QC of more than 30% were omitted for further investigation. [167]. Then, to restrict biological and analytical variances,

normalization was completed by correcting the peak intensities (Equation 1) of each lipid for both (1) the amount of protein in the extract injected (μg) measured by the Bradford method and (2) the variation in the response of QCs dispersed evenly throughout the batch (by the Lowess algorithm). Manually, lipids containing either a large number of unsaturations or odd-chain fatty acids were omitted. A description of the entire lipid metabolism was presented as the sum of the individual lipids per subclass after normalization (an example is shown in Equation 2). Fold change was eventually calculated against the control group, and its SD was considered after scaling each variable for the mean of the same variable in the control group (Equation 3)

$$\text{Amount}_X = \frac{\text{Peak intensity}_X \text{ after normalization}}{\mu\text{g protein injected}} \quad (1)$$

$$\text{Amount}_{Cer} = \text{Amount}_{Cer1} + \text{Amount}_{Cer2} + .. \text{Amount}_{Cer\ n} \quad (2)$$

$$\text{Fold change}_X = \frac{(\text{Amount}_X)\text{SAMPLE}}{(\text{Amount}_X)\text{CTR}} \quad (3)$$

Table 2. Characteristic MS/MS fragmentation pattern for the correct lipids identification

Lipid subclasses	Adducts	MS/MS (m/z)	Identification
Ceramides	M+H+	PI 264.26 or 282.27	sphingosine d18:1
Dihydroceramides	M+H+	PI 266.26 or 284.28	dihydrosphingosine d18:0
Sphingomyelins	M+H+	PI 184.07	phosphocholine head group
Neutral glycosphingolipids (HexCer, LacCer, Gb3)	M+H+	PI 264.26 or 282.27	sphingosine d18:1
Acidic glycosphingolipids (GM3, aGM1..)	M+H+	PI 520.5 or 548.5 or 605.5 or 632.5 …	Loss of water by ceramide residues
Phosphatidylcholines	M+H+	PI 184.07	phosphocholine head group
Phosphatidyletanolamines	M+H+	NL 141.01	phosphoethanolamine head group
Cholesterol esters	$M+NH_4+$	PI 369.35	free cholesterol [$M-H_2O+H+$]
Free cholesterol	$M-H_2O+H+$	PI 147.1 or 161.1	
Acylcarnitines	M+	PI 85.0	CH2CH=CHCOOH cation
Cardiolipins	$M+NH_4+$	PI DAG moieties	
Triacylglycerols	$M+NH_4+$		
with FA 16:0		NL 273.2	FA 16:0 + NH_3
with FA 18:0		NL 301.2	FA 18:0 + NH_3
with FA 18:1		NL 299.2	FA 18:1 + NH_3
with FA 18:2		NL 297.2	FA 18:2 + NH_3
with FA 18:3		NL 295.2	FA 18:3 + NH_3
with FA 20:0		NL 329.2	FA 20:0 + NH_3
with FA 22:0		NL 357.2	FA 22:0 + NH_3
with FA 22:1		NL 355.2	FA 22:1 + NH_3
with FA 24:0		NL 385.2	FA 24:0 + NH_3
with FA 24:1		NL 383.2	FA 24:1 + NH_3
Phosphatidylinositoles	M-H-	PI 241.0	Rearrangement of inositol head group
Phosphatidylserine	M-H-	NL 87.0	Serine head group
Phosphatidylglycerols	M-H-	PI 171.0	Glycerols head group
Phospatidic acid	M-H-	PI 152.9	Polar head

NL, neutral loss; PI, product ions

3.8 Targeted sphingolipidomics

3.8.1 Sphingolipid extraction

Sphingolipids were extracted from both mesenchymal stem cells and EVs using a monophasic extraction with alkaline methanolysis [168–170]. Cell pellets were diluted with 100 µL of PBS + 0.1% protease inhibitor. A small aliquot was used to determine the total protein content by the Bradford method. The internal standard mix was added to the purified sample (10 µl, Cer C12, SM C12, and Sph d17:1 each at 20 µM) along with a mixture of methanol/chloroform (2:1, v/v), then sonicated for 30 min. Samples were then incubated overnight in an oscillator bath at 48 °C. Once at room temperature, 75 µl of KOH 1 M in MeOH were added to the samples, then subjected to 2 hours incubation at 37 °C. The pH was adjusted at 7.0 by adding 75 µl acetic acid 1 M in MeOH. After evaporation with a gentle stream of nitrogen, samples were dissolved in 100 µl of methanol, then centrifuged for 10 min at 13000 rpm and withdrawn in a glass-vials.

3.8.2 LC-MS/MS Targeted Method for ceramides, dihydroceramides and sphingomyelins analysis

The LC-MS/MS consisted of a UPLC (Dionex 3000 UltiMate - Thermo Fisher Scientific, USA) connected to a 3200 QTRAP Sciex (Concord, ON, CA). The instrument parameters were: CUR 25, GS1 45, GS2 50, capillary voltage 5.5 kV, and source temperature 300 °C. The analytical data were processed using Analyst software (version 1.2). The dwell time was set at 0.1 s, and the MS scan was performed in positive ion modes (ESI+). Compound-dependent parameters were optimized via direct infusion. Multiple reaction monitoring (MRM) mode was used (Table 3).

Separation was attained on an Acquity BEH C8 1.7 µm, 2.1 x 100 mm (Waters, Franklin, MA, USA), equipped with a precolumn by mixing eluent A (water +2 mM ammonium formate + 0.2% formic acid) and eluent B (methanol + 1 mM ammonium formate + 0.2% formic acid). The flow rate was 0.3 mL/min, and the column temperature was 30 °C. The elution gradient was set as below: 0-3 min (80-90%), 3-6 min (90%), 6-15 min (90-99%), 15-18 min (99%), 18-20 min (99-80%), 20-24 (80%).

Table 3. LC/MS-MS conditions for the analysis of ceramides, dihydroceramides and sphingomyelins.

Analytes	MS/MS (m/z)	DP (eV)	CE (eV)
Cer 12:0 (Cer IS)[1]	482.7 > 264.4	40	29
Cer 14:0	510.7 > 264.4	40	29
Cer 16:0	538.8 > 264.4	40	32
Cer 18:1	566.8 > 264.4	40	34
Cer 18:0	564.8 > 264.4	40	35
Cer 20:0	594.8 > 264.4	40	36
Cer 22:0	622.9 > 264.4	40	37
Cer 24:1	650.9 > 264.4	40	41
Cer 24:0	648.9 > 264.4	40	38
DHCer 16:0	540.4 > 266.4	40	33
DHCer 18:1	568.5 > 266.4	40	35
DHCer 18:0	566.5 > 266.4	40	35
DHCer 24:1	652.5 > 266.4	40	40
DHCer 24:0	650.5 > 266.4	40	38
Sm 12:0 (SM IS)[2]	649.6 > 184.1	40	50
Sm 16:0	705.6 > 184.1	40	50
Sm 18:0	733.6 > 184.1	40	50
Sm 18:1	731.6 > 184.1	40	50
Sm 24:0	817.6 > 184.1	40	50
Sm 24:1	815.6 > 184.1	40	50

[1]Cer 12:0 was used as internal standard to counterbalance the variations of ceramides and dihydroceramides
[2]Sm 12:0 was used as internal standard to counterbalance the variations of sphingomyelins

3.*8.3 LC-MS/MS Targeted Method for S1P analysis*

The LC-MS/MS consisted of a UPLC (Dionex 3000 UltiMate - Thermo Fisher Scientific, USA) connected to a 3200 QTRAP Sciex (Concord, ON, CA). The instrument parameters were: CUR 25, GS1 45, GS2 50, capillary voltage 5.5 kV, and source temperature 300 °C. The analytical data were processed using Analyst software (version 1.2). The dwell time was set at 0.1 s, and the MS scan was performed in positive ion modes (ESI+). Compound-dependent parameters were optimized via direct infusion. Multiple reaction monitoring (MRM) mode was used (Table 4).

Separation was attained on an Restek Raptor C18 2.7 µm, 2.1 x 100 mm (Cernusco sul Naviglio, Milan, Italy), equipped with a precolumn by mixing eluent A (water +2 mM ammonium formate + 0.2% formic acid) and eluent B

(methanol + 1 mM ammonium formate + 0.2% formic acid). The flow rate was 0.3 mL/min, and the column temperature was 30 °C. The elution gradient was set as below: 0-2 min (20%), 2-4 min (20-99%), 4-7 min (99%), 7-7.5 min (99-20%), 7.5-10 min (20%).

Table 4. LC/MS-MS conditions for the analysis of S1P

Analytes	MS/MS (m/z)	DP (eV)	CE (eV)
Sphinganine d17:0 (Sph IS)[1]	288.4 > 252.0	21	20
Sphingosine-1-phosphate (S1P)	380.2 > 264.3	26	21

[1]Sphinganine d17:0 was used as internal standard to counterbalance the variations of sphingoid bases

3.8.4 Sphingolipid absolute quantification: analytical performances

Quantitative analysis was performed interpolating the ratio area of analyte/area of the appropriate IS (Cer 12:0 for ceramides and dihydroceramides, SM 12:0 for sphingomyelins and Sphinganine d17:0 for S1P) against the calibration curve of each sphingolipid (Table 5). The sphingolipids amount was normalized by total protein content, expressed in milligram, in each sample (Equation 4).

$$\left(\frac{\text{pmol}}{\text{mg protein}}\right)_X = \frac{\text{Peak Area}_X}{\text{Peak Area}_{IS} \cdot m_{\text{std curve}} \cdot \text{mg protein}} \quad (4)$$

Table 5. Calibration curves for each sphingolipid

Analytes	Slope	R^2	LOQ[1] ($pmol_{vial}$)	Range (pmol)
Cer 14:0	0.0058	0.998	1	4-400
Cer 16:0	0.0041	0.997	1	4-400
Cer 18:1	0.0063	0.991	1	4-400
Cer 18:0	0.0080	0.995	1	4-400
Cer 20:0	0.0092	0.990	1	4-400
Cer 22:0	0.0136	0.985	1	4-400
Cer 24:1	0.0118	0.972	1	4-400
Cer 24:0	0.0089	0.977	1	4-400
DHCer 16:0	0.0053	0.996	1	4-400
DHCer 18:1	0.0019	0.991	1	4-400
DHCer 18:0	0.0079	0.992	1	4-400
DHCer 24:1	0.0051	0.961	1	4-400
DHCer 24:0	0.0046	0.975	1	4-400
Sm 16:0	0.0095	0.983	0.3	5-1000
Sm 18:0	0.0104	0.974	0.3	5-1000
Sm 18:1	0.0112	0.985	0.3	5-1000
Sm 24:0	0.0080	0.977	0.3	5-1000
Sm 24:1	0.0115	0.963	0.3	5-1000
S1P	0.0329	0.997	0.2	4-400

[1]LOQ limit of quantification was calculated as the concentration that presented a signal-to-noise > 10

3.9 Cytokines determination

Pro-inflammatory cytokines levels were determined in IB3 culture media by biomarker multiplex immunoassays on Luminex Platform [171]. Cell protein concentration was determined by Bradford assay and used for normalization.

3.10 Confocal analysis

Cells were seeded on glass slides and grown for 24 hours (70% confluency). To label lipid biosynthesis products, BODIPY™ 558/568 C12 (4,4-Difluoro-5-(2-Thienyl)-4-Bora-3a,4a-Diaza-s-Indacene-3-Dodecanoic Acid) was added to the culture medium, according to the manufacturer's instruction, and cells were labelled overnight. For neutral lipid staining, BODIPY 493/503 (4,4-difluoro-1,3,5,7,8-pentamethyl-4-bora-3a,4a-diaza-s-indacene) was added to the culture medium, according to manufactures instruction, and cells were labelled for 30 minutes. Next, the slides were washed and dried for 3 minutes at room

temperature, fixed in 4% buffered formalin for 30 minutes, rinsed twice in PBS. Sections on a glass slide were inverted and mounted onto glass slides using anti-fading and DAPI (4',6-diamidino-2-phenylindole) containing mounting reagent for nuclei counterstaining. Confocal images were acquired using Nikon A1 Laser Scanning Confocal microscope (60x oil immersion objective). Image quantitation was performed using Fiji analysis software. All values were normalized onto nuclei count.

3.11 Statistical and Data Analysis

3.11.1 Statistical analysis for targeted approach

Statistical analysis for the targeted approach was investigated by the software GraphPad Prism 7.0 (GraphPad Software, Inc, La Jolla, CA, USA). Normally was tested by the Kolmogorov-Smirnow-Lilliefors test. Continuous variables were presented as mean $\pm$ standard deviation (SD), whereas categorical variables as absolute numbers and percentages. Comparisons between two groups were performed using either paired t-test or unpaired t-test, accordingly. Categorical variables were compared using the chi-square test or Fisher's exact test, as appropriate. Comparisons between more than two groups were performed by one-way ANOVA with Bonferroni post-hoc test for multiple comparisons. All tests were two-sided, and statistical significance was set to p-value < 0.05.

3.11.2 Statistical analysis for untargeted approach

The different lipid groups (sum of species concentrations) were compared by t-test with GraphPad Prism 7.0 (GraphPad Software, Inc, La Jolla, CA, USA) to prove differences in lipid metabolisms between cell phenotypes. Then for biomarker discovery, data tables with lipids detected were uploaded to the MetaboAnalyst server. (version 4.0) [172,173]. Data were checked for integrity, filtered by interquartile range, log-transformed (generalized logarithmic transformation), and auto-scaled. The sum of their abundances will be further considered if multiple isomeric lipid species were found because the exact position and stereochemistry of the unsaturations could not be deduced from this experiment. The comparison between CF and healthy cells was performed by both univariate and multivariate methods. The volcano plot showed the statistical significance and the fold change of each lipid identified by selecting

only those with a *p*-value < 0.05 (corrected for false discovery rate) and a fold change (FC) >2. Partial least squares discriminant analysis (PLS-DA) was performed in order to increase the group separation and investigate the variables with a Variance Importance in Projection (VIP) score >1. These features could be considered as a potential biomarker of CF [174]. The quality of the PLS-DA models was assessed by cross-validation: R^2 and Q^2 (i.e. cross-validated R^2). In order to prevent overfitting or inaccurate estimations, they should be above 0.8 [175]. Visualization by hierarchical clustering heatmaps was performed by Ward clustering and setting distance as Euclidean. Enrichment analysis was performed on normalized data from MetaboAnalyst, using LION/web by the ranking mode, with a one-tailed Welch 2-sample *t*-test as the local statistics [109]. The LION ontology and, specifically, lipid structure, cellular components, and physical-chemical properties were related to changes in lipid patterns between CF and healthy phenotypes. The chi-square or binomial tests were used to compare observed with expected data distributions.

4. RESULTS

4.1 Sphingolipid profile and function of EVs derived from MSC

4.1.1 The profile of sphingolipids in ctr EVs and CF-EVs is differently expressed

To investigate the possible mediators that underlie the various anti-inflammatory activities of ctr- and inh-Evs (model of CF), the composition of bioactive sphingolipids has been determined [171]. In CF-EVs, we obtained a substantial increase in the content of total Cer and dhCer (Figure 6), its precursor along the de-novo biosynthesis pathway, with values ranging from 991.1 ± 401.4 against 790.9 ± 229 (mean ± SD, CTR) and to 25.75 ± 10.4 against 18.17 ± 5.1 (CTR) pmoles/mg protein, respectively.

Moving to the single ceramide species, we found that the Cer with C16:0 fatty acid accumulated 15% more in CF-EVs than in ctr EVs, and it is the most representative one (Figure 7, panel B). In addition, ceramides with longer saturated and unsaturated fatty acid chains, namely C20:0, C22:0, C24:0, and C24:1, increased significantly in CF-EVs by 25%, 60%, 100%, and 25%, respectively.

EVs levels of sphingosine-1-phosphate, one of the most bioactive catabolites of ceramide, were slightly elevated in CF-Evs (5.0±1.7 vs. 4.0±0.7), and this behaviour will be further investigated with a higher number of patients.

The same sphingolipid profile was established in CF mesenchymal stem cells (MSC-inh), from which Evs derived, with a significant 30% increase in the levels of total Cer (3387±1111 vs. 2605 ±1032 pmoles/mg protein, $p<0.05$) and specifically an accumulation of 35% in the most representative Cer species, namely C16:0, C22:0, and C24:0 (Figure 7, panel A). Moreover, we observer 40% decrease in the class of sphingomyelins (13680±2072 vs. 9585±1696 pmoles/mg protein, $p<0.05$) were observed.

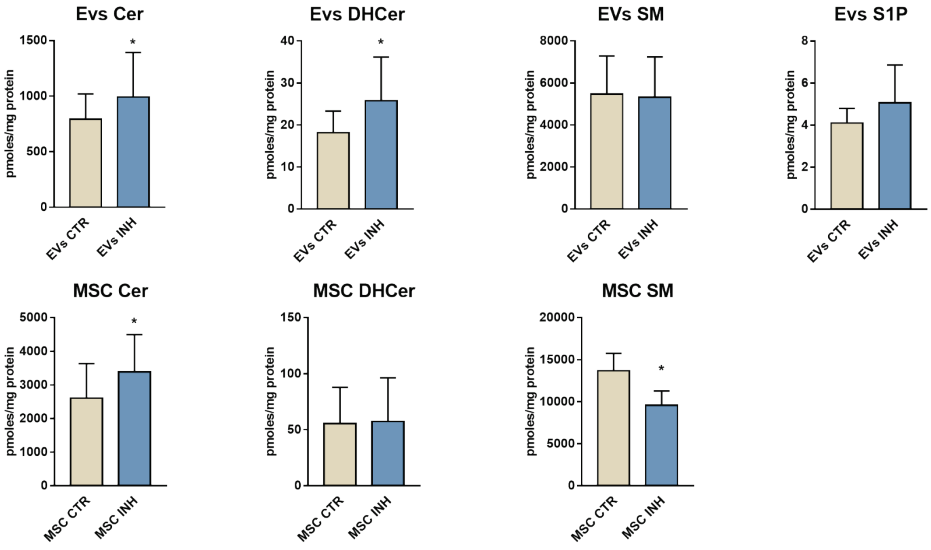

Figure 6. Sphingolipids profile of healthy (CTR) and cystic fibrosis induced (INH) mesenchymal stem cells (MSC) and extracellular vesicles (EVs). Data are expressed as mean ± SD of five to seven independent experiments. The statistical significance was evaluated by two-tailed, paired, Student t-test (*, $p < 0.05$).

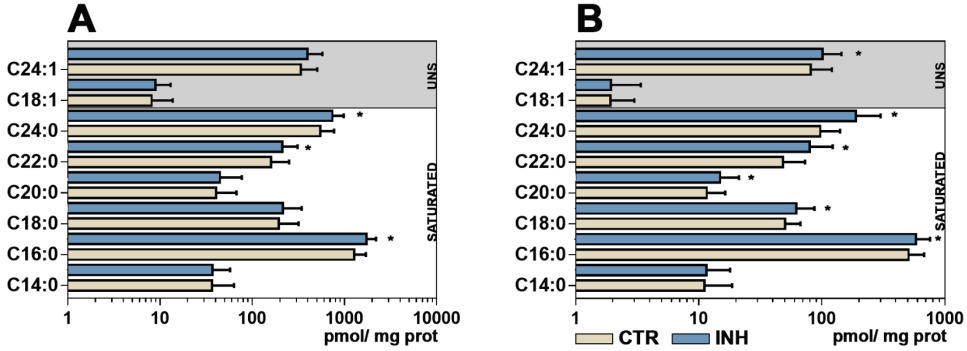

Figure 7. Ceramide species with saturated fatty acids from C14 to C24 and the monounsaturated (UNS) C18:1, C24:1 in healthy (CTR) and cystic fibrosis induced (INH) (**A**) mesenchymal stem cells and (**B**) extracellular vesicles. Ceramide concentrations are expressed as pmol/mg protein. Data are expressed as mean ± SD of five to seven independent experiments. The statistical significance was evaluated by two-tailed, paired, Student t-test (*, $p < 0.05$).

4.1.2 The role of EVs in modulating inflammation in CF

We investigate the hypothesis that lung MSCs and their EVs may be implicated in immunity and inflammatory responses in CF [171]. Basal cultured IB3 cells were treated with 30 μL of EVs released from either I-172-treated or untreated MSCs (namely CF-EVs or ctr EVs) for 24 hours.

Treatment with CF-EVs did not affect cell viability, and neither signs of early apoptosis nor autophagy were noted.

With regard to the expression of pro-inflammatory cytokines in IB3-1 cells after supplementation with ctr-EVs, we obtained a significant decrease in mRNA and protein expression of IL-1β and IL-6 (Figure 8). IL-1β tends to be the most receptive, showing a substantial reduction of 35% in protein levels, while the amount of IL-6 showed a global reduction of 40%. As a whole, CF-EVs seem less effective in attenuating the pro-inflammatory profile of IB3-1 cells than ctr EVs, demonstrated by no significant variations in cytokines levels.

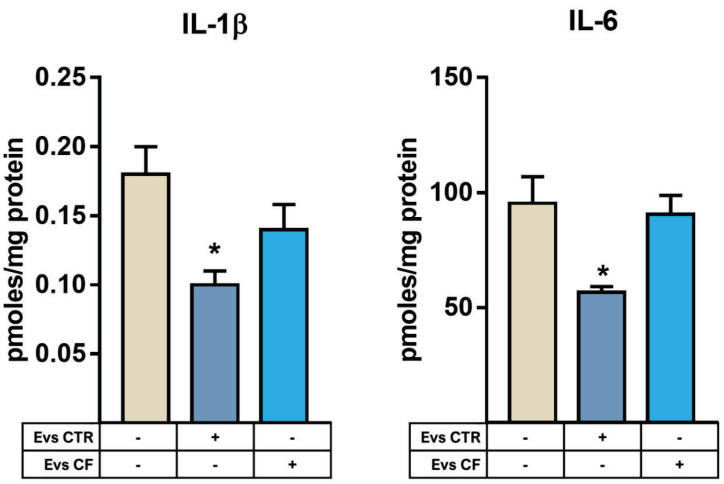

Figure 8. Effect of CF-EVs media supplementation on cytokynes expression in IB3 cell culture. The cytokines were expressed as pmoles/mg protein by ELISA. Statistical significance was evaluated by one-way ANOVA (*$p<0.05$; ** $p<0.01$), followed by Newman-Keuls post-test against basal IB3. Data, expressed as mean ± SEM, are obtained from seven individual MSCs - derived EVs populations.

4.2 Characterization of the lipidomic profile in CF phenotype

4.2.1 Optimization of the pre-analytical procedures

The gold-standard for sphingolipid quantification is methanol/chloroform extraction supplemented with alkaline methanolysis [169,176]. This unique extraction protocol warranties a higher rate of extraction of sphingolipids species, especially sphingomyelins, by reducing pre-eminent interference of phospholipids [170,177]. It was verified that the samples treated with alkaline methanolysis showed higher sphingolipid intensity (Figure 9, panel A). Curiously, the total lipid approach yielded a greater number of correctly labeled sphingolipids (84 vs. 104, taking into account the major subclasses: ceramides, hexosylceramides, and sphingomyelins). When using the two extraction protocols, the profile of sphingolipids, calculated as fold changes between the two cell lines, not significantly differed each other (Figure 9, panels B-D). Taking these findings overall, in the untargeted lipidomics method, we chose to avoid methanolysis, limiting this particular treatment to those experiments which need to study specifically sphingolipids [178].

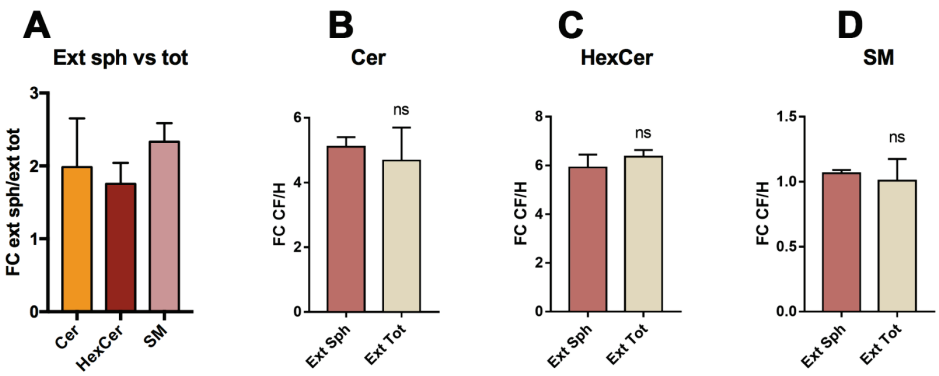

Figure 9. Sphingolipidomics: comparison between the specific extraction of sphingolipid with alkaline methanolysis (Ext sph) and total lipid extraction (Ext tot). (**A**) Fold-change (FC) of the main sub-classes of sphingolipids (ceramides, hexosylceramides and sphingomyelins) within the two extraction protocols: the alkaline methanolysis logically increases the intensity (about 2-fold) of the species due to the removal of the interferences of phospholipids in the extract. Fold-change of the concentration of (**B**) ceramides, (**C**) hexosylceramides and (**D**) sphingomyelins in cystic fibrosis (CF) and healthy phenotypes (H) as the function of the extraction protocols. Taking into account these results, the extraction methods appear to be comparable.

4.1.2 Optimization of the analytical conditions

To optimize chromatographic separation, two distinct mobile-phase modifiers and two separate columns were tested using a mixture of 14 chemically pure lipids (Differential ion mobility system suitability package, synthetic lipid mix, Avanti Polar, Alabaster, AL, USA) covering all the subclasses. The maximum peak intensity (Tables 6-7) and the best lipidome coverage (Figure 10) were provided by ammonium acetate and the Acquity CSH column. In the runs with the ammonium acetate, as a buffer, it was assessed a fold-change in the measured lipids of 1.5 (mean) in respect to ammonium formate, whereas 1.9 (mean) was achieved in CSH in respect to BEH.

In biological QC pools (n=5), the CSH column was confirmed at +34 % in lipids coverage (995 vs. 741, Figure S2). This was possibly due to the improved separation of the multiple lipids. The number of IDA experiments in a cycle period was also taken into account: not surprisingly, using the 20 spectra/cycle configuration, the number of total spectra acquired was around double compared to the top 10 (Figure S3).

Table 6. Performance comparison between buffers selection (10 mM ammonium acetate vs. 10 mM ammonium formate) in HPLC mobile phases. A mixture of different lipids (10 ng injected for each lipid, except 25 ng injected for PI) was used to monitor shift in retention times and peak intensities.

Analytes	m/z	R_T acetate	R_T formate	FC in peak height $_{\text{acetate vs formate}}$
Cholesterol	369.3515	14.06	13.96	1.05
SM 18:1	729.5905	14.59	14.55	1.32
Cer 18:1	564.5350	15.47	15.48	1.34
LPC 18:1	522.3554	3.36	3.19	1.52
CE 19:0	689.6207	18.26	18.33	3.59
DAG 28:2	526.4466	13.7	13.35	2.11
CL 56:6	1233.7917	16.16	16.25	1.66
PC 28:2	674.4755	7.66	7.43	1.27
TAG 54:3	902.8171	18.9	18.98	1.15
PS 28:2	676.41841	6.11	6.00	1.37
PE 28:2	632.4285	8.25	7.99	1.21
PI 28:2	768.4657	6.32	6.21	0.74
PG 28:2	680.4497	6.51	6.36	1.34
PA 28:2	606.4129	7.43	7.25	1.21

Table 7. Performance comparison between analytical columns (Acquity CSH 1.7 µm 2.1x100 mm *vs* Acquity BEH 1.7 µm 2.1x50 mm) using appropriate LC conditions[1] and the same MS methods. A mixture of different lipids (10 ng injected for each lipid, except 25 ng injected for PI) was used to monitor shift in retention times and peak intensities.

Analytes	m/z	R_T CSH	R_T BEH	FC in peak height $_{CSH\ vs\ BEH}$
Cholesterol	369.3515	14.14	6.73	1.03
SM 18:1	729.5905	14.63	7.38	2.28
Cer 18:1	564.5350	15.50	8.08	3.01
LPC 18:1	522.3554	3.47	1.52	1.83
CE 19:0	689.6207	15.90	8.24	1.57
DAG 28:2	526.4466	13.85	6.41	1.34
CL 56:6	1233.7917	16.16	9.13	3.91
PC 28:2	674.4755	7.83	4.82	1.27
TAG 54:3	902.8171	18.90	11.52	7.76
PS 28:2	676.41841	6.18	4.15	0.90
PE 28:2	632.4285	8.42	5.06	0.92
PI 28:2	768.4657	6.32	4.08	0.10
PG 28:2	680.4497	6.57	4.38	1.00
PA 28:2	606.4129	7.44	4.69	0.26

In the whole dataset (Figure 11), MS-DIAL recorded, considering data from both polarities n.15845, which after blank filtration, account for n.13375 mass spectra. The essential MS/MS information was presented by only n.7787 (49.1%), and the species annotated as lipids were n.1159 (7.3%), grouped into various classes and subclasses (Figure 12).

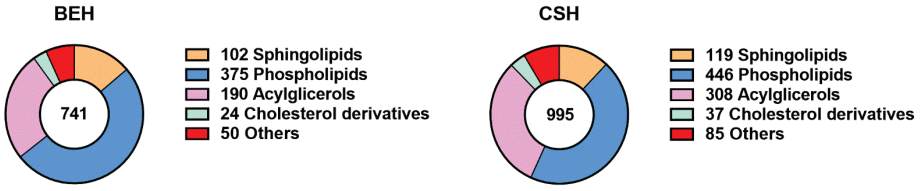

Figure 10. Lipids coverage between different chemical stationary phases in the analytical column: BEH and CSH

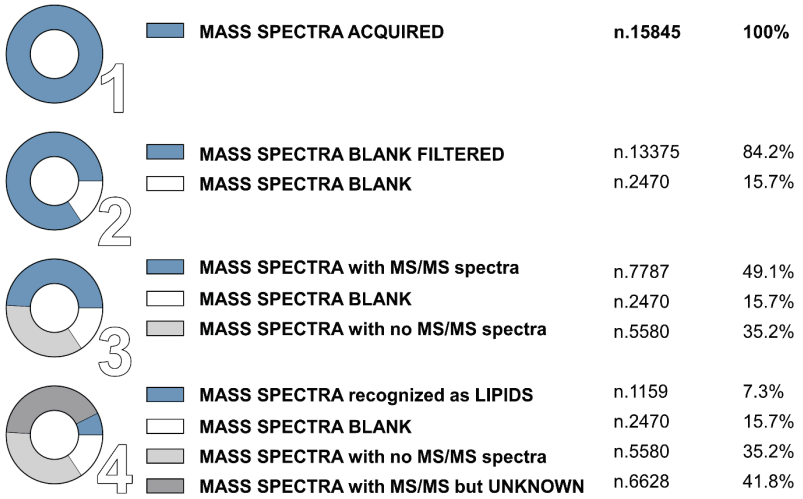

Figure 11. Workflow for the spectra data cleaning: the mass spectra acquired (1) were filtered for (2) the blank impurities, (3) spectra without MS/MS information, and (4) spectra with MS/MS information but not referable to lipid structures.

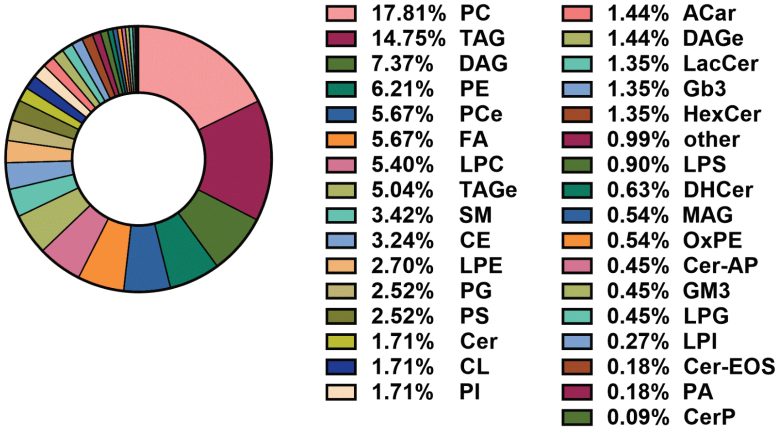

Figure 12. Distribution of the lipids recognized by lipidomics analysis on the whole set of samples divided by sub-class. ACar, Acylcarnitines; CE, cholesterol esters; Cer, ceramides; DAG, diacylglycerols; DHCer, dihydroceramides; FA, fatty acids; Gb3, globotriaosylceramide; GM3, gangliosides; HexCer, hexosylceramides; LacCer, lactosylceramides; LPC, lysophosphatidylcholines;
LPG, lysophosphatidylglicerols; LPE, lysophosphatidylethanolamines; LPI, lysophosphatidylinositole; LPS, lysophosphatidylserines; MAG, monoacylglycerols; PC, phosphatidylcholines; PCe, ether linked phosphatidylcholines; PG, phosphatidylglicerols; PE, phosphatidylethanolamines; PI, phosphatidylinositoles; PS, phosphatidylserines; SM, sphingomyelins; TAG, triacylglycerols.

4.2.2 Performances of the untargeted approach

Running standard samples containing a mixture of chemically pure lipids (Differential ion mobility system suitability package, synthetic lipid mix, Avanti Polar, Alabaster, AL, USA) with a concentration of 1 µg/mL (10 ng injected), MS-DIAL correctly identified 65% of the lipids contained.

To balance differences and eradicate experimental or biological biases, the normalization approach is of utmost importance. The gold-standard for targeted analysis is internal standard-based normalisation, but it has been shown for untargeted analysis that the process is outperformed by other approaches. The use of a small number of internal standards is not appropriate for an unbiased study of complex biological mixtures, because various chemical structures (e.g. the fatty acid chain) and chromatographic behaviours have been displayed in lipids, which also belong to the same class. The alternative of internal standardisation was avoided for the above reasons.

The use of total ion count (TIC) [179,180] may be an alternate approach to reducing analytical and biological variability. In our experiment, the TIC was measured (ochre curve in Figure 13), producing satisfactory results for both cell lines and also displaying a linearity response with the total amount of protein in each sample (R^2 0.70).

To calibrate symmetric biases, we used the weighted scatterplot smoothing (Lowess) on QC sample for analytical signal correction [163,181,182]. With the goal of minimising variance not only in QC but also in experimental groups, the option of normalization should be carried out [183,184]. Therefore by normalising data on total protein content of the samples, we minimise biological variability. Lowess, combined with biological normalisation, is shown in Figure 13 as a single curve (green). The latter showed the same TIC efficiency, with approximately 70-90 % of acceptable features (CV %< 30%), and was thus finally chosen for our intent. The raw, non-normalized data were contrasted with these normalisation techniques (red curve in Figure 13). The various methods of normalisation showed minimal experimental differences between them in this restricted context, specifically in the comparison between two phenotypes, and so we suggested choosing the Lowless coupled with

biological normalisation (green in Figure 1). Results on the HBE cell line were significantly affected by the lack of normalisation (Figure 1B).
The variability of the intra-batch, which is the variance coefficient (CV%) of the QC sample distributed in the batch, was around 16 percent.

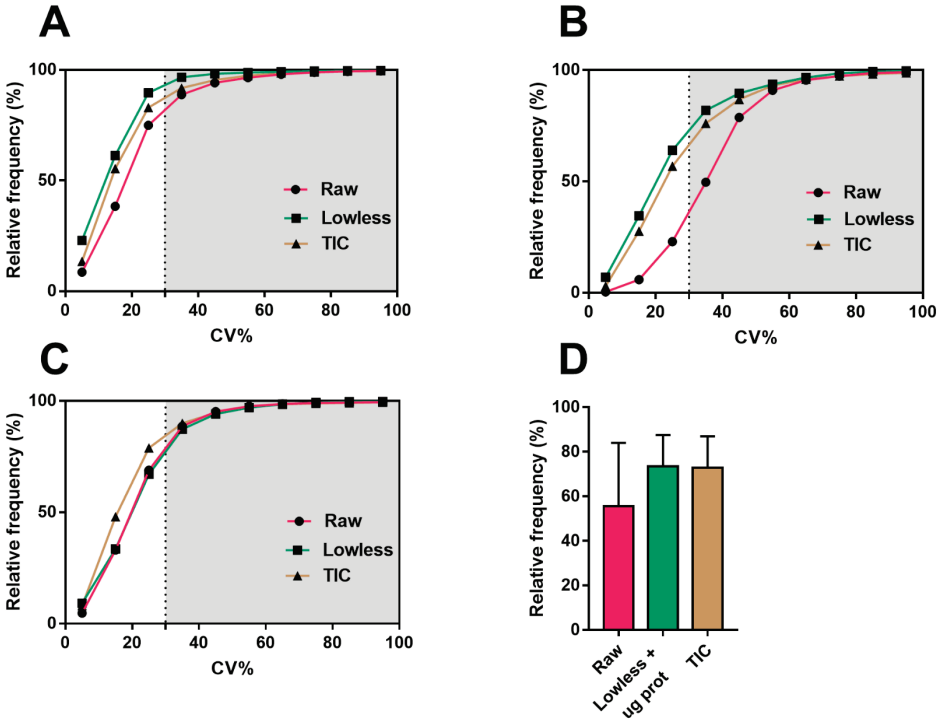

Figure 13. Cumulative frequency distribution of CVs % in (**A**) QC samples, (**B**) healthy HBE and (**C**) CF cells collected from both polarities for the evaluation of the various normalization protocols. The dotted line shows the separation within 30% of the CV between features, which is intended to be the maximum permissible for the validation purpose. The white area indicates features with acceptable CV%, and the gray area designates those above the maximum permitted. (**D**) Graphs display the mean ± SD of the percentage of validated features between the different normalization techniques. No statistical differences was found between TIC and Lowess.

4.2.3 Lipids abnormalities in Cystic Fibrosis cell model

A substantial general accumulation of all lipid species, in particular ceramides, hexosylceramides, lactosylceramides, GM3, and cholesterol esters, has been found in CF (Figure 14) [86,178]. Furthermore, it was found that ether-linked phospholipids (etherPL) were highly modulated by the disease. Specifically, the

most abundant class recognised in our cell model is ether-linked phosphatidylcholine (fold-change CF/H: 14.56), followed by ether-linked phosphatidylethanolamine (fold-change CF/H: 4.75). The concentrations of free fatty acids, dihydroceramides, sphingomyelins, phosphatidylcholines, phosphatidylinositols, sphingosine, free cholesterol, acylglycerols, cardiolipins, and acylcarnitines did not show any statistical differences.

In order to select relevant lipids for cellular phenotype discrimination, univariate and multivariate statistical approaches were employed. Volcano Plot Analysis highlighted n. 632 lipids (81.3% elevated and 18.7 % decreased in CF vs healthy) with a fold-change > 2 and a corrected p-value < 0.05 at the same time (Figure 15).Chemometric analysis by supervised PLS-DA (Figure 17, panel A) was then used to enhance the group separation and to evaluate significant lipids that change, with a VIP value of >1, in CF phenotype, which were n.709. Since PLS-DA tends to overfit results, the Leave-one-out cross-validation method (LOOCV) was used to estimate R2 and Q2 that assessed at 0.96 and 0.94, respectively [185].

Among the discriminating lipids, there was a high prevalence of etherPL, cholesterol esters, and sphingolipids (particularly hexosyl and lactosyl ceramides). Future validation of the identified biomarkers is highly suggested, likely with a high number of primary cells coming from different patients. The altered lipid composition was also reflected in the different lipid ontologies, which are lipid structure, cellular compartment, chemical, and physical properties (Figure 16). The enrichment analysis revealed a highly important modification in the lipids involved in the composition of cell membranes. In CF versus healthy cells, the lipids in the endoplasmic reticulum and mitochondrial compartments are greatly modified. Finally, changes in chemical and biophysical properties reflect these lipid alterations, specifically affecting chain lengths, saturation, and ether-bound glycerol structure- and sphingo- lipids. We observed a quantitative rise in CF levels of saturated and monounsaturated fatty acids (SFAs and MUFAs), while the polyunsaturated species (PUFAs) were unchanged (Figure 14). Otherwise, the percentual prevalence of PUFAs was found elevated in the subgroup of the top-100 discriminant lipids (Figure 5B) as well as the prevalence of ether-PL over ester-bound phospholipids (Figure 5C).

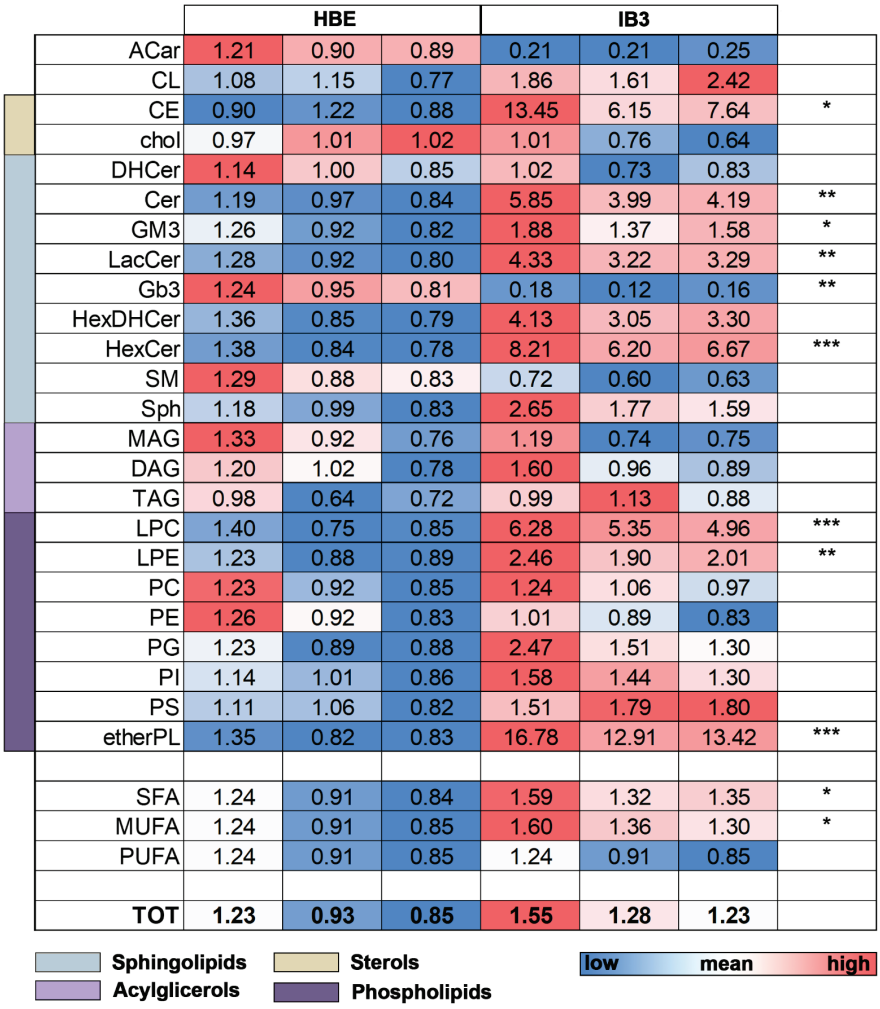

Figure 14. Heatmap shows the alteration in lipid profile in CF immortalized cell model (HBE vs. IB3). The color scale differentiates values from low (blue) to high (red) per each row, passing through the baseline (white). Values are normalized against the control mean. Statistical differences were evaluated by unpaired t-test.

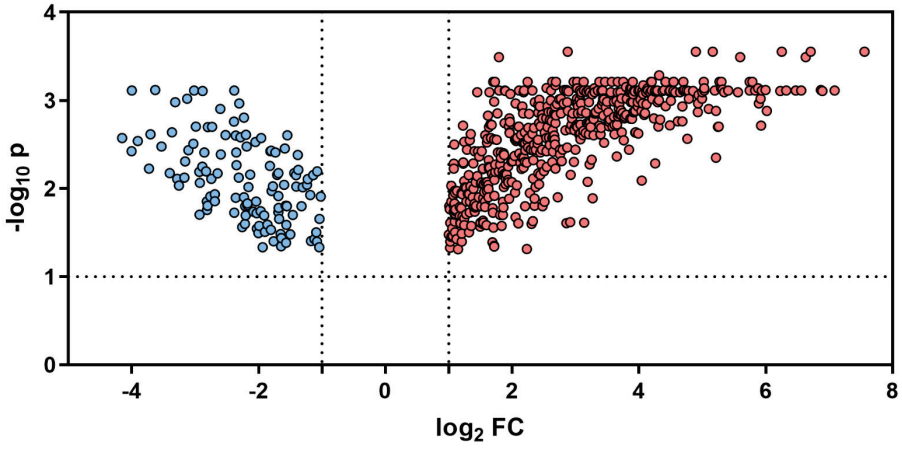

Figure 15. Volcano Plot Analysis highlighted n. 632 lipids correlated with CF with a fold-change > 2 and a corrected p-value < 0.05 at the same time. The 81.3% of lipids are elevated (red) and 18.7 % decreased (blue) in CF vs healthy.

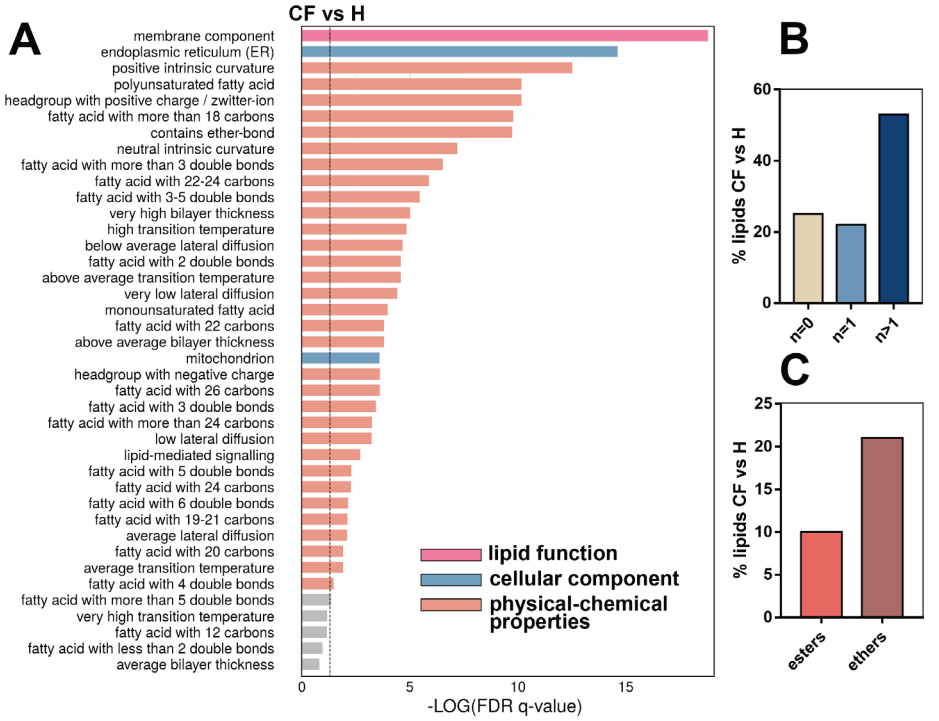

Figure 16. (**A**) Enrichment analysis (top-40) of CF phenotype against control. The cut-off value of essential enrichments ($q < 0.05$) is shown by the dotted line. Bar length is correlated with enrichment (-log q-values corrected for false discovery rate, FDR), while colors suggest lipid function, physical-chemical properties, and cellular components. (**B**) The distributions, in top-100 discriminant lipid group, of (**B**) the acyl chain unsaturation from all lipid fraction (%) and (**C**) the ester and ether linkages in phospholipids in CF vs. H. In (**B**) Chi-square test and in (**C**) binomial test revealed a p-value<0.05.

4.2.4 Lipids abnormalities in Cystic Fibrosis patients derived cells

The general lipid accumulation found in immortalized cell models was not totally reflected in the patient-derived primary broncho-epithelial cells, for the intrinsic inter-individual biological differences. The lipidome differences in the immortalized cell model were visualized by PLS-DA and estimated on the first component 74% and also in patient-derived primary cells at about 34% (Figure 17, panel B).

In particular, we evidenced a significant increase (Figure 18) in the content of pro-inflammatory ceramides (fold-change 1.64) and in the cholesterol esters (fold-change 7).

The lipid profile of apical membrane fractions from human primary bronchial epithelial cells was investigated. By radioactivity assays, the authors found a rise in ceramides, glucosylceramides, gangliosides, but no change was verified in the content of sphingomyelins and phosphatidylethanolamine [140].

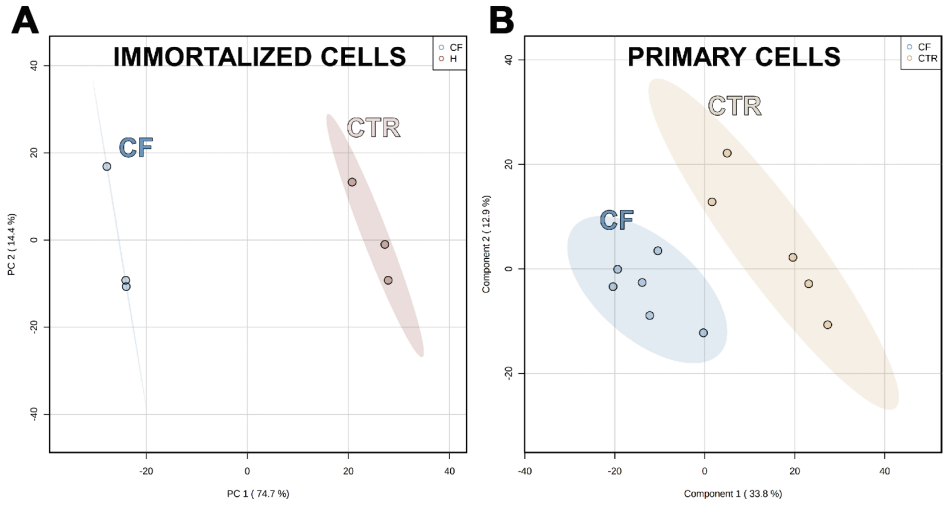

Figure 17. Partial least squares discriminant analysis (PLS-DA) significantly differentiate the CF and healthy phenotypes in both immortalized cell model (**A**) and also in patient-derived primary cells (**B**) at about 75% and 34%, respectively.

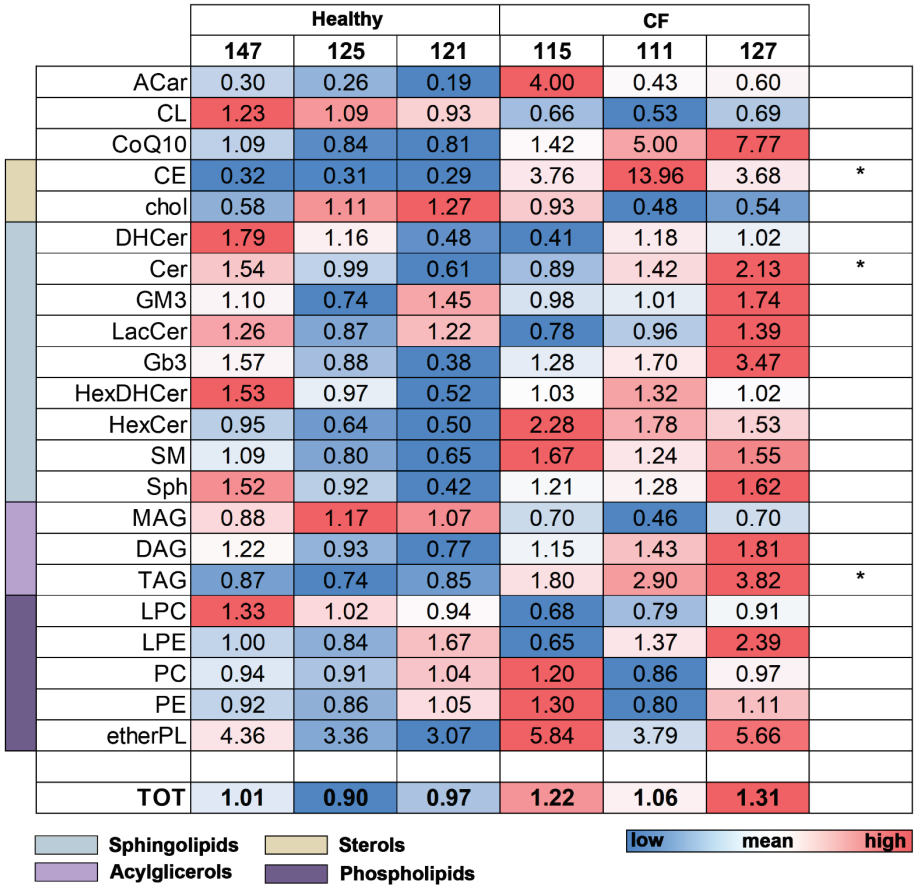

Figure 18. Heatmap shows the alteration in lipid profile in patients derived broncho-epithelial cells (healthy vs. CF). The color scale differentiates values from low (blue) to high (red) per each row, passing through the baseline (white). Values are normalized against the control mean. Statistical differences were evaluated by unpaired t-test.

4.3 In-vitro myriocin treatment for restoring lipid imbalances

4.3.1 Myriocin effect on immortalized CF cell model

Myr blocks ceramide and sphingolipid de novo biosynthesis acting on serine palmitoyltransferase. We compared the effect of Myr administration on the content of different lipid species in healthy and CF cells. As already mentioned, sphingolipids - including ceramides (Cer), glycosphingolipids (HexCer), and sphingomyelins (SM)- glycerophospholipids - especially phosphatidylcholine (PC)- triacylglycerols (TAG) and cholesterol esters (CE) are significantly higher in CF cells (Figures 19-21). We found that Myr not only directly decreases the content of sphingolipids, but it also decreases the phospholipids (PC, and phosphatidylethanolamine, PE), lysophosphatidylcholine (LPC), TAG, and cholesterol esters (CE). Therefore, the inhibition of the biosynthesis of sphingolipids induces a generalized depletion of various groups of cellular lipids. CF shows a substantial increase (+70%) in the total amount of lipids that can be diminished by the treatment with Myriocin (-60%), which attempts to restore physiological conditions (Figure 22).

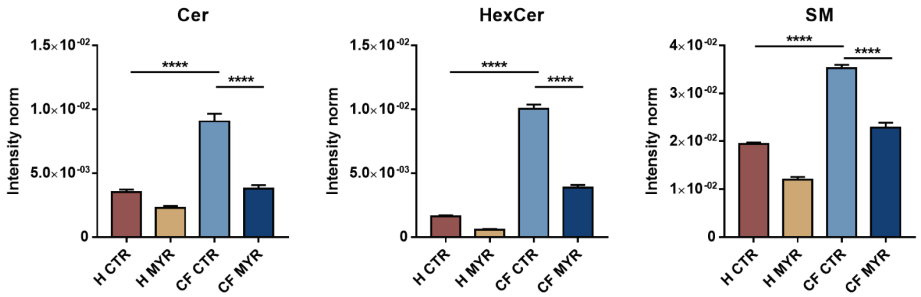

Figure 19. Myriocin by the inhibition of serine-palmitoyl transferase diminish de-novo sphingolipids synthesis and their levels. Statistical differences were evaluated by one-way ANOVA coupled with Bonferroni post-hoc test. Cer: ceramide, HexCer: hexosylceramide and SM: sphingomyelin.

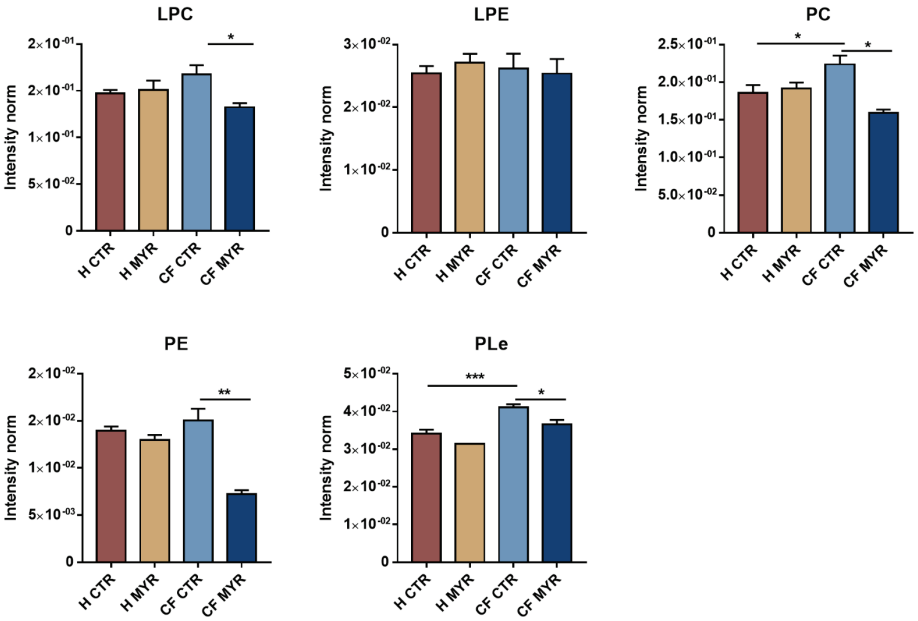

Figure 20. Myriocin effect on phospholipids levels. Statistical differences were evaluated by one-way ANOVA coupled with Bonferroni post-hoc test. LPC: lyso-phosphatidylcholine; LPE: lyso-phosphatidylethanolamine; PC: phosphatidylcholine; PC: phosphatidylethanolamine; PLe: ether-linked phospholipids.

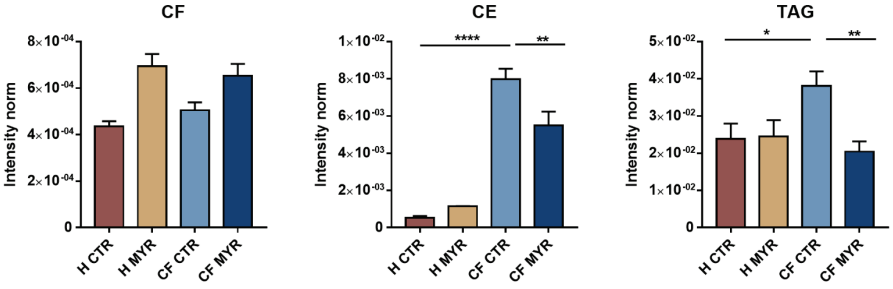

Figure 21. Myriocin effect on storage lipids levels. Statistical differences were evaluated by one-way ANOVA coupled with Bonferroni post-hoc test. CF: cholesterol free; CE: cholesteryl ester; TAG: triacylglycerol.

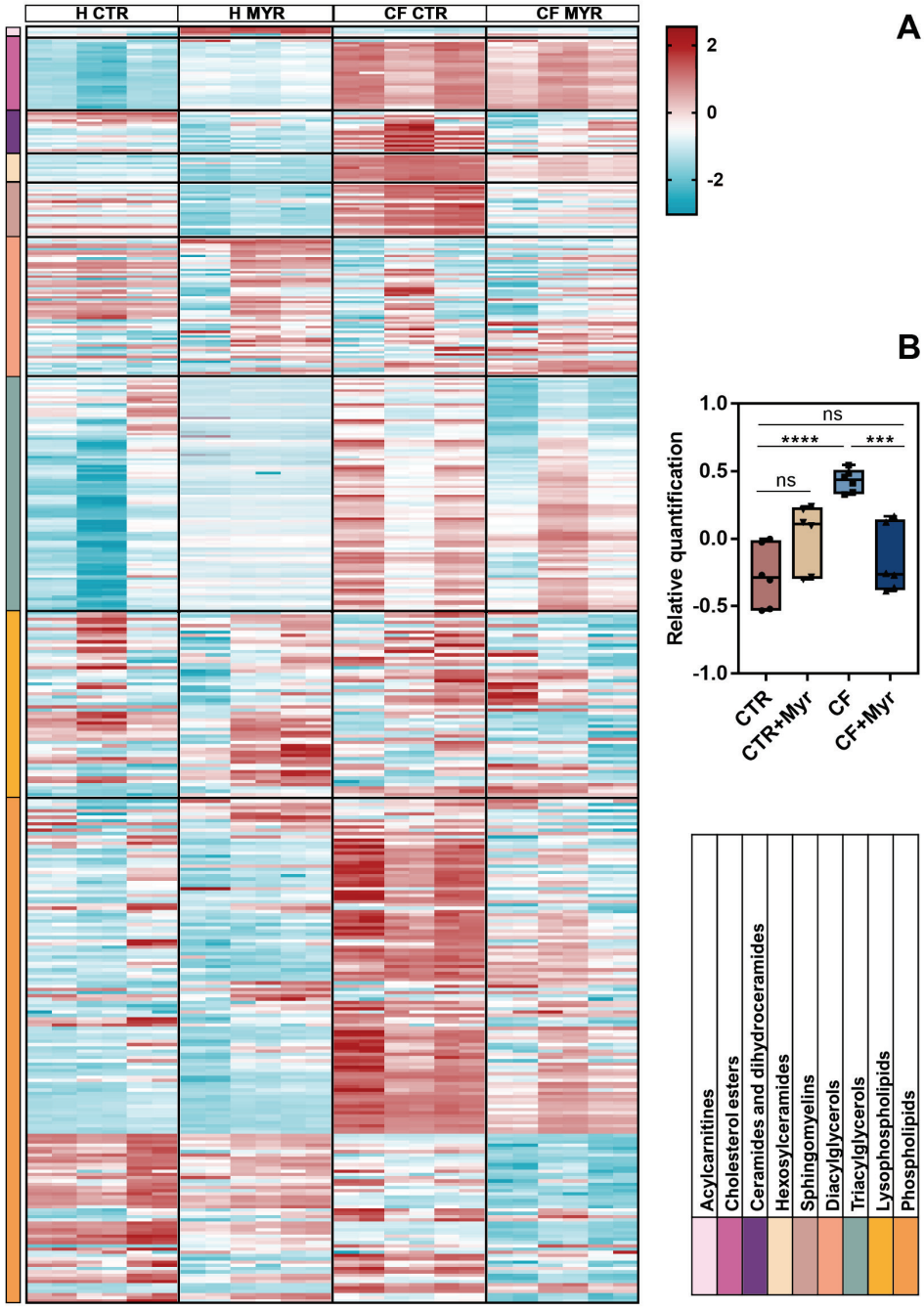

Caption next page

Figure 22. (**A**) Heatmap of the entire lipidome in immortalized cell models (n=625 species) divided per lipid class. Features were log-transformed and auto-scaled for visualization. The color-scale differentiates values as high (red), mid (white), and low (blue). (**B**) Relative quantification of all the lipids identified in cell pellets (n=6 for each class). Boxplots are defined with the first and third quartiles (25th and 75th percentile) for lower and upper hinges, mix-max for the length of the whiskers, and median for the middle-line. Statistical significance was investigated by unpaired one-way ANOVA with Bonferroni post-hoc test.

It was evidenced that there is an accumulation of diffuse lipids in the CF cells and a diminished capacity to form compartmentalized lipid droplets. We labelled neutral lipids in CF and healthy cells in order to understand the role of Myr in lipid mobilization and catabolism. Myr was able to significantly reduce lipids in CF but not in control cells (Figure 23). Myr is a well-known sphingolipid synthesis inhibitor and is also capable of decreasing the content of several lipid species in CF epithelial cells. Moreover, we investigated the effects of Myr on de novo lipid biosynthesis. In this way, cells were labelled with a fluorescent derivate of lauric acid, which is integrated into lipid, especially into phospholipids (Figure 23).

In relation to healthy cells, we found an elevated amount of new synthesized fatty acids in CF. Second, we found that treatment with Myr induced a foremost reduction in fluorescence in CF cells. The evidence mentioned above indicates that Myr effects may be mediated by its ability to restrain lipid synthesis while increasing lipid catabolism and oxidation.

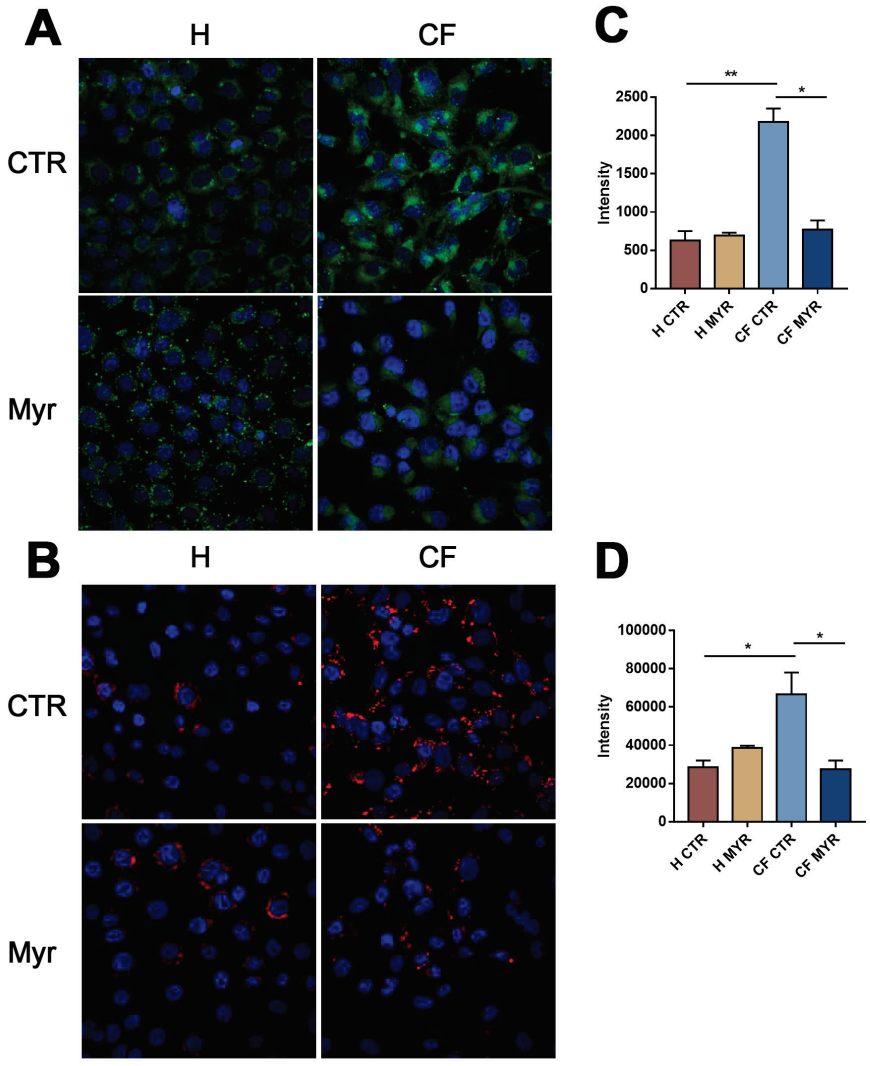

Figure 23. (**A**) Confocal immunofluorescent images displaying intracellular lipid aggregate (green) in CF (IB3) and healthy (H, HBE) broncho epithelial cells, either treated or not with 50 μM Myriocin 24 hours. (**B**) Confocal immunofluorescent images displaying de novo synthesized fatty acids (red) in CF (IB3) and healthy (H, HBE) broncho epithelial cells, either treated or not with 50 μM Myriocin 24 hours In both panel **A** and **B** DAPI (blue) was used for nuclear counterstaining. The fluorescence intensity was recorded and depicted as histograms for intracellular neutral lipids aggregate (**C**) and de novo synthesized fatty acids (**D**). Data are presented as means ± SEM (* $p<0.05$; ** $p<0.01$); one way ANOVA test followed by Bonferroni correction was used.

4.3.1 Myriocin effect on patient-derived primary CF cell

The effect of Myr in patient-derived broncho-epithelial cells is principally relegated to its direct activity against sphingolipids (Figures 24-26). Some tendencies can be found, even if not significant, on the reduction of neutral storage lipids such as TAG (-20%) and CE (-82%). The whole lipidome seems to be not modified by myriocin but is quantitatively altered in the sphingolipids levels (Figure 27).

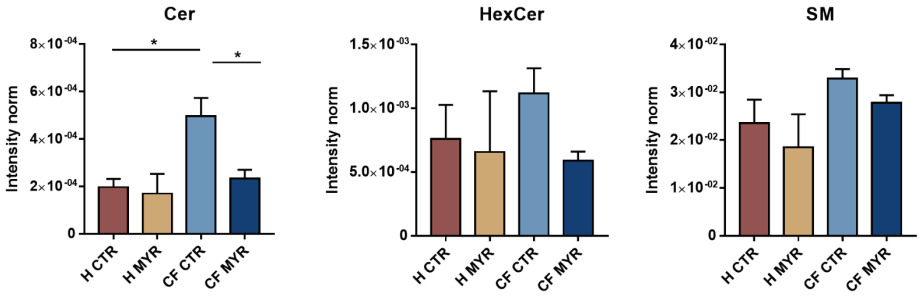

Figure 24. Myriocin by the inhibition of serine-palmitoyl transferase diminish de-novo sphingolipids synthesis and their levels in patient-derived primary cells. Statistical differences were evaluated by one-way ANOVA coupled with Bonferroni post-hoc test. Cer: ceramide, HexCer: hexosylceramide and SM: sphingomyelin.

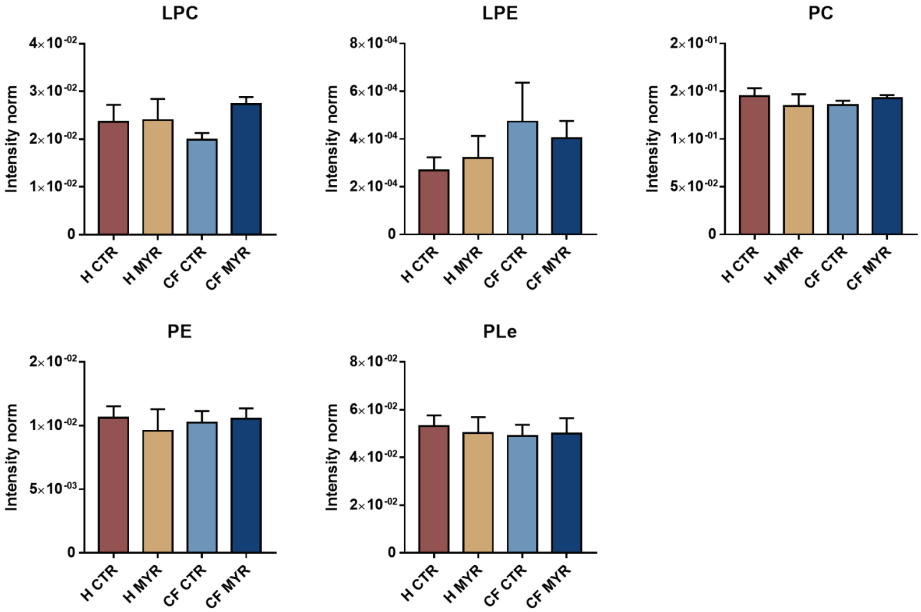

Figure 25. Myriocin effect on phospholipids levels in patient-derived primary cells. Statistical differences were evaluated by one-way ANOVA coupled with Bonferroni post-hoc test. LPC: lyso-phosphatidylcholine; LPE: lyso-phosphatidylethanolamine; PC: phosphatidylcholine; PC: phosphatidylethanolamine; PLe: ether-linked phospholipids.

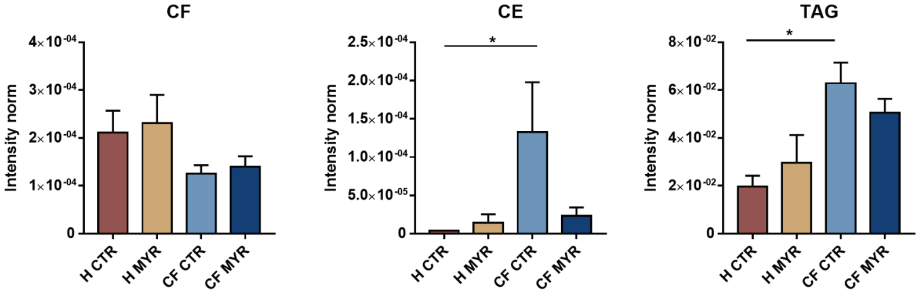

Figure 26. Myriocin effect on storage lipids levels in patient-derived primary cells. Statistical differences were evaluated by one-way ANOVA coupled with Bonferroni post-hoc test. CF: cholesterol free; CE: cholesteryl ester; TAG: triacylglycerol.

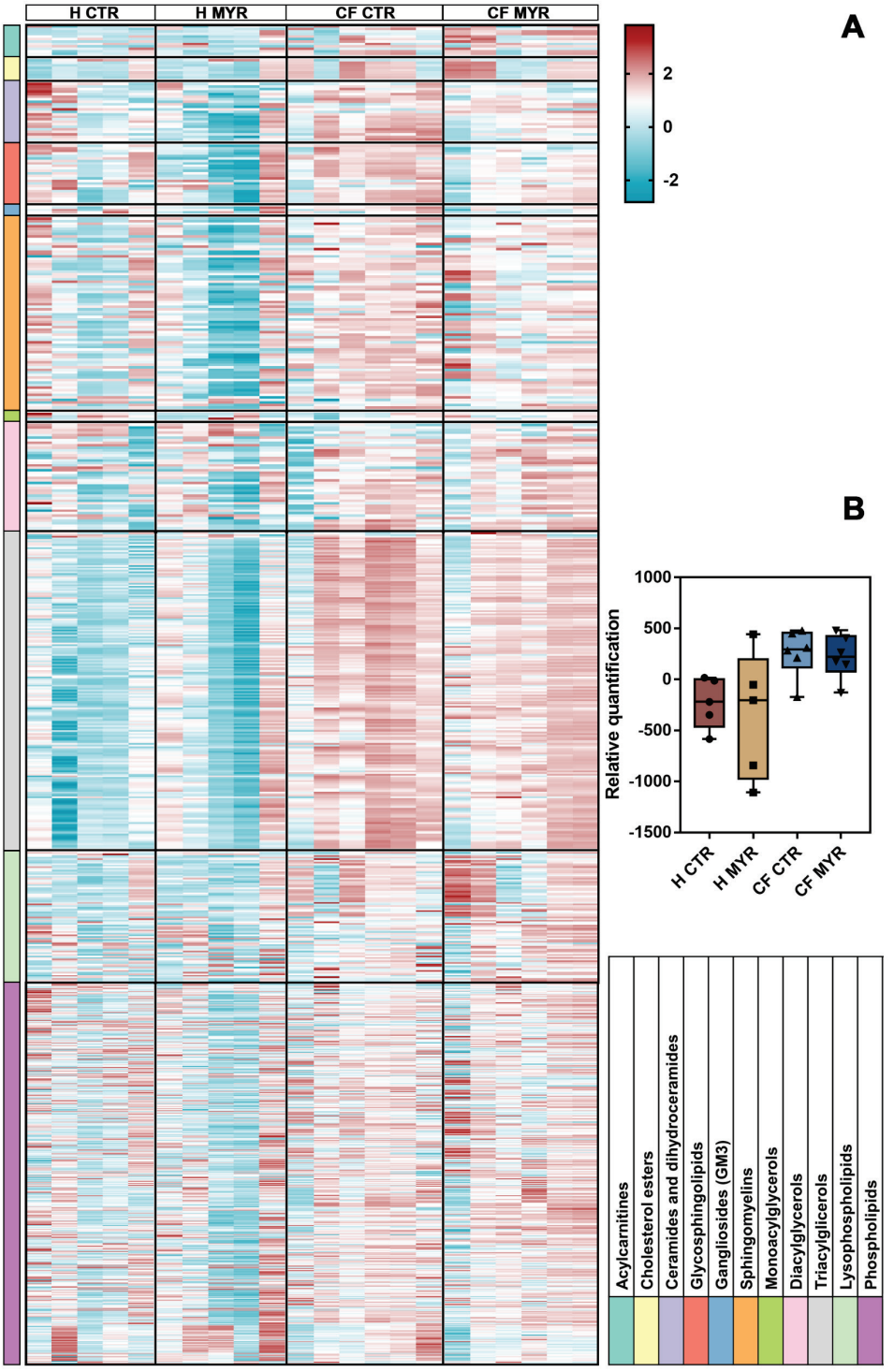

Caption next page

Figure 27. (**A**) Heatmap of the entire lipidome in patient-derived primary cells (n=893 species) divided per lipid class. Features were log-transformed and auto-scaled for visualization. The color-scale differentiates values as high (red), mid (white), and low (blue). (**B**) Relative quantification of all the lipids identified in cell pellets (n=6 for each class). Boxplots are defined with the first and third quartiles (25th and 75th percentile) for lower and upper hinges, mix-max for the length of the whiskers, and median for the middle-line. No statistical significance was found by unpaired one-way ANOVA with Bonferroni post-hoc test.

5. DISCUSSION

The effect of lipid deposition may reflect an important insight into CFTR pathophysiology and therapeutic outcomes by current modulator therapy [144].

Firstly, our research focuses on assessing whether the inflammatory chronic state that characterizes CF can be affected by MSCs and their secreted EVs. We obtain an in vitro cellular model of CF-MSC by treating control human lung MSCs with a particular CFTR inhibitor (I-172) to obtain CF-EVs that imitate those physiologically released in the lung of the CF patient.

IB3, immortalized human bronchial epithelial cell line from a CF patient (ΔF508/W1282X), was used to acquire the basal inflammatory CF phenotype and compared the anti-inflammatory ability of CF-EVs with the control EVs. The persistent chronic inflammatory status in CF is uncontested, even if the scientific community keep asking themselves if inflammation is part of the disease or a reaction to the genetic defect in CF [186,187].

It was demonstrated that EVs from control MSCs discharged the pro-inflammatory profile of IB3 cells by reducing the expression of cytokines and relieving the transcription of PPARΔ, which is highly inflammatory in anti-inflammatory pathways (data not shown). On the other hand, CF-EVs supplementation is less effective on both cytokines and PPARΔ expression, providing a rationale for the basal physiological inflammatory phenotype [171].

MSCs were previously recognized as an effective candidate for the treatment of chronic infection and inflammation-related diseases by secrete anti-inflammatory (i.e, increase in IL-6 and CCL2 expression, while decreasing IL-8 expression) and antimicrobial (i.e, chemokine CCL20) mediators. These mediators could redefine the function of the tissue, improving the recruitment of macrophages that can be involved in immunosurveillance [188,189].

In addition, MSCs secretoma could confine lung injury and prevent fibrosis [190]. In our model, the substantial accumulation of both Cer and dhCer species in CF-EVs suggests an active secretion of signalling lipids. Moreover, Cer-enriched exosomes have been reported to mediate cytotoxic effects in recipient cells by stimulating cytokine-induced cell death [191]. Thus, we speculate that inflammation could trigger Cer *de novo* synthesis and accumulation [84,85]

that can be released during the exocytosis of new generated vesicles, which disperse a paracrine inflammatory signal.

Altered lipid homeostasis, consisting of inflammatory ceramide accumulation in the lung, sterol accumulation in the airways, hepatic steatosis and plasma dyslipidemia, is associated with CFTR deficiency [120,192–196]. We aimed to validate the untargeted lipidomics approach by the application to an immortalized CF cell line (IB3). Secondly, the mentioned lipid modifications are confirmed and potentially associated with CF signatures. This is a challenging task that can be accomplished only by combining multidisciplinary research branches such as proteomics, transcriptomics, and metabolomics [192].

The first evidence is that ceramide and glycosphingolipids accumulate in CF epithelial cells such as hexosylceramides, lactosylceramides, and GM3. Ceramides are involved in inflammation [197,198], and their levels accrual has been seen previously by us and others in CF models [85,139,147,199]. The importance of Cer in the pathophysiological alterations found in CF also lies on the evidence, that even without lung infection, its concentrations are increased and mediate inflammation and cell death [200].

Notably, we establish a substantial rise in hexosylceramides, while poorly characterized so far, hexosylceramide accretion has been shown to worsen inflammation [34,201], and its synthesis was demonstrated to be increased in damaged tissues [202]. Glycosylated ceramides induce the release of mediators of inflammation such as MIP-1β, TNF-α, MCP-1 and IL-6 in atherosclerosis plaque and vascular smooth muscle apoptosis [203]. In addition, oxidative stress and inflammatory pathway promotion could be driven by hexosylceramides, which can bind either glucose or galactose to ceramide, and lactosylceramides [204].

In order to reduce its accrual and associated inflammatory responses, we speculate that CF cells could increase ceramide glycosylation, which is also improved in tumour metabolism [205].

Another lipid marker of inflammation are LPC, which is augmented in CF broncho-epithelial cells and were seen to increase during chronic inflammation [21,22,206]. This accumulation can be associated with the increased activity of

Phospholipase A2, that catalyses the hydrolysis of fatty acid from the glycerol of PC generating LPC [206].

Besides, we measure a substantial increase in lipid storage, such as cholesterol esters. This may be linked, as previously described, to the inflammatory status associated with intracellular lipids clumping and to altered lipids intracellular traffic. These data are consistent with documented evidence of cholesterol accumulation in CF bronchi [119,121,207] and, most prominently, with elevated cholesterol esters concentrations in bronchoalveolar lavage fluid in pediatric CF patients [138,208]. Cholesterol synthesis aberrations are related to mutated CFTR cells and consisted of a defective in endosomal/lysosomal storage, high cholesterol content in the plasma membrane [119]. Such biochemical changes could maintain chronic inflammation and inadequate infection response [84,209].

It was also noted a large rise in etherPL, which are characterized by ether bond between glycerol and the fatty acid in position *sn-1*. They are important regulators of membrane fluidity, and their modification can be somehow linked to the abnormal CFTR membrane composition [210,211]. Their incremented deposition was also evidenced in human CF bronchoalveolar lavage fluid [206] and could be a reaction to boost membrane stability [212].

Our theories raise new concerns regarding the pathophysiological function of lipids and calls for more studies to establish novel biomarkers for inflammatory disorders and possible therapeutic targets. We firmly agree that our results require further validation, using numerous patients-derived primary cell or directly lung biopsies. The first set of patient-derived primary cells - here presented - displayed an accumulation of ceramide and storage lipids. However, it can be considered just a preliminary experiment, and we need to investigate further.

Myr has been widely used as therapeutic agent by inhibiting the sphingolipids synthesisand thus their abnormal accrual. Currently, it is tested in pre-clinical trials for the treatment of multiple diseases, including retinitis pigmentosa [76,77], myocardial infarction [78–80], atherosclerosis [81], fatty liver disease [82] and cystic fibrosis [83–86]. Our group previously demonstrated the benefits of Myr treatment in CF murine and cell models, which decreased systemic inflammation and promoted the removal of fungi

and bacteria in the lungs [75,84,85]. In line with the literature documenting peripheral tissue lipid aggregation in CF, we shown that CF bronchial epithelial cells are enriched in most systemic lipid species and also their metabolism and organisation are disrupted [86,178]. The accumulation of lipids can be the result of impaired lipid trafficking in the cell and might be responsible for blocking the ER-Golgi network, exacerbating the ROS production and inflammation in CF [86]. In CF cell line, the intracellular lipid concentrations were greatly decreased by Myr treatment. A clear decline was evidenced in the class of storage lipid, such as cholesterol esters and triacylglycerols, and in ceramides, which drive inflammatory responses. Another evidence was that healthy cells were only modestly affected by the Myr treatment. It suggests that Myr works mainly on CF specific lipid alterations.

6. CONCLUSION

The CFTR dysfunction leads to increased lipid metabolism and subsequent deposition of a broad span of lipids, especially the pro-inflammatory sphingolipids. This thesis suggests, more specifically, that:

1. The substantial accumulation of both Cer and DhCer species in CF-EVs suggests an active secretion of signalling lipids. We speculate that cells inflammation could trigger Cer *de novo* synthesis and accumulation that can be released during the exocytosis of newly generated vesicles, which disperse a paracrine inflammatory signal.
2. We validate an untargeted lipidomics approach based on high-resolution mass spectrometry by applying it to an immortalized CF cell line. This way, we demonstrate the involvement of bioactive lipids in CF pathophysiology. Specifically, we evidence a substantial general accumulation of all lipid species: ceramides, hexosylceramides, lactosylceramides, GM3, and cholesterol esters.
3. In a cell model of CF the intracellular lipid concentrations were significantly decreased by the treatment with Myr, a well-known sphingolipid inhibitor. An evident decline was evidenced in the class of storage lipid, such as cholesterol esters and triacylglycerols, and obviously in ceramides, which drive inflammatory responses. This suggests a possible pharmacological application of Myr thanks to its ability to restrain lipid synthesis while increasing lipids catabolism and oxidation.

ACKNOWLEDGMENTS

I would like to thank my mentors, Prof. Riccardo Ghidoni, Prof.Rita Paroni and Prof. Gabriella Roda, for their guidance throughout the project and for being those who have always believed in me. No scientific work could be accomplished without the contribution of Prof. Anna Caretti, Prof. Michele Samaja, Prof. Paola Signorelli, whom I would sincerely like to thank.

This PhD thesis was evaluated by four independent reviewers which I really want to thank for the excellent feedback and the valuable help: Prof. Elisabetta Albi, Professor in Biochemistry, Department of Pharmaceutical Sciences, University of Perugia (IT); Prof. Gemma Fabrias, Professor in Chemistry, Institute for Advanced Chemistry of Catalonia – Spanish Council for Scientific Research (IQAC-CSIC)/Department of Biological Chemistry; Dr. Laura Gatti, Professor in Biochemistry, Applied Biology, Clinical Neurosciences Department, Cerebrovascular Diseases, Unit Fondazione IRCCS Istituto Neurologico "Carlo Besta", Milano (IT); Dr. Vittorio Maglione, Professor in Biochemistry, IRCCS Neuromed, Isernia (IT).

REFERENCES

[1] S. Chapman, G. Robinson, J. Stradling, S. West, J. Wrightson, Oxford Handbook of Respiratory Medicine, Oxford University Press, 2014. doi:10.1093/med/9780198703860.001.0001.

[2] C. Bergeron, A.M. Cantin, Cystic Fibrosis: Pathophysiology of Lung Disease, Semin. Respir. Crit. Care Med. (2019) 40, 715–726. doi:10.1055/s-0039-1694021.

[3] F. Ratjen, G. Döring, Cystic fibrosis, Lancet. (2003) 361, 681–689. doi:10.1016/S0140-6736(03)12567-6.

[4] M.M. Rafeeq, H.A.S. Murad, Cystic fibrosis: Current therapeutic targets and future approaches, J. Transl. Med. (2017) 15, 84. doi:10.1186/s12967-017-1193-9.

[5] A. Hamosh, S.C. FitzSimmons, J. Macek M., M.R. Knowles, B.J. Rosenstein, G.R. Cutting, Comparison of the clinical manifestations of cystic fibrosis in black and white patients, J. Pediatr. (1998) 132, 255–259. doi:10.1016/S0022-3476(98)70441-X.

[6] M.P. Boyle, K. De Boeck, A new era in the treatment of cystic fibrosis: Correction of the underlying CFTR defect, Lancet Respir. Med. (2013) 1, 158–163. doi:10.1016/S2213-2600(12)70057-7.

[7] K. De Boeck, F. Vermeulen, L. Dupont, The diagnosis of cystic fibrosis, Press. Medicale. (2017) 46, e97–e108. doi:10.1016/j.lpm.2017.04.010.

[8] G. Villanueva, G. Marceniuk, M.S. Murphy, M. Walshaw, R. Cosulich, Diagnosis and management of cystic fibrosis: summary of NICE guidance, BMJ. (2017) 359, j4574. doi:10.1136/bmj.j4574.

[9] J.M. Littlewood, A. Bevan, G. Connett, S. Conway, J. Govan, M. Hodson, Antibiotic treatment for cystic fibrosis: report of the UK Cystic Fibrosis Trust Antibiotic Group, UK Cyst. Fibros. Trust. (2009) 1–50.

[10] W.W. Christie, F.B. Jungalwala, High-performance liquid chromatography and lipids: A practical guide, Pergamon Press, Oxford, 1990. doi:10.1016/0009-3084(90)90051-R.

[11] E. Fahy, S. Subramaniam, H.A. Brown, C.K. Glass, A.H. Merrill, R.C. Murphy, C.R.H.H. Raetz, D.W. Russell, Y. Seyama, W. Shaw, T. Shimizu, F. Spener, G. Van Meer, M.S. VanNieuwenhze, S.H. White, J.L. Witztum, E.A. Dennis, A comprehensive classification system for lipids, J. Lipid Res. (2005) 46, 839–862. doi:10.1194/jlr.E400004-JLR200.

[12] G. Van Meer, D.R. Voelker, G.W. Feigenson, Membrane lipids: Where they are and how they behave, Nat. Rev. Mol. Cell Biol. (2008) 9, 112–124. doi:10.1038/nrm2330.

[13] D. Casares, P. V. Escribá, C.A. Rosselló, Membrane Lipid Composition: Effect on Membrane and Organelle Structure, Function and Compartmentalization and Therapeutic Avenues, Int. J. Mol. Sci. (2019) 20, 2167. doi:10.3390/ijms20092167.

[14] N.D. Ridgway, R.S. McLeod, Biochemistry of Lipids, Lipoproteins and Membranes: Sixth Edition, 2015. doi:10.1016/c2013-0-18457-7.

[15] R.B. Gennis, The Structures and Properties of Membrane Lipids, in: 1989: pp. 36–84. doi:10.1007/978-1-4757-2065-5_2.

[16] A. Trostchansky, H. Rubbo, Bioactive Lipids in Health and Disease, Springer International Publishing, Cham, 2019. doi:10.1007/978-3-030-11488-6.

[17] A.Z. Fernandis, M.R. Wenk, Membrane lipids as signaling molecules, Curr. Opin. Lipidol. (2007) 18, 121–128. doi:10.1097/MOL.0b013e328082e4d5.

[18] K. V Honn, D.C.Z. Editors, The Role of Bioactive Lipids in Cancer , Infl ammation and Related Diseases, 2019.

[19] M.D. Cas, G. Roda, F. Li, F. Secundo, Functional lipids in autoimmune inflammatory diseases, Int. J. Mol. Sci. (2020) 21, 1–19. doi:10.3390/ijms21093074.

[20] D.W. Gilroy, D. Bishop-Bailey, Lipid mediators in immune regulation and resolution, Br. J. Pharmacol. (2019) 1009–1023. doi:10.1111/bph.14587.

[21] A.D. Tselepis, M.J. Chapman, Inflammation, bioactive lipids and atherosclerosis: Potential roles of a lipoprotein-associated phospholipase A2, platelet activating factor-acetylhydrolase, Atheroscler. Suppl. (2002) 3, 57–68. doi:10.1016/S1567-5688(02)00045-4.

[22] V. Chiurchiù, A. Leuti, M. Maccarrone, Bioactive lipids and chronic inflammation: Managing the fire within, Front. Immunol. (2018) 9, 38. doi:10.3389/fimmu.2018.00038.

[23] E. Leishman, P.E. Kunkler, J.H. Hurley, S. Miller, H.B. Bradshaw, Bioactive Lipids in Cancer, Inflammation and Related Diseases, Switzerland, 2019. doi:10.1007/978-3-030-21735-8_16.

[24] E.A. Dennis, P.C. Norris, Eicosanoid storm in infection and inflammation, Nat. Rev. Immunol. (2015) 15, 511–523. doi:10.1038/nri3859.

[25] W.L. Smith, D.L. DeWitt, R.M. Garavito, Cyclooxygenases: Structural, Cellular, and Molecular Biology, Annu. Rev. Biochem. (2000) 69, 145–182. doi:10.1146/annurev.biochem.69.1.145.

[26] M.C. Basil, B.D. Levy, Specialized pro-resolving mediators: Endogenous regulators of infection and inflammation, Nat. Rev. Immunol. (2016) 16, 51–67. doi:10.1038/nri.2015.4.

[27] T. Aoki, S. Narumiya, Prostaglandins and chronic inflammation, Trends Pharmacol. Sci. (2012) 33, 304–11. doi:10.1016/j.tips.2012.02.004.

[28] T. Honda, E. Segi-Nishida, Y. Miyachi, S. Narumiya, Prostacyclin-IP signaling and prostaglandin E2-EP2/EP4 signaling both mediate joint inflammation in mouse collagen-induced arthritis, J. Exp. Med. (2006) 203, 325–35. doi:10.1084/jem.20051310.

[29] T. Hirata, S. Narumiya, Prostanoids as Regulators of Innate and Adaptive Immunity, Adv. Immunol. (2012) 116, 143–174. doi:10.1016/B978-0-12-394300-2.00005-3.

[30] C. Yao, D. Sakata, Y. Esaki, Y. Li, T. Matsuoka, K. Kuroiwa, Y. Sugimoto, S. Narumiya, Prostaglandin E2-EP4 signaling promotes immune inflammation through TH1 cell differentiation and TH17 cell expansion, Nat. Med. (2009) 15, 633–40. doi:10.1038/nm.1968.

[31] S.J. Burke, J.J. Collier, The gene encoding cyclooxygenase-2 is regulated by IL-1β and prostaglandins in 832/13 rat insulinoma cells, Cell. Immunol. (2011) 271, 379–84. doi:10.1016/j.cellimm.2011.08.004.

[32] T. Hu, C. Tie, Z. Wang, J.L. Zhang, Highly sensitive and specific derivatization strategy to profile and quantitate eicosanoids by UPLC-MS/MS, Anal. Chim. Acta. (2017) 950, 108–118. doi:10.1016/j.aca.2016.10.046.

[33] A.A. Spector, X. Fang, G.D. Snyder, N.L. Weintraub, Epoxyeicosatrienoic acids (EETs): Metabolism and biochemical function, Prog. Lipid Res. (2004) 43, 55–90. doi:10.1016/S0163-7827(03)00049-3.

[34] Y.A. Hannun, L.M. Obeid, Sphingolipids and their metabolism in physiology and disease, Nat. Rev. Mol. Cell Biol. (2018) 19, 175–191. doi:10.1038/nrm.2017.107.

[35] L.J. Siskind, T.D. Mullen, K.R. Rosales, C.J. Clarke, M.J. Hernandez-Corbacho, A.L. Edinger, L.M. Obeid, The BCL-2 protein BAK is required for long-chain ceramide generation during apoptosis, J. Biol. Chem. (2010) 285, 11818–26. doi:10.1074/jbc.M109.078121.

[36] T.D. Mullen, R.W. Jenkins, C.J. Clarke, J. Bielawski, Y.A. Hannun, L.M. Obeid, Ceramide synthase-dependent ceramide generation and programmed cell death: Involvement of salvage pathway in regulating postmitochondrial events, J. Biol. Chem. (2011) 286, 15929–42. doi:10.1074/jbc.M111.230870.

[37] M. Kohno, M. Momoi, M.L. Oo, J.-H. Paik, Y.-M. Lee, K. Venkataraman, Y. Ai, A.P. Ristimaki, H. Fyrst, H. Sano, D. Rosenberg, J.D. Saba, R.L. Proia, T. Hla, Intracellular Role for Sphingosine Kinase 1 in Intestinal Adenoma Cell Proliferation, Mol. Cell. Biol. (2006) 26, 7211–23. doi:10.1128/mcb.02341-05.

[38] G. Wang, S.D. Spassieva, E. Bieberich, Ceramide and S1P signaling in embryonic stem cell differentiation, Methods Mol. Biol. (2018) 1697, 153–171. doi:10.1007/7651_2017_43.

[39] S.K. Mishra, Y.G. Gao, Y. Deng, C.E. Chalfant, E.H. Hinchcliffe, R.E. Brown, CPTP: A sphingolipid transfer protein that regulates autophagy and inflammasome activation, Autophagy. (2018) 14, 862–879. doi:10.1080/15548627.2017.1393129.

[40] M. Taniguchi, K. Kitatani, T. Kondo, M. Hashimoto-Nishimura, S. Asano, A. Hayashi, S. Mitsutake, Y. Igarashi, H. Umehara, H. Takeya, J. Kigawa, T. Okazaki, Regulation of autophagy and its associated cell death by "sphingolipid rheostat": Reciprocal role of ceramide and sphingosine 1-phosphate in the mammalian target of rapamycin pathway, J. Biol. Chem. (2012) 287, 39898–910. doi:10.1074/jbc.M112.416552.

[41] Y. Yu, M. Skočaj, M.E. Kreft, N. Resnik, P. Veranič, P. Franceschi, K. Sepčić, G. Guella, Comparative lipidomic study of urothelial cancer models: Association with urothelial cancer cell invasiveness, Mol. Biosyst. (2016) 12, 3266–3279. doi:10.1039/c6mb00477f.

[42] T.H. Beckham, P. Lu, J.C. Cheng, D. Zhao, L.S. Turner, X. Zhang, S. Hoffman, K.E. Armeson, A. Liu, T. Marrison, Y.A. Hannun, X. Liu, Acid ceramidase-mediated production of sphingosine 1-phosphate promotes prostate cancer invasion through upregulation of cathepsin B, Int. J. Cancer. (2012) 131, 2034–43. doi:10.1002/ijc.27480.

[43] A.C. Carreira, A.E. Ventura, A.R.P. Varela, L.C. Silva, Tackling the biophysical properties of sphingolipids to decipher their biological roles, Biol. Chem. (2015) 396, 597–609. doi:10.1515/hsz-2014-0283.

[44] K. Trajkovic, Ceramide triggers budding of exosome vesicles into multivesicular endosomes, Science (80-.). (2008) 319, 1244–7. doi:10.1126/science.320.5873.179.

[45] V.A. Blaho, S. Galvani, E. Engelbrecht, C. Liu, S.L. Swendeman, M. Kono, R.L. Proia, L. Steinman, M.H. Han, T. Hla, HDL-bound sphingosine-1-phosphate restrains lymphopoiesis and neuroinflammation, Nature. (2015) 523, 342–6. doi:10.1038/nature14462.

[46] G.A. Patwardhan, L.J. Beverly, L.J. Siskind, Sphingolipids and mitochondrial apoptosis, J. Bioenerg. Biomembr. (2016) 48, 153–168. doi:10.1007/s10863-015-9602-3.

[47] M. Maceyka, S.G. Payne, S. Milstien, S. Spiegel, Sphingosine kinase, sphingosine-1-phosphate, and apoptosis, Biochim. Biophys. Acta - Mol. Cell Biol. Lipids. (2002) 1585, 193–201. doi:10.1016/S1388-1981(02)00341-4.

[48] T.A. Taha, T.D. Mullen, L.M. Obeid, A house divided: Ceramide, sphingosine, and sphingosine-1-phosphate in programmed cell death, Biochim. Biophys. Acta - Biomembr. (2006) 1758, 2027–36. doi:10.1016/j.bbamem.2006.10.018.

[49] C.R. Gault, L.M. Obeid, Y.A. Hannun, An overview of sphingolipid metabolism: From synthesis to breakdown, Adv. Exp. Med. Biol. (2010) 688, 1–23. doi:10.1007/978-1-4419-6741-1_1.

[50] M. Dei Cas, R. Ghidoni, Cancer prevention and therapy with polyphenols: Sphingolipid-mediated mechanisms, Nutrients. (2018) 10, 940. doi:10.3390/nu10070940.

[51] M. Alhouayek, G.G. Muccioli, The endocannabinoid system in inflammatory bowel diseases: From pathophysiology to therapeutic opportunity, Trends Mol. Med. (2012) 18, 615–625. doi:10.1016/j.molmed.2012.07.009.

[52] H. Gui, Q. Tong, W. Qu, C.M. Mao, S.M. Dai, The endocannabinoid system and its therapeutic implications in rheumatoid arthritis, Int. Immunopharmacol. (2015) 26, 86–91. doi:10.1016/j.intimp.2015.03.006.

[53] M.T. Cencioni, V. Chiurchiù, G. Catanzaro, G. Borsellino, G. Bernardi, L. Battistini, M. Maccarrone, Anandamide suppresses proliferation and cytokine release from primary human T-lymphocytes mainly via CB2 receptors, PLoS One. (2010) 5, e8688. doi:10.1371/journal.pone.0008688.

[54] A. Ribeiro, S. Pontis, L. Mengatto, A. Armirotti, V. Chiurchiù, V. Capurro, A. Fiasella, A. Nuzzi, E. Romeo, G. Moreno-Sanz, M. Maccarrone, A. Reggiani, G. Tarzia, M. Mor, F. Bertozzi, T. Bandiera, D. Piomelli, A Potent Systemically Active N-Acylethanolamine Acid Amidase Inhibitor that Suppresses Inflammation and Human Macrophage Activation, ACS Chem. Biol. (2015) 10, 1838–46. doi:10.1021/acschembio.5b00114.

[55] G.J.M. Maestroni, The endogenous cannabinoid 2-arachidonoyl glycerol as in vivo chemoattractant for dendritic cells and adjuvant for Th1 response to a soluble protein, FASEB J. (2004) 18, 1914–6. doi:10.1096/fj.04-2190fje.

[56] R. Gallily, A. Breuer, R. Mechoulam, 2-Arachidonylglycerol, an endogenous cannabinoid, inhibits tumor necrosis factor-α production in murine macrophages, and in mice, Eur. J. Pharmacol. (2000) 406, 5–7. doi:10.1016/S0014-2999(00)00653-1.

[57] Y.H. Chang, S.T. Lee, W.W. Lin, Effects of cannabinoids on LPS-stimulated inflammatory mediator release from macrophages: Involvement of eicosanoids, J. Cell. Biochem. (2001) 81, 715–23. doi:10.1002/jcb.1103.

[58] N. Barrie, N. Manolios, The endocannabinoid system in pain and inflammation: Its relevance to rheumatic disease, Eur. J. Rheumatol. (2017) 4, 210–218. doi:10.5152/eurjrheum.2017.17025.

[59] I. Sevastou, E. Kaffe, M.A. Mouratis, V. Aidinis, Lysoglycerophospholipids in chronic inflammatory disorders: The PLA 2/LPC and ATX/LPA axes, Biochim. Biophys. Acta - Mol. Cell Biol. Lipids. (2013) 1831, 42–60. doi:10.1016/j.bbalip.2012.07.019.

[60] X. Ye, Lysophospholipid signaling in the function and pathology of the reproductive system, Hum. Reprod. Update. (2008) 14, 519–536. doi:10.1093/humupd/dmn023.

[61] S. Knowlden, S.N. Georas, The Autotaxin–LPA Axis Emerges as a Novel Regulator of Lymphocyte Homing and Inflammation, J. Immunol. (2014) 192, 851–7. doi:10.4049/jimmunol.1302831.

[62] S. Heimerl, M. Fischer, A. Baessler, G. Liebisch, A. Sigruener, S. Wallner, G. Schmitz, Alterations of plasma lysophosphatidylcholine species in obesity and weight loss, PLoS One. (2014) 9, e111348. doi:10.1371/journal.pone.0111348.

[63] R. Piñeiro, M. Falasca, Lysophosphatidylinositol signalling: New wine from an old bottle, Biochim. Biophys. Acta - Mol. Cell Biol. Lipids. (2012) 1821, 694–705. doi:10.1016/j.bbalip.2012.01.009.

[64] B. Fuchs, J. Schiller, U. Wagner, H. Häntzschel, K. Arnold, The phosphatidylcholine/lysophosphatidylcholine ratio in human plasma is an indicator of the severity of rheumatoid arthritis: Investigations by 31P NMR and MALDI-TOF MS, Clin. Biochem. (2005) 38, 925–33. doi:10.1016/j.clinbiochem.2005.06.006.

[65] D. Kluepfel, J. Bagli, H. Baker, M.P. Charest, A. Kudelski, S.N. Sehgal, C. Vézina, Myriocin, a new antifungal antibiotic from myriococcum albomyces, J. Antibiot. (Tokyo). (1972) 25, 109–115. doi:10.7164/antibiotics.25.109.

[66] R. Craveri, P.L. Manachini, F. Aragozzini, Thermozymocidin new antifungal antibiotic from a thermophilic eumycete, Experientia. (1972) 28, 867–868. doi:10.1007/BF01923181.

[67] T. Fujita, Patent EP 0436 020 A1, EP 0 436 020 A1, 1991.

[68] K. Chiba, Discovery of fingolimod based on the chemical modification of a natural product from the fungus, Isaria sinclairii, J. Antibiot. (Tokyo). (2020) 73, 666–678. doi:10.1038/s41429-020-0351-0.

[69] S. Sasaki, R. Hashimoto, M. Kiuchi, K. Inoue, T. Ikumoto, R. Hirose, K. Chiba, Y. Hoshino, T. Okumoto, T. Fujita, M. Kiuchi, T. Fujita, R. Hashimoto, K. Inoue, K. Chiba, Y. Hoshino, T. Okumoto, M. Kiuchi, K. Inoue, T. Ikumoto, R. Hirose, K. Chiba, Y. Hoshino, T. Okumoto, T. Fujita, Fungal metabolites. Part 14. Novel potent immunosuppressants, mycestericins, produced by Mycelia sterilia., J. Antibiot. (Tokyo). (1994) 47, 420–433. doi:10.7164/antibiotics.47.420.

[70] T. Fujita, K. Inoue, S. Yamamoto, T. Ikumoto, S. Sasaki, R. Toyama, K. Chiba, Y. Hoshino, T. Okumoto, Fungal metabolites. Part 12. Potent immunosuppressant, 14-deoxomyriocin, (2S,3R,4R)-(E)-2-amino-3,4-dihydroxy-2-hydroxymethyleicos-6-enoic acid and structure-activity relationships of myriocin derivatives., J. Antibiot. (Tokyo). (1994). doi:10.7164/antibiotics.47.216.

[71] W.-M. Cheng, Q.-L. Zhang, Z.-H. Wu, Z.-Y. Zhang, Y.-R. Miao, F. Peng, C.-R. Li, Identification and determination of myriocin in Isaria cicadae and its allies by LTQ-Orbitrap-HRMS., Mycology. (2017) 8, 286–292. doi:10.1080/21501203.2017.1383319.

[72] M. Yoshikawa, Y. Yokokawa, Y. Okuno, N. Murakami, Total synthesis of a novel immunosuppressant, myriocin (thermozymocidin, isp-i), and z-myriocin, Chem. Pharm. Bull. (1994) 42, 994–996. doi:10.1248/cpb.42.994.

[73] Y. Miyake, Y. Kozutsumi, S. Nakamura, T. Fujita, T. Kawasaki, Serine palmitoyltransferase is the primary target of a sphingosine-like immunosuppressant, ISP-1/myriocin, Biochem. Biophys. Res. Commun. (1995). doi:10.1006/bbrc.1995.1827.

[74] S. Nakamura, Y. Kozutsumi, Y. Sun, Y. Miyake, T. Fujita, T. Kawasaki, Dual roles of sphingolipids in signaling of the escape from and onset of apoptosis in a mouse cytotoxic T-cell line, CTLL-2, J. Biol. Chem. (1996) 271, 1255–1257. doi:10.1074/jbc.271.3.1255.

[75] A. Mingione, E. Ottaviano, M. Barcella, I. Merelli, L. Rosso, T. Armeni, N. Cirilli, R. Ghidoni, E. Borghi, P. Signorelli, Cystic Fibrosis Defective Response to Infection Involves Autophagy and Lipid Metabolism, Cells. (2020) 9,. doi:10.3390/cells9081845.

[76] E. Strettoi, C. Gargini, E. Novelli, G. Sala, I. Piano, P. Gasco, R. Ghidoni, Inhibition of ceramide biosynthesis preserves photoreceptor structure and function in a mouse model of retinitis pigmentosa, Proc. Natl. Acad. Sci. (2010). doi:10.1073/pnas.1007644107.

[77] I. Piano, E. Novelli, P. Gasco, R. Ghidoni, E. Strettoi, C. Gargini, Cone survival and preservation of visual acuity in an animal model of retinal degeneration, Eur. J. Neurosci. (2013). doi:10.1111/ejn.12196.

[78] R. Ji, H. Akashi, K. Drosatos, X. Liao, H. Jiang, P.J. Kennel, D.L. Brunjes, E. Castillero, X. Zhang, L.Y. Deng, S. Homma, I.J. George, H. Takayama, Y. Naka, I.J. Goldberg, P.C. Schulze, Increased de novo ceramide synthesis and accumulation in failing myocardium, JCI Insight. (2017). doi:10.1172/jci.insight.96203.

[79] M.R. Reforgiato, G. Milano, G. Fabriï¿½s, J. Casas, P. Gasco, R. Paroni, M. Samaja, R. Ghidoni, A. Caretti, P. Signorelli, Inhibition of ceramide de novo synthesis as a postischemic strategy to reduce myocardial reperfusion injury, Basic Res. Cardiol. (2016). doi:10.1007/s00395-016-0533-x.

[80] F. Bonezzi, M. Piccoli, M.D. Cas, R. Paroni, A. Mingione, M.M. Monasky, A. Caretti, C. Riganti, R. Ghidoni, C. Pappone, L. Anastasia, P. Signorelli, P.B. Chase, Sphingolipid Synthesis Inhibition by Myriocin Administration Enhances Lipid Consumption and Ameliorates Lipid Response to Myocardial Ischemia Reperfusion Injury, (2019) 10, 1–14. doi:10.3389/fphys.2019.00986.

[81] Z. Yu, Q. Peng, S. Li, H. Hao, J. Deng, L. Meng, Z. Shen, W. Yu, D. Nan, Y. Bai, Y. Huang, Myriocin and d-PDMP ameliorate atherosclerosis in ApoE-/- mice via reducing lipid uptake and vascular inflammation, Clin. Sci. (Lond). (2020) 134, 439–458. doi:10.1042/CS20191028.

[82] R.X. Yang, Q. Pan, X.L. Liu, D. Zhou, F.Z. Xin, Z.H. Zhao, R.N. Zhang, J. Zeng, L. Qiao, C.X. Hu,

G.W. Xu, J.G. Fan, Therapeutic effect and autophagy regulation of myriocin in nonalcoholic steatohepatitis, Lipids Health Dis. (2019) 18, 1–11. doi:10.1186/s12944-019-1118-0.

[83] A. Caretti, M. Vasso, F.T. Bonezzi, A. Gallina, M. Trinchera, A. Rossi, R. Adami, J. Casas, M. Falleni, D. Tosi, A. Bragonzi, R. Ghidoni, C. Gelfi, P. Signorelli, Myriocin treatment of CF lung infection and inflammation: complex analyses for enigmatic lipids, Naunyn. Schmiedebergs. Arch. Pharmacol. (2017). doi:10.1007/s00210-017-1373-4.

[84] A. Caretti, R. Torelli, F. Perdoni, M. Falleni, D. Tosi, A. Zulueta, J. Casas, M. Sanguinetti, R. Ghidoni, E. Borghi, P. Signorelli, Inhibition of ceramide de novo synthesis by myriocin produces the double effect of reducing pathological inflammation and exerting antifungal activity against A. fumigatus airways infection, Biochim. Biophys. Acta - Gen. Subj. (2016) 1860, 1089–97. doi:10.1016/j.bbagen.2016.02.014.

[85] A. Caretti, A. Bragonzi, M. Facchini, I. De Fino, C. Riva, P. Gasco, C. Musicanti, J. Casas, G. Fabriàs, R. Ghidoni, P. Signorelli, Anti-inflammatory action of lipid nanocarrier-delivered myriocin: Therapeutic potential in cystic fibrosis, Biochim. Biophys. Acta - Gen. Subj. (2014) 1840, 586–94. doi:10.1016/j.bbagen.2013.10.018.

[86] A. Mingione, M.D. Cas, F. Bonezzi, A. Caretti, M. Piccoli, L. Anastasia, R. Ghidoni, R. Paroni, P. Signorelli, M. Dei Cas, F. Bonezzi, A. Caretti, M. Piccoli, L. Anastasia, R. Ghidoni, R. Paroni, P. Signorelli, Inhibition of sphingolipid synthesis as a phenotype-modifying therapy in cystic fibrosis, Cell. Physiol. Biochem. (2020) 54, 110–125. doi:10.33594/000000208.

[87] M. Casasampere, Y.F. Ordóñez, J. Casas, G. Fabrias, Dihydroceramide desaturase inhibitors induce autophagy via dihydroceramide-dependent and independent mechanisms, Biochim. Biophys. Acta - Gen. Subj. (2017) 1861, 264–275. doi:10.1016/j.bbagen.2016.11.033.

[88] S. Agatonovic-Kustrin, D.W. Morton, V. Smirnov, A. Petukhov, V. Gegechkori, V. Kuzina, N. Gorpinchenko, G. Ramenskaya, Analytical strategies in lipidomics for discovery of functional biomarkers from human saliva, Dis. Markers. (2019) 2019,. doi:10.1155/2019/6741518.

[89] S. Zhong, L. Li, X. Shen, Q. Li, W. Xu, X. Wang, Y. Tao, H. Yin, An update on lipid oxidation and inflammation in cardiovascular diseases, Free Radic. Biol. Med. (2019) 144, 266–278. doi:10.1016/j.freeradbiomed.2019.03.036.

[90] B.H. Mishra, P.P. Mishra, N. Mononen, M. Hilvo, H. Sievänen, M. Juonala, M. Laaksonen, N. Hutri-Kähönen, J. Viikari, M. Kähönen, O.T. Raitakari, R. Laaksonen, T. Lehtimäki, Lipidomic architecture shared by subclinical markers of osteoporosis and atherosclerosis: The Cardiovascular Risk in Young Finns Study, Bone. (2020) 131,. doi:10.1016/j.bone.2019.115160.

[91] J. Lu, S. ManLam, Q. Wan, L. Shi, Y. Huo, L. Chen, X. Tang, B. Li, X. Wu, K. Peng, M. Li, S. Wang, Y. Xu, M. Xu, Y. Bi, G. Ning, G. Shui, W. Wang, High-coverage targeted lipidomics reveals novel serum lipid predictors and lipid pathway dysregulation antecedent to type 2 diabetes onset in normoglycemic Chinese adults, Diabetes Care. (2019) 42, 2117–2126. doi:10.2337/dc19-0100.

[92] T. Suvitaival, I. Bondia-Pons, L. Yetukuri, P. Pöhö, J.J. Nolan, T. Hyötyläinen, J. Kuusisto, M. Orešič, Lipidome as a predictive tool in progression to type 2 diabetes in Finnish men, Metabolism. (2018) 78, 1–12. doi:10.1016/j.metabol.2017.08.014.

[93] F. Zhong, M. Xu, R.S. Bruno, K.D. Ballard, J. Zhu, Targeted High Performance Liquid Chromatography Tandem Mass Spectrometry-based Metabolomics differentiates metabolic syndrome from obesity, Exp. Biol. Med. (2017) 242, 773–780. doi:10.1177/1535370217694098.

[94] L. li Gong, S. Yang, W. Zhang, F. fei Han, Y. li Lv, L. ling Xuan, H. Liu, L. hong Liu, Discovery of metabolite profiles of metabolic syndrome using untargeted and targeted LC–MS

based lipidomics approach, J. Pharm. Biomed. Anal. (2020) 177,. doi:10.1016/j.jpba.2019.112848.

[95] K. Kus, A. Kij, A. Zakrzewska, A. Jasztal, M. Stojak, M. Walczak, S. Chlopicki, Alterations in arginine and energy metabolism, structural and signalling lipids in metastatic breast cancer in mice detected in plasma by targeted metabolomics and lipidomics, Breast Cancer Res. (2018) 20,. doi:10.1186/s13058-018-1075-y.

[96] R. Farrokhi Yekta, M. Rezaie Tavirani, A. Arefi Oskouie, M.R. Mohajeri-Tehrani, A.R. Soroush, The metabolomics and lipidomics window into thyroid cancer research, Biomarkers. (2017) 22, 595–603. doi:10.1080/1354750X.2016.1256429.

[97] L. Zhang, B. Zhu, Y. Zeng, H. Shen, J. Zhang, X. Wang, Clinical lipidomics in understanding of lung cancer: Opportunity and challenge, Cancer Lett. (2020) 470, 75–83. doi:10.1016/j.canlet.2019.08.014.

[98] E.G. Armitage, A.D. Southam, Monitoring cancer prognosis, diagnosis and treatment efficacy using metabolomics and lipidomics, Metabolomics. (2016) 12,. doi:10.1007/s11306-016-1093-7.

[99] M.W. Wong, N. Braidy, A. Poljak, P.S. Sachdev, The application of lipidomics to biomarker research and pathomechanisms in Alzheimer's disease, Curr. Opin. Psychiatry. (2017) 30, 136–144. doi:10.1097/YCO.0000000000000303.

[100] P. Proitsi, M. Kim, L. Whiley, A. Simmons, M. Sattlecker, L. Velayudhan, M.K. Lupton, H. Soininen, I. Kloszewska, P. Mecocci, M. Tsolaki, B. Vellas, S. Lovestone, J.F. Powell, R.J.B. Dobson, C. Legido-Quigley, Association of blood lipids with Alzheimer's disease: A comprehensive lipidomics analysis, Alzheimer's Dement. (2017) 13, 140–151. doi:10.1016/j.jalz.2016.08.003.

[101] D. Gao, L. Zhang, D. Song, J. Lv, L. Wang, S. Zhou, Y. Li, T. Zeng, Y. Zeng, J. Zhang, X. Wang, Values of integration between lipidomics and clinical phenomes in patients with acute lung infection, pulmonary embolism, or acute exacerbation of chronic pulmonary diseases: A preliminary study, J. Transl. Med. (2019) 17,. doi:10.1186/s12967-019-1898-z.

[102] S. Zarini, R.M. Barkley, M.A. Gijón, R.C. Murphy, Overview of lipid mass spectrometry and lipidomics, 2019. doi:10.1007/978-1-4939-9236-2_6.

[103] J.A. Bowden, A. Heckert, C.Z. Ulmer, C.M. Jones, J.P. Koelmel, L. Abdullah, L. Ahonen, Y. Alnouti, A.M. Armando, J.M. Asara, T. Bamba, J.R. Barr, J. Bergquist, C.H. Borchers, J. Brandsma, S.B. Breitkopf, T. Cajka, A. Cazenave-Gassiot, A. Checa, M.A. Cinel, R.A. Colas, S. Cremers, E.A. Dennis, J.E. Evans, A. Fauland, O. Fiehn, M.S. Gardner, T.J. Garrett, K.H. Gotlinger, J. Han, Y. Huang, A.H. Neo, T. Hyötyläinen, Y. Izumi, H. Jiang, H. Jiang, J. Jiang, M. Kachman, R. Kiyonami, K. Klavins, C. Klose, H.C. Köfeler, J. Kolmert, T. Koal, G. Koster, Z. Kuklenyik, I.J. Kurland, M. Leadley, K. Lin, K.R. Maddipati, D. McDougall, P.J. Meikle, N.A. Mellett, C. Monnin, M.A. Moseley, R. Nandakumar, M. Oresic, R. Patterson, D. Peake, J.S. Pierce, M. Post, A.D. Postle, R. Pugh, Y. Qiu, O. Quehenberger, P. Ramrup, J. Rees, B. Rembiesa, D. Reynaud, M.R. Roth, S. Sales, K. Schuhmann, M.L. Schwartzman, C.N. Serhan, A. Shevchenko, S.E. Somerville, L. St John-Williams, M.A. Surma, H. Takeda, R. Thakare, J.W. Thompson, F. Torta, A. Triebl, M. Trötzmüller, S.J.K. Ubhayasekera, D. Vuckovic, J.M. Weir, R. Welti, M.R. Wenk, C.E. Wheelock, L. Yao, M. Yuan, X.H. Zhao, S. Zhou, Harmonizing lipidomics: NIST interlaboratory comparison exercise for lipidomics using SRM 1950-Metabolites in frozen human plasma, J. Lipid Res. (2017) 58, 2275–2288. doi:10.1194/jlr.M079012.

[104] F. Afshinnia, T.M. Rajendiran, S. Wernisch, T. Soni, A. Jadoon, A. Karnovsky, G. Michailidis, S. Pennathur, Lipidomics and Biomarker Discovery in Kidney Disease, Semin. Nephrol. (2018) 38, 127–141. doi:10.1016/j.semnephrol.2018.01.004.

[105] A.M. Evans, C. O'Donovan, M. Playdon, C. Beecher, R.D. Beger, J.A. Bowden, D. Broadhurst,

C.B. Clish, S. Dasari, W.B. Dunn, J.L. Griffin, T. Hartung, P.C. Hsu, T. Huan, J. Jans, C.M. Jones, M. Kachman, A. Kleensang, M.R. Lewis, M.E. Monge, J.D. Mosley, E. Taylor, F. Tayyari, G. Theodoridis, F. Torta, B.K. Ubhi, D. Vuckovic, Dissemination and analysis of the quality assurance (QA) and quality control (QC) practices of LC–MS based untargeted metabolomics practitioners, Metabolomics. (2020) 16,. doi:10.1007/s11306-020-01728-5.

[106] M.R. Wenk, Lipidomics: New tools and applications, Cell. (2010) 143, 888–95. doi:10.1016/j.cell.2010.11.033.

[107] M.R. Wenk, The emerging field of lipidomics, Nat. Rev. Drug Discov. (2005) 4, 594–610. doi:10.1038/nrd1776.

[108] S. Sethi, E. Brietzke, Recent advances in lipidomics: Analytical and clinical perspectives, Prostaglandins Other Lipid Mediat. (2017) 128–9, 8–16. doi:10.1016/j.prostaglandins.2016.12.002.

[109] M.R. Molenaar, A. Jeucken, T.A. Wassenaar, C.H.A. Van De Lest, J.F. Brouwers, J.B. Helms, LION/web: A web-based ontology enrichment tool for lipidomic data analysis, Gigascience. (2019). doi:10.1093/gigascience/giz061.

[110] C.M. Farinha, E. Miller, N. McCarty, Protein and lipid interactions – Modulating CFTR trafficking and rescue, J. Cyst. Fibros. (2018) 17, S9–S13. doi:10.1016/j.jcf.2017.08.014.

[111] D.M. Cholon, W.K. O'Neal, S.H. Randell, J.R. Riordan, M. Gentzsch, Modulation of endocytic trafficking and apical stability of CFTR in primary human airway epithelial cultures, Am. J. Physiol. - Lung Cell. Mol. Physiol. (2010) 298, L304–L314. doi:10.1152/ajplung.00016.2009.

[112] A. Abu-Arish, E. Pandzic, J. Goepp, E. Matthes, J.W. Hanrahan, P.W. Wiseman, Cholesterol Modulates CFTR Confinement in the Plasma Membrane of Primary Epithelial Cells, Biophys. J. (2015) 109, 85–94. doi:10.1016/j.bpj.2015.04.042.

[113] T.S. Worgall, Lipid metabolism in cystic fibrosis, Curr. Opin. Clin. Nutr. Metab. Care. (2009) 12, 105–109. doi:10.1097/MCO.0b013e32832595b7.

[114] V. Figueroa, C. Milla, E.J. Parks, S.J. Schwarzenberg, A. Moran, Abnormal lipid concentrations in cystic fibrosis, Am. J. Clin. Nutr. (2002) 75, 1005–11. doi:10.1093/ajcn/75.6.1005.

[115] A.R.T.O. Tjon Tham, H.G.M. Heyerman, T.H.M. Falke, A.H. Zwinderman, J.L. Bloem, W. Bakker, C.B.H.W. Lamers, Cystic fibrosis: MR imaging of the pancreas, Radiology. (1991) 179, 183–186. doi:10.1148/radiology.179.1.2006275.

[116] D.S. Hardin, A. LeBlanc, L. Para, D.K. Seilheimer, Hepatic insulin resistance and defects in substrate utilization in cystic fibrosis, Diabetes. (1999) 48, 1082–1087. doi:10.2337/diabetes.48.5.1082.

[117] A. Chryssostalis, D. Hubert, J. Coste, R. Kanaan, P.R. Burgel, N. Desmazes-Dufeu, O. Soubrane, D. Dusser, P. Sogni, Liver disease in adult patients with cystic fibrosis: A frequent and independent prognostic factor associated with death or lung transplantation, J. Hepatol. (2011) 55, 1377–1382. doi:10.1016/j.jhep.2011.03.028.

[118] M. Wilschanski, P.R. Durie, Patterns of GI disease in adulthood associated with mutations in the CFTR gene, Gut. (2007) 56, 1153–1163. doi:10.1136/gut.2004.062786.

[119] N.M. White, D. Jiang, J.D. Burgess, I.R. Bederman, S.F. Previs, T.J. Kelley, Altered cholesterol homeostasis in cultured and in vivo models of cystic fibrosis, Am. J. Physiol. - Lung Cell. Mol. Physiol. (2007) 292, 476–86. doi:10.1152/ajplung.00262.2006.

[120] M. Gelzo, C. Sica, A. Elce, A. Dello Russo, P. Iacotucci, V. Carnovale, V. Raia, D. Salvatore, G. Corso, G. Castaldo, Reduced absorption and enhanced synthesis of cholesterol in patients with cystic fibrosis: A preliminary study of plasma sterols, Clin. Chem. Lab. Med. (2016) 54, 1461–6. doi:10.1515/cclm-2015-1151.

[121] W.L. Ernst, K. Shome, C.C. Wu, X. Gong, R.A. Frizzell, M. Aridor, VAMP-associated proteins (VAP) as receptors that couple cystic fibrosis transmembrane conductance regulator (CFTR) proteostasis with lipid homeostasis, J. Biol. Chem. (2016) 291, 5206–20. doi:10.1074/jbc.M115.692749.

[122] A.Z. Buzatto, M.A. Jabar, I. Nizami, M. Dasouki, L. Li, A.M.A. Rahman, Lipidome Alterations Induced by Cystic Fibrosis , CFTR Mutation , and Lung Function, (2020). doi:10.1021/acs.jproteome.0c00556.

[123] A. López-Neyra, L. Suárez, M. Muñoz, A. de Blas, M. Ruiz de Valbuena, M. Garriga, J. Calvo, C. Ribes, R. Girón Moreno, L. Máiz, D. González, C. Bousoño, J. Manzanares, Ó. Pastor, J. Martínez-Botas, R. del Campo, R. Cantón, G. Roy, M. Menacho, D. Arroyo, J. Zamora, J.B. Soriano, A. Lamas, Long-term docosahexaenoic acid (DHA) supplementation in cystic fibrosis patients: a randomized, multi-center, double-blind, placebo-controlled trial, Prostaglandins Leukot. Essent. Fat. Acids. (2020) 162, 102186. doi:10.1016/j.plefa.2020.102186.

[124] S.D. Freedman, P.G. Blanco, M.M. Zaman, J.C. Shea, M. Ollero, I.K. Hopper, D.A. Weed, A. Gelrud, M.M. Regan, M. Laposata, J.G. Alvarez, B.P. O'Sullivan, Association of Cystic Fibrosis with Abnormalities in Fatty Acid Metabolism, N. Engl. J. Med. (2004) 350, 560–569. doi:10.1056/nejmoa021218.

[125] C. Vandebrouck, T. Ferreira, Glued in lipids: Lipointoxication in cystic fibrosis, EBioMedicine. (2020) 61,. doi:10.1016/j.ebiom.2020.103038.

[126] C.E. Wheelock, B. Strandvik, Abnormal n-6 fatty acid metabolism in cystic fibrosis contributes to pulmonary symptoms, Prostaglandins Leukot. Essent. Fat. Acids. (2020) 160, 102156. doi:10.1016/j.plefa.2020.102156.

[127] M.S. Muhlebach, W. Sha, B. MacIntosh, T.J. Kelley, J. Muenzer, Metabonomics reveals altered metabolites related to inflammation and energy utilization at recovery of cystic fibrosis lung exacerbation, Metab. Open. (2019) 3, 100010. doi:10.1016/j.metop.2019.100010.

[128] P. Witters, L. Dupont, F. Vermeulen, M. Proesmans, D. Cassiman, P. Wallemacq, K. De Boeck, Lung transplantation in cystic fibrosis normalizes essential fatty acid profiles, J. Cyst. Fibros. (2013) 12, 222–228. doi:10.1016/j.jcf.2012.09.004.

[129] L. Hanssens, J. Duchateau, S.A. Namane, A. Malfroot, C. Knoop, G. Casimir, Influence of lung transplantation on the essential fatty acid profile in cystic fibrosis, Prostaglandins Leukot. Essent. Fat. Acids. (2020) 158, 102060. doi:10.1016/j.plefa.2020.102060.

[130] J. Colomba, R. Rabasa-Lhoret, A. Bonhoure, C. Bergeron, V. Boudreau, F. Tremblay, P. Senior, K. Potter, Dyslipidemia is not associated with the development of glucose intolerance or diabetes in cystic fibrosis, J. Cyst. Fibros. (2020) 19, 704–711. doi:10.1016/j.jcf.2020.04.004.

[131] B. Rhodes, E.F. Nash, E. Tullis, P.B. Pencharz, M. Brotherwood, A. Dupuis, A. Stephenson, Prevalence of dyslipidemia in adults with cystic fibrosis, J. Cyst. Fibros. (2010) 9, 24–28. doi:10.1016/j.jcf.2009.09.002.

[132] M.J. Slesinski, M.F. Gloninger, J.P. Costantino, D.M. Orenstein, Lipid levels in adults with cystic fibrosis, J. Am. Diet. Assoc. (1994) 94, 402–408. doi:10.1016/0002-8223(94)90095-7.

[133] J.K. Nowak, M. Szczepanik, I. Wojsyk-Banaszak, E. Mądry, A. Wykrętowicz, P. Krzyżanowska-Jankowska, S. Drzymała-Czyż, A. Nowicka, A. Pogorzelski, E. Sapiejka, W. Skorupa, A. Miśkiewicz-Chotnicka, A. Lisowska, J. Walkowiak, Cystic fibrosis dyslipidaemia: A cross-sectional study, J. Cyst. Fibros. (2019) 18, 566–571. doi:10.1016/j.jcf.2019.04.001.

[134] V. V. GEORGIOPOULOU, A. DENKER, K.L. BISHOP, J.M. BROWN, B. HIRSH, L. WOLFENDEN, L. SPERLING, Metabolic abnormalities in adults with cystic fibrosis, Respirology. (2010)

15, 823–829. doi:10.1111/j.1440-1843.2010.01771.x.

[135] J.W. Woestenenk, D.A. Schulkes, H.S. Schipper, C.K. Van Der Ent, R.H.J. Houwen, Dietary intake and lipid profile in children and adolescents with cystic fibrosis, J. Cyst. Fibros. (2017) 16, 410–417. doi:10.1016/j.jcf.2017.02.010.

[136] B. Lu, L. Li, M. Schneider, C.A. Hodges, C.U. Cotton, J.D. Burgess, T.J. Kelley, Electrochemical measurement of membrane cholesterol correlates with CFTR function and is HDAC6-dependent, J. Cyst. Fibros. (2019) 18, 175–181. doi:10.1016/j.jcf.2018.06.005.

[137] M. Gelzo, P. Iacotucci, C. Sica, R. Liguori, M. Comegna, V. Carnovale, A. Dello Russo, G. Corso, G. Castaldo, Influence of pancreatic status on circulating plasma sterols in patients with cystic fibrosis, Clin. Chem. Lab. Med. (2020) 58,. doi:10.1515/cclm-2019-1112.

[138] D.C. Ma, A.J. Yoon, K.F. Faull, R. Desharnais, E.T. Zemanick, E. Porter, Cholesteryl esters are elevated in the lipid fraction of bronchoalveolar lavage fluid collected from pediatric cystic fibrosis patients, PLoS One. (2015) 10, e0125326. doi:10.1371/journal.pone.0125326.

[139] V. Teichgräber, M. Ulrich, N. Endlich, J. Riethmüller, B. Wilker, C.C. De Oliveira-Munding, A.M. Van Heeckeren, M.L. Barr, G. Von Kürthy, K.W. Schmid, M. Weller, B. Tümmler, F. Lang, H. Grassme, G. Döring, E. Gulbins, Ceramide accumulation mediates inflammation, cell death and infection susceptibility in cystic fibrosis, Nat. Med. (2008) 14, 382–91. doi:10.1038/nm1748.

[140] N. Loberto, G. Mancini, R. Bassi, E.V. Carsana, A. Tamanini, N. Pedemonte, M.C. Dechecchi, S. Sonnino, M. Aureli, Sphingolipids and plasma membrane hydrolases in human primary bronchial cells during differentiation and their altered patterns in cystic fibrosis, Glycoconj. J. (2020) 37, 623–633. doi:10.1007/s10719-020-09935-x.

[141] N. Liessi, E. Pesce, C. Braccia, S.M. Bertozzi, A. Giraudo, T. Bandiera, N. Pedemonte, A. Armirotti, Distinctive lipid signatures of bronchial epithelial cells associated with cystic fibrosis drugs, including Trikafta, JCI Insight. (2020) 5,. doi:10.1172/jci.insight.138722.

[142] S.N. Lavrentiadou, C. Chan, T'Nay Kawcak, T. Ravid, A. Tsaba, A. Van der Vliet, R. Rasooly, T. Goldkorn, Ceramide-mediated apoptosis in lung epithelial cells is regulated by glutathione, Am. J. Respir. Cell Mol. Biol. (2001) 25, 676–684. doi:10.1165/ajrcmb.25.6.4321.

[143] C. Chan, T. Goldkorn, Ceramide path in human lung cell death, Am. J. Respir. Cell Mol. Biol. (2000) 22, 460–468. doi:10.1165/ajrcmb.22.4.3376.

[144] T.L. Bonfield, Membrane Lipids and CFTR: The Yin/Yang of Efficient Ceramide Metabolism, Am. J. Respir. Crit. Care Med. (2020) 202, 1074–1075. doi:10.1164/rccm.202006-2362ed.

[145] Y. Pewzner-Jung, S. Tavakoli Tabazavareh, H. Grassmé, K.A. Becker, L. Japtok, J. Steinmann, T. Joseph, S. Lang, B. Tuemmler, E.H. Schuchman, A.B. Lentsch, B. Kleuser, M.J. Edwards, A.H. Futerman, E. Gulbins, Sphingoid long chain bases prevent lung infection by Pseudomonas aeruginosa , EMBO Mol. Med. (2014) 6, 1205–1214. doi:10.15252/emmm.201404075.

[146] S. Tavakoli Tabazavareh, A. Seitz, P. Jernigan, C. Sehl, S. Keitsch, S. Lang, B.C. Kahl, M. Edwards, H. Grassmé, E. Gulbins, K.A. Becker, Lack of Sphingosine Causes Susceptibility to Pulmonary Staphylococcus Aureus Infections in Cystic Fibrosis, Cell. Physiol. Biochem. (2016) 38, 2094–2102. doi:10.1159/000445567.

[147] H. Grassmé, B. Henry, R. Ziobro, K.A. Becker, J. Riethmüller, A. Gardner, A.P. Seitz, J. Steinmann, S. Lang, C. Ward, E.H. Schuchman, C.C. Caldwell, M. Kamler, M.J. Edwards, M. Brodlie, E. Gulbins, β1-Integrin Accumulates in Cystic Fibrosis Luminal Airway Epithelial Membranes and Decreases Sphingosine, Promoting Bacterial Infections, Cell Host Microbe. (2017) 21, 707-718.e8. doi:10.1016/j.chom.2017.05.001.

[148] K.A. Becker, R. Verhaegh, H.-L. Verhasselt, S. Keitsch, M. Soddemann, B. Wilker, G.C. Wilson, J. Buer, S.A. Ahmad, M.J. Edwards, E. Gulbins, Acid ceramidase rescues cystic fibrosis mice from pulmonary infections, Infect. Immun. (2020). doi:10.1128/IAI.00677-20.

[149] H. Horati, H.M. Janssens, C. Margaroli, M. Veltman, M. Stolarczyk, M.B. Kilgore, J. Chou, L. Peng, H.A.M.W. Tiddens, J.D. Chandler, R. Tirouvanziam, B.J. Scholte, Airway profile of bioactive lipids predicts early progression of lung disease in cystic fibrosis, J. Cyst. Fibros. (2020). doi:10.1016/j.jcf.2020.01.010.

[150] B.J. Scholte, H. Horati, M. Veltman, R.J. Vreeken, L.W. Garratt, H.A.W.M. Tiddens, H.M. Janssens, S.M. Stick, Oxidative stress and abnormal bioactive lipids in early cystic fibrosis lung disease, J. Cyst. Fibros. (2019) 18, 781–789. doi:10.1016/j.jcf.2019.04.011.

[151] I. Petrache, K. Kamocki, C. Poirier, Y. Pewzner-Jung, E.L. Laviad, K.S. Schweitzer, M. Van Demark, M.J. Justice, W.C. Hubbard, A.H. Futerman, Ceramide Synthases Expression and Role of Ceramide Synthase-2 in the Lung: Insight from Human Lung Cells and Mouse Models, PLoS One. (2013) 8, e62968. doi:10.1371/journal.pone.0062968.

[152] D. Garić, J.B. De Sanctis, J. Shah, D.C. Dumut, D. Radzioch, Biochemistry of very-long-chain and long-chain ceramides in cystic fibrosis and other diseases: The importance of side chain, Prog. Lipid Res. (2019) 74, 130–144. doi:10.1016/j.plipres.2019.03.001.

[153] M. Maceyka, K.B. Harikumar, S. Milstien, S. Spiegel, Sphingosine-1-phosphate signaling and its role in disease, Trends Cell Biol. (2012) 22, 50–60. doi:10.1016/j.tcb.2011.09.003.

[154] Y. Xu, A. Krause, M. Limberis, T.S. Worgall, S. Worgall, Low sphingosine-1-phosphate impairs lung dendritic cells in cystic fibrosis, Am. J. Respir. Cell Mol. Biol. (2013) 48, 250–257. doi:10.1165/rcmb.2012-0021OC.

[155] F.A. Malik, A. Meissner, I. Semenkov, S. Molinski, S. Pasyk, S. Ahmadi, H.H. Bui, C.E. Bear, D. Lidington, S.S. Bolz, Sphingosine-1-phosphate is a novel regulator of cystic fibrosis transmembrane conductance regulator (CFTR) activity, PLoS One. (2015) 10,. doi:10.1371/journal.pone.0130313.

[156] H.B. Tran, M.G. Macowan, A. Abdo, M. Donnelley, D. Parsons, S. Hodge, Enhanced inflammasome activation and reduced sphingosine-1 phosphate S1P signalling in a respiratory mucoobstructive disease model, J. Inflamm. (United Kingdom). (2020) 17,. doi:10.1186/s12950-020-00248-2.

[157] M. Veltman, M. Stolarczyk, D. Radzioch, G. Wojewodka, J.B. De Sanctis, W.A. Dik, O. Dzyubachyk, T. Oravecz, I. de Kleer, B.J. Scholte, Correction of lung inflammation in a F508del CFTR murine cystic fibrosis model by the sphingosine-1-phosphate lyase inhibitor LX2931, Am. J. Physiol. Cell. Mol. Physiol. (2016) 311, L1000–L1014. doi:10.1152/ajplung.00298.2016.

[158] D.L. Ebenezer, E. V. Berdyshev, I.A. Bronova, Y. Liu, C. Tiruppathi, Y. Komarova, E. V. Benevolenskaya, V. Suryadevara, A.W. Ha, A. Harijith, R.M. Tuder, V. Natarajan, P. Fu, Pseudomonas aeruginosa stimulates nuclear sphingosine-1-phosphate generation and epigenetic regulation of lung inflammatory injury, Thorax. (2019) 74, 579–591. doi:10.1136/thoraxjnl-2018-212378.

[159] E. Halilbasic, E. Fuerst, D. Heiden, L. Japtok, S.C. Diesner, M. Trauner, A. Kulu, P. Jaksch, K. Hoetzenecker, B. Kleuser, L. Kazemi-Shirazi, E. Untersmayr, Plasma Levels of the Bioactive Sphingolipid Metabolite S1P in Adult Cystic Fibrosis Patients: Potential Target for Immunonutrition?, Nutrients. (2020) 12, 765. doi:10.3390/nu12030765.

[160] D. Mattoscio, V. Evangelista, R. De Cristofaro, A. Recchiuti, A. Pandolfi, S. Di Silvestre, S. Manarini, N. Martelli, B. Rocca, G. Petrucci, D.F. Angelini, L. Battistini, I. Robuffo, T. Pensabene, L. Pieroni, M.L. Furnari, F. Pardo, S. Quattrucci, S. Lancellotti, G. Davì, M. Romano, Cystic fibrosis transmembrane conductance regulator (CFTR) expression in

human platelets: Impact on mediators and mechanisms of the inflammatory response, FASEB J. (2010) 24, 3970–3980. doi:10.1096/fj.10-159921.

[161] M. Bonzini, L. Pergoli, L. Cantone, M. Hoxha, A. Spinazzè, L. Del Buono, C. Favero, M. Carugno, L. Angelici, L. Broggi, A. Cattaneo, A.C. Pesatori, V. Bollati, Short-term particulate matter exposure induces extracellular vesicle release in overweight subjects, Environ. Res. (2017) 155, 228–234. doi:10.1016/j.envres.2017.02.014.

[162] A. Della Corte, G. Chitarrini, I.M. Di Gangi, D. Masuero, E. Soini, F. Mattivi, U. Vrhovsek, A rapid LC-MS/MS method for quantitative profiling of fatty acids, sterols, glycerolipids, glycerophospholipids and sphingolipids in grapes, Talanta. (2015) 140, 52–61. doi:10.1016/j.talanta.2015.03.003.

[163] T. Cajka, J.T. Smilowitz, O. Fiehn, Validating Quantitative Untargeted Lipidomics Across Nine Liquid Chromatography-High-Resolution Mass Spectrometry Platforms, Anal. Chem. (2017) 89, 12360–368. doi:10.1021/acs.analchem.7b03404.

[164] T. Huan, E.M. Forsberg, D. Rinehart, C.H. Johnson, J. Ivanisevic, H.P. Benton, M. Fang, A. Aisporna, B. Hilmers, F.L. Poole, M.P. Thorgersen, M.W.W.W. Adams, G. Krantz, M.W. Fields, P.D. Robbins, L.J. Niedernhofer, T. Ideker, E.L. Majumder, J.D. Wall, N.J.W.W. Rattray, R. Goodacre, L.L. Lairson, G. Siuzdak, Systems biology guided by XCMS Online metabolomics, Nat. Methods. (2017) 14, 461–462. doi:10.1038/nmeth.4260.

[165] H. Tsugawa, T. Cajka, T. Kind, Y. Ma, B. Higgins, K. Ikeda, M. Kanazawa, J. Vandergheynst, O. Fiehn, M. Arita, MS-DIAL: Data-independent MS/MS deconvolution for comprehensive metabolome analysis, Nat. Methods. (2015) 12, 523–526. doi:10.1038/nmeth.3393.

[166] J. Shan, W. Qian, C. Shen, L. Lin, T. Xie, L. Peng, J. Xu, R. Yang, J. Ji, X. Zhao, High-resolution lipidomics reveals dysregulation of lipid metabolism in respiratory syncytial virus pneumonia mice, RSC Adv. (2018) 8, 29368–377. doi:10.1039/c8ra05640d.

[167] C. Hu, Y. Zhou, J. Feng, S. Zhou, C. Li, S. Zhao, Y. Shen, L. Hong, Q. Xuan, X. Liu, Q. Li, X. Wang, Y. Zhang, G. Xu, Untargeted Lipidomics Reveals Specific Lipid Abnormalities in Nonfunctioning Human Pituitary Adenomas, J. Proteome Res. (2019) 19, 455–63. doi:10.1021/acs.jproteome.9b00637.

[168] N. Dalmau, J. Jaumot, R. Tauler, C. Bedia, Epithelial-to-mesenchymal transition involves triacylglycerol accumulation in DU145 prostate cancer cells, Mol. Biosyst. (2015). doi:10.1039/c5mb00413f.

[169] C.B.M. Platania, M. Dei Cas, S. Cianciolo, A. Fidilio, F. Lazzara, R. Paroni, R. Pignatello, E. Strettoi, R. Ghidoni, F. Drago, C. Bucolo, Novel ophthalmic formulation of myriocin: implications in retinitis pigmentosa, Drug Deliv. (2019) 26, 237–243. doi:10.1080/10717544.2019.1574936.

[170] A.H. Merrill, M.C. Sullards, J.C. Allegood, S. Kelly, E. Wang, Sphingolipidomics: High-throughput, structure-specific, and quantitative analysis of sphingolipids by liquid chromatography tandem mass spectrometry, Methods. (2005) 36, 207–24. doi:10.1016/j.ymeth.2005.01.009.

[171] A. Zulueta, V. Peli, M. Dei Cas, M. Colombo, R. Paroni, M. Falleni, A. Baisi, V. Bollati, R. Chiaramonte, E. Del Favero, R. Ghidoni, A. Caretti, Inflammatory role of extracellular sphingolipids in Cystic Fibrosis, Int. J. Biochem. Cell Biol. (2019) 116, 105622. doi:10.1016/j.biocel.2019.105622.

[172] J. Xia, D.S. Wishart, Using metaboanalyst 3.0 for comprehensive metabolomics data analysis, Curr. Protoc. Bioinforma. (2016) 55, 14.10.1-14.10-91. doi:10.1002/cpbi.11.

[173] J. Chong, O. Soufan, C. Li, I. Caraus, S. Li, G. Bourque, D.S. Wishart, J. Xia, MetaboAnalyst 4.0: Towards more transparent and integrative metabolomics analysis, Nucleic Acids Res. (2018) 46, 486–94. doi:10.1093/nar/gky310.

[174] M.A. Rahman, M. Akond, M.A. Babar, C. Beecher, J. Erickson, K. Thomason, F.A. De Jong,

R.E. Mason, LC-HRMS Based Non-Targeted Metabolomic Profiling of Wheat (Triticum aestivum; L.) under Post-Anthesis Drought Stress, Am. J. Plant Sci. (2017) 8, 3024–61. doi:10.4236/ajps.2017.812205.

[175] W. Jiang, L. Gao, P. Li, H. Kan, J. Qu, L. Men, Z.Z. Liu, Z.Z. Liu, Metabonomics study of the therapeutic mechanism of fenugreek galactomannan on diabetic hyperglycemia in rats, by ultra-performance liquid chromatography coupled with quadrupole time-of-flight mass spectrometry, J. Chromatogr. B Anal. Technol. Biomed. Life Sci. (2017) 1044–5, 8–16. doi:10.1016/j.jchromb.2016.12.039.

[176] E. La Corte, M. Dei Cas, A. Raggi, M. Patan, M. Broggi, S. Schiavolin, C. Calatozzolo, B. Pollo, C. Pipolo, M.G. Bruzzone, G. Campisi, R. Paroni, R. Ghidoni, P. Ferroli, E. La Corte, M.D. Cas, A. Raggi, M. Patan, M. Broggi, S. Schiavolin, C. Calatozzolo, B. Pollo, C. Pipolo, M.G. Bruzzone, G. Campisi, R. Paroni, R. Ghidoni, P. Ferroli, Long and Very-Long-Chain Ceramides Correlate with A More Aggressive Behavior in Skull Base Chordoma Patients, (2019) 1–16.

[177] X. Jiang, H. Cheng, K. Yang, R.W. Gross, X. Han, Alkaline methanolysis of lipid extracts extends shotgun lipidomics analyses to the low-abundance regime of cellular sphingolipids, Anal. Biochem. (2007) 371, 135–45. doi:10.1016/j.ab.2007.08.019.

[178] M. Dei Cas, A. Zulueta, A. Mingione, A. Caretti, R. Ghidoni, P. Signorelli, R. Paroni, An Innovative Lipidomic Workflow to Investigate the Lipid Profile in a Cystic Fibrosis Cell Line, Cells. (2020) 9, 1–17. doi:10.3390/cells9051197.

[179] X. Liu, Z. Ser, J.W. Locasale, Development and quantitative evaluation of a high-resolution metabolomics technology, Anal. Chem. (2014) 86, 2175–84. doi:10.1021/ac403845u.

[180] C. Rombouts, M. De Spiegeleer, L. Van Meulebroek, W.H. De Vos, L. Vanhaecke, Validated comprehensive metabolomics and lipidomics analysis of colon tissue and cell lines, Anal. Chim. Acta. (2019) 1066, 79–92. doi:10.1016/j.aca.2019.03.020.

[181] T.-L. Han, Y. Yang, H. Zhang, K.P. Law, Analytical challenges of untargeted GC-MS-based metabolomics and the critical issues in selecting the data processing strategy, F1000Research. (2017) 6, 967. doi:10.12688/f1000research.11823.1.

[182] F.M. Van Der Kloet, I. Bobeldijk, E.R. Verheij, R.H. Jellema, Analytical error reduction using single point calibration for accurate and precise metabolomic phenotyping, J. Proteome Res. (2009) 8, 5132–41. doi:10.1021/pr900499r.

[183] B. Drotleff, M. Lämmerhofer, Guidelines for Selection of Internal Standard-based Normalization Strategies in Untargeted Lipidomic Profiling by LC-HR-MS/MS, Anal. Chem. (2019) 91, 9836–43. doi:10.1021/acs.analchem.9b01505.

[184] D.K. Barupal, S. Fan, B. Wancewicz, T. Cajka, M. Sa, M.R. Showalter, R. Baillie, J.D. Tenenbaum, G. Louie, R. Kaddurah-Daouk, O. Fiehn, Generation and quality control of lipidomics data for the alzheimer's disease neuroimaging initiative cohort, Sci. Data. (2018) 5, 1–13. doi:10.1038/sdata.2018.263.

[185] C.-Y. Chiu, K.-W. Yeh, G. Lin, M.-H. Chiang, S.-C. Yang, W.-J. Chao, T.-C. Yao, M.-H. Tsai, M.-C. Hua, S.-L. Liao, S.-H. Lai, M.-L. Cheng, J.-L. Huang, Metabolomics Reveals Dynamic Metabolic Changes Associated with Age in Early Childhood, PLoS One. (2016) 11, e0149823. doi:10.1371/journal.pone.0149823.

[186] R. Tirouvanziam, S. De Bentzmann, C. Hubeau, J. Hinnrasky, J. Jacquot, B. Péault, E. Puchelle, Inflammation and infection in naive human cystic fibrosis airway grafts, Am. J. Respir. Cell Mol. Biol. (2000) 23, 121–127. doi:10.1165/ajrcmb.23.2.4214.

[187] D.S. Armstrong, K. Grimwood, J.B. Carlin, R. Carzino, J.P. Gutièrrez, J. Hull, A. Olinsky, E.M. Phelan, C.F. Robertson, P.D. Phelan, Lower Airway Inflammation in Infants and Young Children with Cystic Fibrosis, 1997.

[188] M.T. Sutton, D. Fletcher, N. Episalla, L. Auster, M. Folz, Mesenchymal Stem Cell Soluble

Mediators and Cystic Fibrosis, J Stem Cell Res Ther. (2017) 7, 400. doi:10.4172/2157-7633.1000400.

[189] T.J. Kean, P. Lin, A.I. Caplan, J.E. Dennis, MSCs: Delivery routes and engraftment, cell-targeting strategies, and immune modulation, Stem Cells Int. (2013). doi:10.1155/2013/732742.

[190] T.L. Bonfield, M. Koloze, D.P. Lennon, B. Zuchowski, S.E. Yang, A.I. Caplan, Human mesenchymal stem cells suppress chronic airway inflammation in the murine ovalbumin asthma model, Am. J. Physiol. - Lung Cell. Mol. Physiol. (2010) 299,. doi:10.1152/ajplung.00182.2009.

[191] M. Podbielska, Z.M. Szulc, E. Kurowska, E.L. Hogan, J. Bielawski, A. Bielawska, N.R. Bhat, Cytokine-induced release of ceramide-enriched exosomes as a mediator of cell death signaling in an oligodendroglioma cell line, J. Lipid Res. (2016) 57, 2028–2039. doi:10.1194/jlr.M070664.

[192] M. Ollero, G. Astarita, I.C. Guerrera, I. Sermet-Gaudelus, S. Trudel, D. Piomelli, A. Edelman, Plasma lipidomics reveals potential prognostic signatures within a cohort of cystic fibrosis patients, J. Lipid Res. (2011) 52, 1011–1022. doi:10.1194/jlr.P013722.

[193] M. Ollero, Methods for the study of lipid metabolites in cystic fibrosis, J. Cyst. Fibros. (2004) 3, 97–98. doi:10.1016/j.jcf.2004.05.022.

[194] I.R.L. Del Ciampo, R. Sawamura, M.I. Machado Fernandes, Cystic fibrosis: From protein-energy malnutrition to obesity with dyslipidemia, Iran. J. Pediatr. (2013) 23, 605–6.

[195] D. Fang, R.H. West, M.E. Manson, J. Ruddy, D. Jiang, S.F. Previs, N.D. Sonawane, J.D. Burgess, T.J. Kelley, Increased plasma membrane cholesterol in cystic fibrosis cells correlates with CFTR genotype and depends on de novo cholesterol synthesis, Respir. Res. (2010) 11, 61. doi:10.1186/1465-9921-11-61.

[196] R. Ziobro, B. Henry, M.J. Edwards, A.B. Lentsch, E. Gulbins, Ceramide mediates lung fibrosis in cystic fibrosis, Biochem. Biophys. Res. Commun. (2013) 434, 705–9. doi:10.1016/j.bbrc.2013.03.032.

[197] Y.A. Hannun, L.M. Obeid, The ceramide-centric universe of lipid-mediated cell regulation: Stress encounters of the lipid kind, J. Biol. Chem. (2002) 277, 25847–25850. doi:10.1074/jbc.R200008200.

[198] Y.A. Hannun, L.M. Obeid, Principles of bioactive lipid signalling: Lessons from sphingolipids, Nat. Rev. Mol. Cell Biol. (2008) 9, 139–150. doi:10.1038/nrm2329.

[199] Y. Ramu, Y. Xu, Z. Lu, Inhibition of CFTR Cl- channel function caused by enzymatic hydrolysis of sphingomyelin, Proc. Natl. Acad. Sci. U. S. A. (2007) 104, 6448–53. doi:10.1073/pnas.0701354104.

[200] H. Grassmé, J. Riethmüller, E. Gulbins, Ceramide in Cystic Fibrosis, in: Handb. Exp. Pharmacol., Handb Exp Pharmacol, 2013: pp. 265–274. doi:10.1007/978-3-7091-1511-4_13.

[201] L. Astudillo, N. Therville, C. Colacios, B. Ségui, N. Andrieu-Abadie, T. Levade, Glucosylceramidases and malignancies in mammals, Biochimie. (2016) 125, 267–80. doi:10.1016/j.biochi.2015.11.009.

[202] M. Nagata, Y. Izumi, E. Ishikawa, R. Kiyotake, R. Doi, S. Iwai, Z. Omahdi, T. Yamaji, T. Miyamoto, T. Bamba, S. Yamasaki, Intracellular metabolite β-glucosylceramide is an endogenous Mincle ligand possessing immunostimulatory activity, Proc. Natl. Acad. Sci. (2017) 114, e3285-94. doi:10.1073/pnas.1618133114.

[203] A. Edsfeldt, P. Dunér, M. Stahlman, I.G. Mollet, G. Asciutto, H. Grufman, M. Nitulescu, A.F. Persson, R.M. Fisher, O. Melander, M. Orho-Melander, J. Borén, J. Nilsson, I. Gonçalves, Sphingolipids contribute to human atherosclerotic plaque inflammation, Arterioscler. Thromb. Vasc. Biol. (2016) 36, 1132–1140. doi:10.1161/ATVBAHA.116.305675.

[204] M. Apostolopoulou, R. Gordillo, C. Koliaki, S. Gancheva, T. Jelenik, E. De Filippo, C. Herder, D. Markgraf, F. Jankowiak, I. Esposito, M. Schlensak, P.E. Scherer, M. Roden, Specific hepatic sphingolipids relate to insulin resistance, oxidative stress, and inflammation in nonalcoholic steato hepatitis, Diabetes Care. (2018) 41, 1235–1243. doi:10.2337/dc17-1318.

[205] B.M. Barth, S.S. Shanmugavelandy, D.M. Tacelosky, M. Kester, S.A.F. Morad, M.C. Cabot, Gaucher's disease and cancer: A sphingolipid perspective, Crit. Rev. Oncog. (2013) 18, 221–34. doi:10.1615/CritRevOncog.2013005814.

[206] E. Seidl, H. Kiermeier, G. Liebisch, M. Ballmann, S. Hesse, K. Paul-Buck, F. Ratjen, E. Rietschel, M. Griese, Lavage lipidomics signatures in children with cystic fibrosis and protracted bacterial bronchitis, J. Cyst. Fibros. (2019) 18, 790–795. doi:10.1016/j.jcf.2019.04.012.

[207] M. Gentzsch, A. Choudhury, X.B. Chang, R.E. Pagano, J.R. Riordan, Misassembled mutant ΔF508 CFTR in the distal secretory pathway alters cellular lipid trafficking, J. Cell Sci. (2007) 120, 447–55. doi:10.1242/jcs.03350.

[208] D. Ma, A. Yoon, J. Bartlett, K.F. Faull, P.B. McCray Jr., E.T. Zemanick, E. Porter, Antimicrobial cholesteryl esters in cystic fibrosis airway secretions, Pediatr. Pulmonol. (2013) 10, e0125326.

[209] R. Ghidoni, A. Caretti, P. Signorelli, Role of sphingolipids in the pathobiology of lung inflammation, Mediators Inflamm. (2015) 2015, 487508. doi:10.1155/2015/487508.

[210] K. Arora, A. P. Naren, Pharmacological Correction of Cystic Fibrosis: Molecular Mechanisms at the Plasma Membrane to Augment Mutant CFTR Function, Curr. Drug Targets. (2016) 17, 1275–81. doi:10.2174/1389450117666151209114343.

[211] A.M. Matos, F.R. Pinto, P. Barros, M.D. Amaral, R. Pepperkok, P. Matos, Inhibition of calpain 1 restores plasma membrane stability to pharmacologically rescued Phe508del-CFTR variant, J. Biol. Chem. (2019) 294, 13396–410. doi:10.1074/jbc.ra119.008738.

[212] S. Wallner, E. Orso, M. Grandl, T. Konovalova, G. Liebisch, G. Schmitz, Phosphatidylcholine and phosphatidylethanolamine plasmalogens in lipid loaded human macrophages, PLoS One. (2018) 13, 1–21. doi:10.1371/journal.pone.0205706.

SCIENTIFIC PRODUCTION

My three-year research activities are concretized in 36 papers published in JCR reviewed journals; in 13 of those, I am the first author (average IF 4.1, HI 8). Moreover, I presented my researches at different national and international conferences through 8 talks and 15 posters.

Original papers

1. Fiorentino, T.V., Monroy, A., Kamath, S., Sotero, R., **Dei Cas M.**, Daniele, G., Chavez, A.O., Abdul-Ghani, M., Hribal, M.L., Sesti, G., Tripathy, D., DeFronzo, R.A., Folli, F., (2020). Pioglitazone corrects dysregulation of skeletal muscle mitochondrial proteins involved in ATP synthesis in type 2 diabetes. Metabolism 0, 154416. https://doi.org/10.1016/j.metabol.2020.154416

2. **Dei Cas M.,** Casagni E., Casiraghi, A. Minghetti P., Fornasari D., Ferri F., Arnoldi S., Gambaro V. and Roda G., Phytocannabinoids profile in Cannabis olive oils: comparison among different preparation methods. Front. Pharmacol.

3. Burrello, J., Biemmi, V., **Dei Cas, M**. et al. Sphingolipid composition of circulating extracellular vesicles after myocardial ischemia. Sci Rep 10, 16182 (2020). https://doi.org/10.1038/s41598-020-73411-7

4. **Dei Cas, M.,** Paroni, R., Saccardo, A., Casagni, E., Arnoldi, S et al. (2020). A straightforward LC-MS/MS analysis to study serum profile of short and medium chain fatty acidsds. Journal of Chromatography B, 1154:121982.

5. Saresella M, Marventano I, Barone M, La Rosa F, Piancone F, Mendozzi L, d'Arma A, Rossi V, Pugnetti L, Roda G, Casagni E, **Dei Cas M**, Paroni R, Brigidi P, Turroni S and Clerici M (2020) Alterations in Circulating Fatty Acid Are Associated With Gut Microbiota Dysbiosis and Inflammation in Multiple Sclerosis. Front. Immunol. 11:1390. doi: 10.3389/fimmu.2020.01390

6. Ramella A, Roda G, Pavlovic R, **Dei Cas M**, Casagni E, Mosconi G, Cecati F, Minghetti P, Grizzetti C. (2020) Impact of Lipid Sources on Quality Traits of Medical Cannabis-Based Oil Preparations. Molecules.25(13):2986.

7. Codini M, Tringaniello C, Cossignani L, Boccuto A, Mirarchi A, Cerquiglini L, Troiani S, Verducci G, Patria FF, Conte C, Cataldi S, Ceccarini MR, Paroni R, **Dei Cas M**, Beccari T, Curcio F, Albi E. (2020). Relationship between Fatty Acids Composition/Antioxidant Potential of Breast Milk and Maternal Diet: Comparison with Infant Formulas Molecules 25(12):2910

8. Fogagnolo P, Quisisana C, Caretti A, Marchina D, **Dei Cas M**, Melardi E, Rossetti L. (2020) Efficacy and Safety of VisuEvo® and Cationorm® for the Treatment of Evaporative and Non-Evaporative Dry Eye Disease: A Multicenter, Double-Blind, Cross-Over, Randomized Clinical Trial. Clin Ophthal

9. **Dei Cas, M**.; Zulueta, A.; Mingione, A.; Caretti, A.; Ghidoni, R.; Signorelli, P.; Paroni, R. (2020). An Innovative Lipidomic Workflow to Investigate the Lipid Profile in a Cystic Fibrosis Cell Line. Cells, 9, 1197.

10. Piano, I., D'Antongiovanni, V., Novelli, E., Biagioni, M., Ghidoni, R., **Dei Cas, M**., ... & Gargini, C. (2020). Myriocin effect on Tvrm4 retina, an Autosomal

Dominant pattern of Retinitis Pigmentosa. Frontiers in Neuroscience, 14, 372.

11. **Dei Cas, M.**; Roda, G.; Li, F.; Secundo, F. Functional Lipids in Autoimmune Inflammatory Diseases. (2020) Int. J. Mol. Sci., 21, 3074.
12. Vitalini, S., **Dei Cas, M.**, Rubino, F. M., Vigentini, I., Foschino, R., Iriti, M., & Paroni, R. (2020). LC-MS/MS-Based Profiling of Tryptophan-Related Metabolites in Healthy Plant Foods. Molecules, 25(2), 311.
13. Mingione, A., **Dei Cas, M.,** Bonezzi, F., Caretti, A., Piccoli, M., Anastasia, L., ... Signorelli, P. (2020). Inhibition of Sphingolipid Synthesis as a Phenotype-Modifying Therapy in Cystic Fibrosis. Cell Physiol Biochem, 54, 110-125.
14. Biemmi V, Milano G, Ciullo A, Cervio E, Burrello J, **Dei Cas M**, Paroni R, Tallone T, Moccetti T, Pedrazzini G, Longnus S, Vassalli G, Barile L. (2020) Inflammatory extracellular vesicles prompt heart dysfunction via TRL4-dependent NF-κB activation. Theranostics; 10(6):2773-2790
15. Rubino F.M., **Dei Cas M.,** Bignotto M., Ghidoni R., Iriti M., Paroni R. (2020). Discovery of Unexpected Sphingolipids in Almonds and Pistachios with an Innovative Use of Triple Quadrupole Tandem Mass Spectrometry. Foods.
16. **Dei Cas M**., Casagni E., Saccardo A., Arnoldi S., Young C., Scotti S., Vieira de Manicor E., Gambaro V., Roda G. (2020). The Italian panorama of Cannabis light preparation: determination of cannabinoids by LC-UV. Forensic Science International.
17. Paroni, R.; Casati, S.; **Dei Cas, M.**; Bignotto, M.; Rubino, F.M.; Ciuffreda, P. (2019) Unambiguous Characterization of p-Cresyl Sulfate, a Protein-Bound Uremic Toxin, as Biomarker of Heart and Kidney Disease. Molecules.
18. Zanaboni, M., Roda, G. , Arnoldi, S. , Casagni, E. , Gambaro, V. and **Dei Cas, M**. (2019), Comparison of Different Analytical Methods for the Determination of Carbon Monoxide in Postmortem Blood. J Forensic Sci.
19. Zulueta A., Peli V., **Dei Cas M**., Colombo M., Paroni R., Falleni M., Baisi A., Bollati V., Chiaramonte R., Del Favero E., Ghidoni R., Caretti A. (2019). Inflammatory role of extracellular sphingolipids in Cystic Fibrosis. The International Journal of Biochemistry & Cell Biology.
20. La Corte, E.; **Dei Cas, M.**; Raggi, A.; Patanè, M.; Broggi, M.; Schiavolin, S.; Calatozzolo, C.; Pollo, B.; Pipolo, C.; Bruzzone, M.G.; Campisi, G.; Paroni, R.; Ghidoni, R.; Ferroli, P (2019) Long and Very-Long-Chain Ceramides Correlate with A More Aggressive Behavior in Skull Base Chordoma Patients. International Journal of Molecular Sciences 20(18):4480
21. **Dei Cas, M.**; Ghidoni, R. (2019) Dietary Curcumin: Correlation between Bioavailability and Health Potential. Nutrients, 11, 2147.

22. Bonezzi, F., Piccoli, M., **Dei Cas, M.**, Paroni, R., Mingione, A., Monasky, M. M., ... & Anastasia, L. (2019). Sphingolipid synthesis inhibition by Myriocin administration enhances lipid consumption and ameliorates lipid response to myocardial ischemia reperfusion injury. Frontiers in Physiology

23. Paroni, R., **Dei Cas, M.**, Rizzo, J., Ghidoni, R., Montagna, M. T., Rubino, F. M., & Iriti, M. (2019). Bioactive phytochemicals of tree nuts. Determination of the melatonin and sphingolipid content in almonds and pistachios. Journal of Food Composition and Analysis.

24. Vizzari G., Sommariva M.C., **Dei Cas M.**, Bertoli S., Vizzuso S., Radaelli G., Battezzati A., Paroni R., Verduci E. (2019) Circulating Salicylic Acid and Metabolic Profile after 1-Year Nutritional–Behavioral Intervention in Children with Obesity. Nutrients

25. **Dei Cas, M.,** Casagni, E., Arnoldi, S., Gambaro, V., Roda, G. (2019). Screening of new psychoactive substances (NPS) by gas-chromatography/time of flight mass spectrometry (GC/MS-TOF) and application to 63 cases of judicial seizure. Forensic Science International: Synergy.

26. Roda G., Faggiani F., Bolchi C., Pallavicini M., **Dei Cas M.** (2019). Ten years of fentanyl-like drugs: a technical-analytical review, Analytical sciences, Volume 35, Issue 5, Pages 479-491

27. **Dei Cas M.,** E. Casagni, V. Gambaro, et al., (2019) Determination of daptomycin in human plasma and breast milk by UPLC/MS-MS, Journal of Chromatography B

28. Alessandri, G., Coccè, V., Pastorino, F., Paroni, R., **Dei Cas, M.**, Restelli, F., … Pessina, A. (2019). Microfragmented human fat tissue is a natural scaffold for drug delivery: Potential application in cancer chemotherapy. Journal of Controlled Release.

29. Platania C., **Dei Cas M.**, Cianciolo S., Fidilio A., Lazzara F., Paroni R., Pignatello R., Strettoi E., Ghidoni R., Drago F., Bucolo C. (2019) Novel ophthalmic formulation of myriocin: implications in retinitis pigmentosa, Drug Delivery, 26:1, 237-243

30. Coccè, V.; Franzè, S.; Brini, A.T.; Giannì, A.B.; Pascucci, L.; Ciusani, E.; Alessandri, G.; Farronato, G.; Cavicchini, L.; Sordi, V.; Paroni, R.; **Dei Cas, M.**; Cilurzo, F.; Pessina, A. (2019) In Vitro Anticancer Activity of Extracellular Vesicles (EVs) Secreted by Gingival Mesenchymal Stromal Cells Primed with Paclitaxel. Pharmaceutics, 11(2): 61.

31. Roda G., Arnoldi S., Casagni E., **Dei Cas M.**, Silva L., Carini M. (2018). Determination of Polycyclic Aromatic Hydrocarbons in Lipstick by Gas-Chromatography coupled to Mass Spectrometry: a case history, Journal of Pharmaceutical and Biomedical Analysis

32. Bifari F., Manfrini R., **Dei Cas M.,** Berra C., Siano M., Zuin M., Paroni R., Folli F. (2018). Multiple target tissue effects of GLP-1 analogues on non-alcoholic fatty liver disease (NAFLD) and non-alcoholic steatohepatitis (NASH), Pharmacological Research, 137, 219-229

33. **Dei Cas, M.;** Ghidoni, R. (2018). Cancer Prevention and Therapy with Polyphenols: Sphingolipid-Mediated Mechanisms. Nutrients, 10, 940.

34. Roda, G., Arnoldi, S., **Dei Cas, M.,** Ottaviano, V., Casagni, E., Tregambe, F., ... & Gambaro, V. (2018). Determination of Cyanide by Microdiffusion Technique Coupled to Spectrophotometry and GC/NPD and Propofol by Fast GC/MS-TOF in a Case of Poisoning. Journal of Analytical Toxicology.

35. Farè, F., **Dei Cas, M**., Arnoldi, S., Casagni, E., Visconti, G. L., Parnisari, G., ... & Roda, G. (2018). Determination of Methyldibromoglutaronitrile (MDBGN) in Skin Care Products by Gaschromatography-Mass Spectrometry Employing an Enhanced Matrix Removal (EMR) Lipid Clean-Up. Eur. J. Lipid Sci. Technol. 2018, 120, 1700525

36. Cesari, E., Roda, G., Visconti, G. L., Ramondino, S., **Dei Cas, M.,** Monina, G., & Gambaro, V. (2017). Daptomycin excretion into human milk. British journal of clinical pharmacology.

Talk

1. Flash communication for young researcher: “Screening of new psychoactive substances (NPS) by gas-chromatography/time of flight mass sprectrometry GC/MS-TOF” International meeting on RDPA Recent Developments in Pharmaceutical Analysis (Rimini, 20-23.09.2017)
2. Flash communication for young researcher: “Mass spectrometry: an essential tool for the study of sphingolipids metabolism in clinical and basic research” Breakfast meeting at DISS (Milano, 24.04.2018)
3. “Sfingolipidomica nei cordomi della base cranio” Giornata italiana degli sfingolipidi (Milano, 5.10.2018)
4. “In-vivo pharmacokinetic of paclitaxel released by devitalized microfragmented adipose tissue” Congresso DISS (Milano, 9.11.2018)
5. “In-vivo pharmacokinetic of paclitaxel released by devitalized microfragmented fat tissue: potential application in chemotherapy” Riunione dei giovani biochimici dell’area milanese (Gargnano, 23-25.06.2019)
6. “LC-MS/MS analysis to study serum profile of short and medium chain fatty acids” Recent development in Pharmaceutical Analysis (Pescara, 8-11.09.2020).
7. “Untargeted lipidomic to study the pathological phenotype of cystic fibrosis. Therapeutic role of myriocin in the sphingolipid synthesis inhibition.” Congresso DISS (Milano, 8.11.2020).
8. “Il contributo di lipidomica e metabolomica in diverse patologie”. Riunione biochimici lombardi (Milano, 13.02.2020).

Poster

1. ID-UPLC-MS-MS analysis of melatonin, tryptophan and related indolic metabolites: pilot applications to vegetables and human matrices Secondo congresso di spettrometria di massa (Milano, 21-22.06.2018)
2. Pharmacokinetics of myriocin in rabbit's eyes IMSC 2018, XXII International Mass Spectrometry Conference (Florence, 26-31.08.2018)
3. Indolome analysis for nutraceutical and physiological studies IMSC 2018, XXII International Mass Spectrometry Conference (Florence, 26-31.08.2018)
4. Ceramidome plasticity through iso-energetic precursor and neutral loss discovery scans IMSC 2018, XXII International Mass Spectrometry Conference (Florence, 26-31.08.2018)
5. Pharmacokinetics and bioavailability of different acetylsalicylic acid formulations assessed by Liquid Chromatography-Tandem Mass Spectrometry in healthy subjects. IMSC 2018, XXII International Mass Spectrometry Conference (Florence, 26-31.08.2018)
6. De-novo ceramide synthesis in skull base chordomas suggests a correlation with tumor proliferation
   13TH European association of neuro-oncology (Stockholm, 10-14.10.2018)
7. In Vitro Anticancer Activity of Extracellular Vesicles (EVs) Secreted by Gingival Mesenchymal Stromal Cells Primed with Paclitaxel. Research challenge for clinical application of MSCs (Genova, 4-5.04.2019)
8. Modulation of ceramide levels in rabbit's eyes by eye-drop myriocin administration. FEBS Special Meeting in Sphingolipid Biology (Cascais, 6-10.05.2019)
9. Myriocin potential as a phenotype-modifying therapeutical in Cystic Fibrosis. FEBS Special Meeting in Sphingolipid Biology (Cascais, 6-10.05.2019)
10. Inflammatory role of extracellular lipids in Cystic Fibrosis. FEBS Special Meeting in Sphingolipid Biology (Cascais, 6-10.05.2019)
11. In-vivo pharmacokinetic of paclitaxel released by devitalized microfragmented fat tissue: potential application in chemotherapy. Riunione dei giovani biochimici dell'area Milanese (Gargnano, 23-25.06.2019)
12. Production of kynurenic acid and other tryptophan derivatives in Saccaromyces and non-Saccharomyces wine yeasts 7th Conference on Physiology of yeasts and filamentous fungi (Milano, 24-27.07.2019)

13. Modulation of sphingolipids by non-invasive myriocin administration: potential treatment for retinitis pigmentosa. European Society for Neurochemistry, biennial conference (Milano, 1-4.09.2019)
14. Determination of polycyclic aromatic hydrocarbons in lipstick by gas-chromatography coupled to mass spectrometry: a case history Recent development in Pharmaceutical Analysis (Pescara 8-11.09.2020)
15. "Cannaboom": an overview of legal and therapeutic cannabis use in Italy Recent development in Pharmaceutical Analysis (Pescara 8-11.09.2020)

APPENDIX

International Journal of Biochemistry and Cell Biology 116 (2019) 105622

Contents lists available at ScienceDirect

International Journal of Biochemistry and Cell Biology

journal homepage: www.elsevier.com/locate/biocel

Inflammatory role of extracellular sphingolipids in Cystic Fibrosis

Aida Zulueta[a], Valeria Peli[a], Michele Dei Cas[a], Michela Colombo[b,g], Rita Paroni[a], Monica Falleni[c], Alessandro Baisi[d], Valentina Bollati[e], Raffaella Chiaramonte[b], Elena Del Favero[f], Riccardo Ghidoni[a], Anna Caretti[a,*]

[a] Biochemistry and Molecular Biology Lab., Health Sciences Department, University of Milan, Via A. di Rudinì, 8, Milan, Italy
[b] Laboratory of Experimental Medicine and Pathophysiology, Health Sciences Department, University of Milan, Via A. di Rudinì, 8, Milan, Italy
[c] Pathology Division, Health Sciences Department, University of Milan, San Paolo Hospital Medical School, Via A. di Rudinì, 8, Milan, Italy
[d] Thoracic Surgery Unit, Health Sciences Department, University of Milan, San Paolo Hospital Medical School, Via A. di Rudinì, 8, Milan, Italy
[e] EPIGET LAB, Department of Clinical Sciences and Community Health, University of Milan, Milan, Italy
[f] Department of Medical Biotechnology and Translational Medicine, University of Milan, Via Fratelli Cervi 93, Milan, Italy
[g] Haematopoietic Stem Cell Biology Laboratory, Medical Research Council(MRC) Weatherall Institute of Molecular Medicine (WIMM), University of Oxford, Oxford OX39DS, UK

ARTICLE INFO

Keywords:
Sphingolipids
Ceramide
Inflammation
Extracellular vesicles
Mesenchymal stem cells

ABSTRACT

Ceramide is emerging as one of the players of inflammation in lung diseases. However, data on its inflammatory role in Cystic Fibrosis (CF) as part of the extracellular machinery driven by lung mesenchymal stem cells (MSCs)-derived extracellular vesicles (EVs) are missing.

We obtained an *in vitro* model of CF-MSC by treating control human lung MSCs with a specific CFTR inhibitor. We characterized EVs populations derived from MSCs (ctr EVs) and CF-MSCs (CF-EVs) and analyzed their sphingolipid profile by LC–MS/MS. To evaluate their immunomodulatory function, we treated an *in vitro* human model of CF, with both EVs populations.

Our data show that the two EVs populations differ for the average size, amount, and rate of uptake. CF-EVs display higher ceramide and dihydroceramide accumulation as compared to control EVs, suggesting the involvement of the *de novo* biosynthesis pathway in the parental CF-MSCs. Higher sphingomyelinase activity in CF-MSCs, driven by inflammation-induced ceramide accumulation, sustains the exocytosis of vesicles that export new formed pro-inflammatory ceramide.

Our results suggest that CFTR dysfunction associates with an enhanced sphingolipid metabolism leading to the release of EVs that export the excess of pro-inflammatory Cer to the recipient cells, thus contributing to maintain the unresolved inflammatory status of CF.

1. Introduction

Long considered structural and metabolic molecules, sphingolipids (SPLs) have been recognized as signaling mediators. SPLs are localized in the plasma and in intracellular organelle membranes, with ceramide (Cer) being the structural unit of membrane-forming SPLs and the main modulator of cellular processes such as cell growth, cell death and inflammation (Hannun and Obeid, 2008; Chiricozzi et al., 2018). Cer can derive from the *de novo* biosynthesis pathway or from the so-called salvage pathway via degradation of complex SPLs, such as sphingomyelin (SM), the most abundant membrane lipid (Gault et al., 2010; Marchesini and Hannun, 2004). Among sphingolipids, Cer is emerging as one of the players of the pulmonary dysfunction in inflammatory lung diseases, such as Chronic Obstructive Pulmonary Disease (COPD) and Cystic Fibrosis (CF) (Petrache and Petrusca, 2013; Grassme et al., 2013). Its accumulation in the airways of CFTR-deficient mice, is related to pulmonary inflammation, death of epithelial cells, and susceptibility to severe *P. aeruginosa* infections in mice and in human (Teichgraber et al., 2008; Riethmuller et al., 2009; Becker et al., 2010). We previously demonstrated that the *de novo* ceramide synthesis contributes to lung inflammation and *P. aeruginosa* infection in a murine CF model (Caretti et al., 2014). Moreover, we observed that reducing

* Corresponding author.
E-mail addresses: aida.zulueta@unimi.it (A. Zulueta), valeria.peli@unimi.it (V. Peli), michele.deicas@unimi.it (M. Dei Cas), michela.colombo1@unimi.it (M. Colombo), rita.paroni@unimi.it (R. Paroni), monica.falleni@unimi.it (M. Falleni), alessandro.baisi@unimi.it (A. Baisi), valentina.bollati@unimi.it (V. Bollati), raffaella.chiaramonte@unimi.it (R. Chiaramonte), elena.delfavero@unimi.it (E. Del Favero), riccardo.ghidoni@unimi.it (R. Ghidoni), anna.caretti@unimi.it (A. Caretti).

https://doi.org/10.1016/j.biocel.2019.105622
Received 3 May 2019; Received in revised form 24 September 2019; Accepted 25 September 2019
Available online 26 September 2019

ceramide accumulation in CF airways, correlates with an up-regulation of the anti-oxidative response of the transcriptional factor NRF2, even under infection by *A. fumigatus* (Caretti et al., 2016) and with a down-regulation of the pro-inflammatory cytokine release (Caretti et al., 2014).

Mesenchymal stem cells (MSCs) are multipotent non-hematopoietic stem cells residing in many tissues, including the lung, with an emergent role in the attenuation of inflammation mainly due to the release of extracellular vesicles (EVs). EVs are membrane-derived particles that comprise both exosomes and microvesicles (MVs). Exosomes are generated inside multivesicular bodies (MVB) and are generally 30–100 nm in diameter. Microvesicles are derived from the plasma membrane and are generally larger than exosomes, ranging from 100 to 300 nm. They are involved in intercellular communication since they carry a large array of bioactive molecules including proteins, mRNA, miRNA and bioactive lipids to distant cells (Fatima et al., 2017; Dostert et al., 2017). We have recently demonstrated the role of EVs produced by human lung MSCs in controlling inflammation process. In an *in vitro* CF bronchial epithelial cellular model, EVs treatment reduces transcription and protein expression of pro-inflammatory cytokines such as IL-1β, IL-8, IL-6, under basal and TNFα stimulated conditions. This effect could be mediated by up-regulation of the PPARγ axis, whose down-stream effectors (NF-kB and HO-1) are well-known modulators of inflammatory and oxidative stress pathways (Zulueta et al., 2018).

SPLs participate in EVs biogenesis and in EVs activity towards target cells, as reviewed by Verderio C. and colleagues (Verderio et al., 2018). Cer derived from SM hydrolysis, promoted by neutral sphingomyelinase 2 (n-SMase2), drives exosomes formation and transport via an ESCRT-independent pathway (Trajkovic et al., 2008). Secretion of neuron-derived exosomes was modulated by the activities of sphingolipid-metabolizing enzymes, including nSMase2, in Alzheimer disease models (Yuyama et al., 2012; Dinkins et al., 2014). As for MVs, the acid sphingomyelinase generates Cer that in turn triggers MVs budding from the plasma membrane (Bianco et al., 2009). SM to Cer conversion alters membrane curvature and fluidity, driving membrane evagination of MVs by means of redistribution of inverted cone-shaped Cer molecules (Subra et al., 2007). Several lines of evidence indicate Cer-enriched exosomes as mediators of cytotoxic effects in target cells. Primary cultured astrocytes secrete prostate apoptosis response 4 (PAR-4)/ceramide-enriched exosomes that represent a novel mechanism of Aβ-dependent apoptosis in Alzheimer disease (Wang et al., 2012). More recently, Podbielska M. and colleagues, demonstrated the pro-apoptotic potential of Cer-enriched exosomes released by a human oligodendroglioma cell line previously stimulated with inflammatory cytokines (Podbielska et al., 2016).

In the present manuscript, we investigated the hypothesis that lung MSCs and MSCs-derived EVs could be immunologically impaired in CF, partially because of altered SPLs content. By means of an *in vitro* model of CF-MSCs, we found higher ceramide and dihydroceramide (dhCer) content in EVs shed from CF-MSCs (CF-EVs) than in control MSCs-derived EVs (ctr EVs), with C16:0 and the long acyl chain ceramides (C22:0; C24:0; C24:1) being the most representative. Moreover, the two EV populations are different in term of average size, amount, and rate of uptake by the recipient cells. As for parental MSCs, total Cer and sphingomyelin content significantly increased and decreased, respectively. By treating IB3-1, a bronchial epithelial cell line derived from a CF patient, with CF-EVs or ctr EVs, we observed that CF-EVs are less efficient in decreasing pro-inflammatory cytokines expression. Overall, we observed an inverse correlation between the anti-inflammatory efficacy of EVs and their Cer content.

In conclusion, our data suggest that lung MSCs compartment may be immunologically altered in CF thus contributing to maintain the chronic, unresolved pulmonary inflammation.

2. Materials and methods

2.1. Reagents and antibodies

The following materials were purchased: bFGF and TNFα from Peprotech LTD (Israel); LHC Basal, LHC-8 w/o gentamicin culture media from Gibco (US); FBS and DMEM from Euro Clone Life Science Division (Italy); protease inhibitors (Roche Italia, Italy); CellBrite Green Cytoplasmic Membrane Dye (Biotium, US); SYBR Green system (Qiagen, Italy); synthetic oligonucleotides from M-Medical (Italy), I-172 CFTR inhibitor (Sigma Aldrich, DE). Methanol, acetonitrile, ammonium formate, acetic acid, potassium hydroxide and formic acid (all analytical grade) were supplied from Merck (Darmstadt, Germany). Water was MilliQ grade. Sphingolipids standards were purchased by Avanti Polar Lipids (Alabaster, USA). Primary antibodies: anti- PPARγ (ElabScience, US), anti-H3 (Cell Signaling, US), anti-β-actin (Sigma, US), anti-CFTR Type A4 (596) (University of North Carolina – Chapel Hill, UNC-CH, on behalf of Cystic Fibrosis Foundation, USA), anti-HO-1 (Abcam, UK), anti-caspase 9 (Cell Signaling, US), anti-LC3 (Cell Signaling, US). The secondary antibodies were from Jackson Laboratories (Bar Harbor, ME, US). All reagents were of the maximal available purity degree.

2.2. Ethic statements

Human lung mesenchymal stem cells (MSCs) were isolated from lung biopsies obtained from seven patients that underwent lung surgery for suspected bullous emphysema or lung tumor. Tissues were obtained under appropriate approval by the Ethical Committee of the ASST Santi Paolo e Carlo, Milano, Area A (n°2211, 12/14/2016). All participants signed informed consent forms approved by the Ethical Committee before surgery and specimen collection. All the procedures followed the Declaration of Helsinki protocols.

2.3. Isolation and treatment of human lung MSCs

Human lung MSCs were isolated and cultured as previously described (Zulueta et al., 2018). Briefly, lung samples were recovered after planned surgery for non infectious diseases (bullous and tumor lesions). Each lung biopsy of about 1 cm^3, was minced with surgical scissors and maintained in DMEM medium containing 18% FBS and 1% penicillin/streptomycin at 37 °C in a humid atmosphere containing 5% CO_2 for ten days. At day tenth, the adherent cells were cultured continuously in the presence of bFGF (5 ng/mL) until the passage seven. To obtain an *in vitro* model of Cystic Fibrosis MSCs (CF-MSCs), control MSCs (ctr MSCs) were treated with 10 μg/ml of I-172 CFTR inhibitor for 48 h, as reported by Mattoscio et al (Mattoscio et al., 2010). Control MSCs are intended as treated with dimethyl sulfoxide (DMSO), the I-172 CFTR inhibitor's solvent.

2.4. Isolation of Extracellular vesicles (EVs) derived from human lung MSCs

EVs were obtained from the supernatants of both ctr- and CF-MSCs cultures (ctr EVs and CF-EVs, respectively) after 48–72 hours, by ultracentrifugation as previously described (Bonzini et al., 2017). After serial centrifugations (1000, 2000 and 3000 *g* for 15 min at 4 °C), supernatants were centrifuged at 110,000 *g* (Beckman Coulter Optima L-90 K ultracentrifuge) for 75 min at 4 °C. EVs were resuspended according to the final MSCs number (10 μl per 1×10^6 cells).

2.5. Cell line and treatments

IB3-1 cells, an adeno-associated virus-transformed human bronchial epithelial cell line derived from a CF patient (ΔF508/W1282X) provided by LGC Promochem (US), were grown in LHC-8 medium

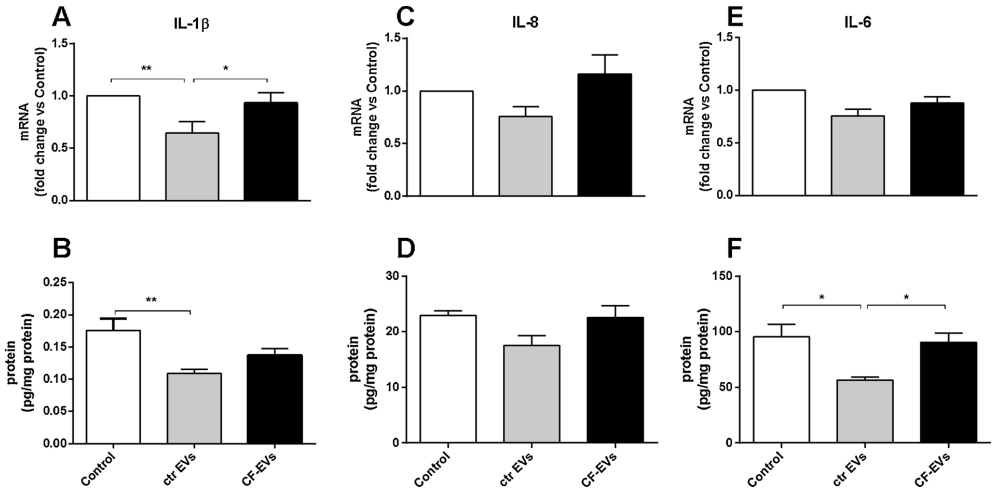

Fig. 1. Effects of EVs derived from ctr and CF-MSCs on cytokines mRNA expression and protein release in IB3-1 cells. The mRNA expression was evaluated by RT-PCR and the results reported as fold change over the control untreated IB3-1 cells. The cytokines content, expressed as picograms per mg of protein (pg/mg), was measured by ELISA in culture media of IB3-1 cells. Panel **A** and **B** refer to IL-1β mRNA and protein; panel **C** and **D**, to IL-8 mRNA and protein; panel **E** and **F**, to IL-6 mRNA and protein, respectively. Control refers to untreated IB3-1 cells at basal condition; ctr EVs refers to cells treated for 24 h with EVs from control MSCs; CF-EVs refers to cells treated for 24 h with EVs from CF-MSCs, meaning MSCs supplemented with 10 μg/ml of CFTR inhibitor, I-172, for 48 h. Data, expressed as mean ± SEM, are obtained from seven individual MSCs - derived EVs populations. The samples were run in triplicate for RT-PCR or in duplicate for ELISA analysis. Significance was evaluated by one-way ANOVA, followed by Newman-Keuls post-test. **, $p < 0.01$; *, $p < 0.05$.

supplemented with 5% FBS, 1% penicillin/streptomycin at 37 °C and 5% CO_2. For the treatments, 2.5×10^5 cells/well in 3 mL medium were plated in 6-well tissue culture dishes for twenty-four hours. Then, the medium was replaced with fresh one (control group), or supplemented with 30 μL of EVs derived from either control or CF-MSCs (ctr EVs and CF-EVs group, respectively) for 24 h. Cells were then harvested to perform different assays. Cell viability was evaluated by Trypan blue exclusion test as previously reported (Fabiani et al., 2017).

2.6. EV uptake

Five millions ctr MSCs and CF-MSCs were labeled with CellBrite Green Cytoplasmic Membrane Dye (Biotium) according to the manufacturer's instructions and supernatants were collected after 72 h and used to isolate EVs' populations by ultracentrifugation. IB3-1 cells were seeded in 24-well culture plates and treated for 16 h with 100 μL of either ctr- or CF-EVs suspension obtained by resuspension in 500 μL of IB3-1 cell medium. Then, the cells were trypsinized and analyzed by flow cytometry.

2.7. Nanoparticle tracking analysis (NTA) of EVs

The size and total number of EVs were calculated with the technology of Nanoparticle Tracking Analysis (NTA) that allows measuring the Brownian motion of suspended vesicles (Pergoli et al., 2017). By using the NanoSight NS300 system (Amesbury, UK), five 30-s recordings were made for each sample and the data were analyzed with NTA software. In order to eliminate the presence of vesicles derived from FBS in the medium, EVs samples were obtained from ctr- and CF-MSCs cultured in FBS free medium for 24 h. The results are provided as high-resolution particle-size distribution and particles concentration.

2.8. Laser light scattering analysis of EVs

Parallel Dynamic and Static Laser Light Scattering (DLS and SLS) experiments were performed on a home-made apparatus equipped with four optical channels, to reach high sensitivity (Lago and Rovati, 1993). Samples were inserted in a quartz cell kept at 25 °C or 37 °C. Light scattering measurements gave information on molecular mass of the particles in solution and on their translational diffusion coefficient, related to their hydrodynamic radius. DLS data were analyzed by both the cumulants method, to detect the weight-average hydrodynamic size of particles, and the non-negative least-squares (NNLS) method (Lawson and Hanson, 1995), suitable to determine the size distribution of EVs. EVs samples were prepared as described for NTA analysis and observed by light scattering to verify the presence/absence of particles in the same size range of EVs. All samples were diluted 1:10 with filtered PBS to avoid multiple scattering.

2.9. Sphingolipid profile of EVs and MSCs

Sphingolipid extraction and LC–MS/MS evaluation were performed according to the procedure already published elsewhere (Platania et al., 2019). Briefly, in order to increase the recovery of low-abundance sphingolipids, samples were extracted by a monophasic Bligh-Dyer method with alkaline methanolysis. Purified samples (10 μL) were directly injected to LC–MS/MS instrumentation (UPLC Dionex 3000 UltiMate - Thermo Fisher Scientific, USA) connected to an ABSciex 3200 QTRAP - AB Sciex S.r.l., Milano, Italy) for quantitative analysis. Separation was attained on a reversed-phase BEH C-8 10 × 2.1 x 1.7 μm analytical column with a linear gradient obtained by mixing eluent A (water + 2 mM ammonium formate + 0.2% formic acid) and eluent B (methanol + μ ammonium formate + 0.2% formic acid). Multiple reaction monitoring (MRM) mode was used. For ceramides and dihydroceramides quantitative analysis was performed interpolating each peak area of analyte/area IS (200 pmol Cer C12) with a calibration curve of each sphingolipid. For sphingomyelins, since the standards were not available, relative quantification was achieved by the ratio of the analyte/area IS (200 pmol SM C12). Then, sphingolipids amount was normalized by total protein content, expressed in milligram, in each sample.

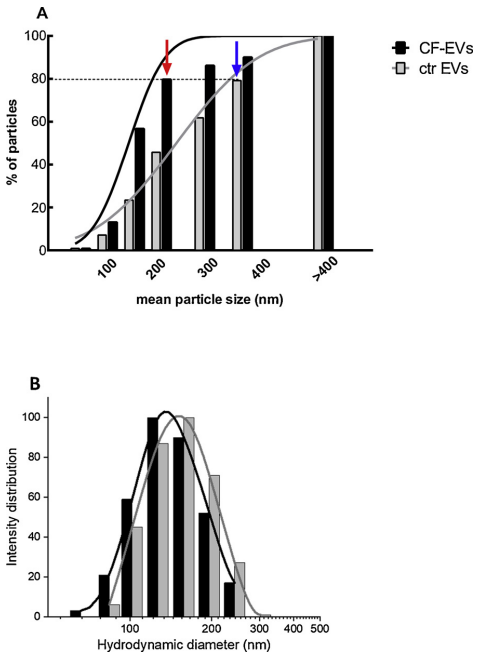

Fig. 2. Morphological features of ctr and CF-EVs populations. Panel **A** shows an example of Nanoparticle Tracking Analysis (NTA) representing the overall distribution of the particles in ctr and CF-EV populations, according to their mean size. On the cumulative plot, data are reported as percentage of particles distributed within a mean size value, expressed as nm. Panel **B** reports an example of Dynamic Light Scattering analysis showing the intensity weighted distribution of hydrodynamic diameters for ctr EVs and CF-EVs. The black bars and the corresponding black plotting curve refer to CF-EV. The gray bars and the corresponding plotting curve refer to EVs from control MSCs. The graphs are the most representative of four different analysis.

2.10. RNA extraction and quantitative RT-PCR

Real-time PCR was performed on RNA from control and ctr EVs and CF-EVs-treated IB3-1 ($2{,}5 \times 10^5$ cells/well). RNA extraction and reverse transcription were performed as previously reported (Zulueta et al., 2018). Human gene primer sequences for SPTLC 1, SPTLC 2, SPTLC 3, nSMase2, PPARγ, IL-1β, IL-8, IL-6 and GAPDH were previously published (Zulueta et al., 2018; Hornemann et al., 2006; Kubota et al., 2015; Dechecchi et al., 2011). RT-PCRs were performed on a StepOnePlus Real-Time PCR Systems (Thermofisher). Results were normalized on GAPDH and the 2-ΔΔCt method was used to calculate the relative value of gene expression *vs* control cells (Arocho et al., 2006). Determinations were done in triplicate.

2.11. Protein extraction and western blotting

Nuclear and cytoplasmic extracts from 5×10^5 IB3-1 cells, either treated or not with EVs, were obtained with the NE-PER Nuclear and Cytoplasmic Extraction Reagents kit (Thermo scientific) according to the manufacturer's instructions, for PPARγ evaluation. To characterize CFTR channel expression, whole cell lysates were prepared by trypsinization of treated and control MSCs, washed in cold PBS containing protease inhibitors, centrifuged at 800 g for 5 min at 4 °C, and finally resuspended in the same PBS solution. Equal amounts of nuclear (10 μg) or cytoplasmic (20 μg) protein's extracts were resuspended in Laemmli solution, separated by electrophoresis and immunoblotted as previously described (Fabiani et al., 2017). Anti-PPARγ (1:500 in TBS-T), anti HO-1 (1:1000 in TBS-T), anti-caspase 9 (1:1000 in TBS-T), anti-LC3 (1:1000 in TBS-T), anti-β-Actin (1:5000 in TBS-T), and anti-H3 (1:500 in TBS-T) antibodies were used. H3 and β-Actin contents were quantified for data normalization of nuclear and cytoplasmic markers, respectively. Specific bands intensity, as revealed by chemiluminescence, was quantified by Alliance UVITEC Cambridge.

2.12. ELISA determinations

The protein expression of the cytokines IL-1β, IL-6 and IL-8 was determined in treated IB3-1 culture media by biomarker multiplex immunoassays on Luminex® Platform. Cell protein concentration, was calculated by Bradford assay and used for data normalization. Determinations have been performed in duplicate.

2.13. Ferric reducing antioxidant power (FRAP) assay

The ferric reducing antioxidant power (FRAP) assay was performed according to previously published method (Benzie and Strain, 1999) with minor modifications (Zulueta et al., 2017).

2.14. Statistical analysis

Data significance was evaluated by paired two-tailed Student *t*-test and by one-way ANOVA followed by the Newman-Keul post-test when significant ($P < 0.05$). The results are the mean value (mean ± SEM) from five to seven individual experiments, depending on the assay. Either duplicate or triplicate samples for each treatment were performed. Western blotting, light scattering and flow cytometry images are the most representative. Statistical analysis was performed by GraphPad Instat software (La Jolla, CA, USA) and graph illustrations by GraphPad Prism software (La Jolla, CA, USA).

3. Results

3.1. EVs released from ctr- and CF-MSCs differently attenuate the pro-inflammatory profile of IB3-1 cells

In order to investigate the hypothesis that lung MSCs and MSC-derived EVs could be immunologically impaired in CF, we obtained an *in vitro* model of CF-MSCs, by treating control MSCs with the specific CFTR inhibitor, I-172 (Mattoscio et al., 2010). At first, we confirmed by Western Blotting analysis that lung MSCs express CFTR protein as it is shown in Supplementary Fig. 1. IB3-1 cells cultured in basal condition, were treated for 24 h with 30 μL of EVs released from either I-172-treated or untreated MSCs (namely CF-EVs or ctr EVs). The cell viability was unaffected by the treatment with CF-EVs and neither signs of early apoptosis nor of autophagy were increased as compared to the ctr EVs-treated cells (Supplementary Fig. 2). Concerning the expression of pro-inflammatory cytokines, following ctr EVs supplementation we observed a trend toward a decrease in the mRNA and protein expression of IL-1β, IL-8 and IL-6 vs control IB3-1 cells not supplemented (Fig. 1). IL-1β seems the most responsive, showing a significant 35% reduction at both the transcriptional and the protein level (Fig. 1, panel A;B) though IL-6 protein amount moves from 95.4 ± 11.4 to 56.6 ± 2.5 pg/mg protein, with a global 40% reduction (Fig. 1, panel F).

As a whole, CF-EVs seem less effective then ctr EVs in attenuating the pro-inflammatory profile of IB3-1 cells. Both the mRNAs and the proteins of the three cytokines slightly increased in the CF-EVs group as compared to the ctr EVs group, though not significantly exceeding the control basal level (Fig. 1). Notably, we observed significant differences in IL-1 β mRNA (Fig. 1, panel A) and IL-6 protein (Fig. 1, panel F) which are significantly higher in the CF-EVs treated group than in the ctr EVs one. In fact, IL-1β mRNA rises by about 45% and IL-6 protein by 60%, moving from 56.6 ± 2.5 to 90.49 ± 8.28 pg/mg protein.

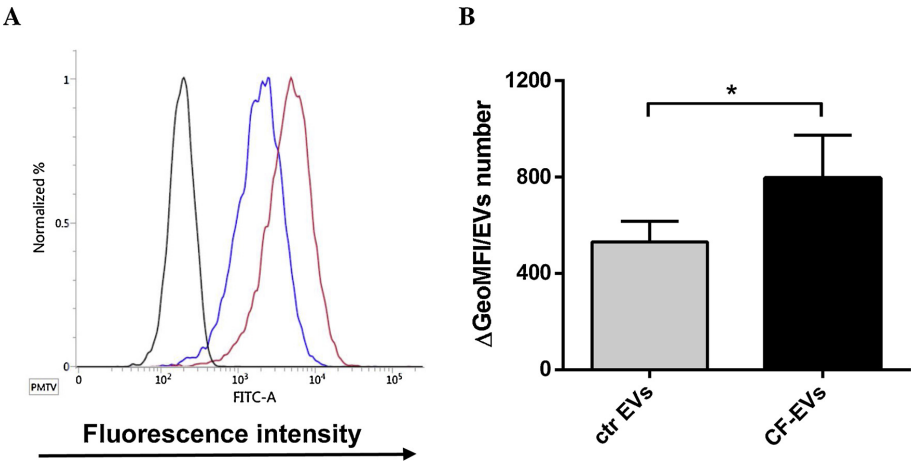

Fig. 3. Labeled EVs incorporation by IB3-1 cells. IB3-1 cells were seeded in 24-well culture plates and treated for 16 h with 100 μL of EVs derived from CellBrite Green Cytoplasmic Membrane Dye-labeled MSCs. Panel **A**: representative graph of the fluorescence intensity values indicating the uptake rate of EVs. The black curve represents the untreated cells; the blue curve represents cells incubated with ctr EVs and the red curve represents cells incubated with CF-EVs. Panel **B**: quantitative determination of EVs uptake by IB3- 1 cells following 16 h of incubation. The gray and black bars represent the internalization value of EVs released from control and CF-MSCs, meaning MSCs added with 10 μg/ml of CFTR inhibitor, I-172, for 48 h. Data are expressed as mean ± SEM of five independent experiments. The statistical significance was evaluated by two-tailed, paired, Student *t*-test (*, $P < 0.05$) performed on the value of geometric mean fluorescent intensity subtracted of the control untreated cells (ΔGeoMFI) and normalized on the number of particles (For interpretation of the references to colour in this figure legend, the reader is referred to the web version of this article.).

We have recently demonstrated that PPARγ, which has an established anti-inflammatory role, is up-regulated in the IB3-1 cell line upon treatment with ctr MSCs-derived EVs (Zulueta et al., 2018). Conversely, here we show that PPARγ transcript is unaffected by CF-EVs treatment, being expressed as in the untreated control IB3-1 cells (Supplementary Fig. 3), supporting the hypothesis of CF-EVs immunological impairment. The EV treatment could interfere with the redox homeostasis of IB3-1 cells, thus indirectly modulating the inflammation status (Supplementary Fig. 4). Control-EVs increase the intrinsic antioxidant power of IB3-1 cells, as shown by the rise in the Fe ions level in the reduced form and by the up-regulation of HO-1 that is a master regulator of the redox-homeostasis. Conversely, CF-EVs treatment fails in improving this protective response, as evidenced by the content of Fe ions in the reduced form and HO-1 that are pretty near to the control value.

3.2. EVs from ctr- and CF-MSCs show different features

We have already specified the composition of the EV population released by human lung MSCs by the classical exosome and microvesicle markers (Zulueta et al., 2018). In this project, we aimed at characterizing ctr EV and CF-EVs in order to understand whether they possess distinct features that might partially account for their different anti-inflammatory potential.

We evaluated the amount of EVs and their size distribution by both Nanoparticles Tracking Analysis (NTA) and Light Scattering. Fig. 2 reports structural result of ctr EVs and CF-EVs prepared in serum-free medium, as described in "material and methods" section, to better characterize the differences among the two particle populations. The cumulative frequency plot (Fig. 2, panel A) shows that ctr EVs exhibit a wide regular distribution with approximately 80% particles distributed within 340 nm in size (as indicated by the blue arrow). Conversely, CF-EVs rather follow a Gaussian distribution that peaks at 150 nm, with approximately 80% particles within 200 nm (as indicated by the red arrow). Those results are in agreement with the mean hydrodynamic size, as assessed by Dynamic Light Scattering (Fig. 2, panel B). As shown, CF-EVs have a hydrodynamic size 20% smaller than the ctr EVs, corresponding to about a 60% smaller volume per EV. Moreover, both NTA and light scattering experiments determined that the number of CF-EVs was approximately 1.5 times higher than the number of ctr EVs, moving from $4.27 \times 10^9 \pm 5.5 \times 10^8$ to $2.99 \times 10^9 \pm 8.0 \times 10^8$/ml (NTA data, not shown). The combined results suggest that EVs released by ctr MSCs and CF-MSCs, have a different supramolecular organization, resulting in more numerous, but smaller CF-EVs.

To study the internalization rate of MSCs-derived EVs by IB3-1 cells, we designed a quantitative flow cytometric assay, as reported in the "Materials and methods" section. Control and CF-MSCs were labeled with the CellBrite Cytoplasmic Membrane Dye, EVs were isolated and used to treat IB3-1 cells and the uptake was assessed by flow cytometry 16 h later. Fig. 3 shows that CF-EVs are more efficiently internalized by IB3-1 cells than ctr EVs, as indicated by the value of the fluorescence intensity, normalized on the number of particles, with an increase of almost 50% (from 531.3 ± 84.63–795.8 ± 177.3 ΔGeoMFI/EVs number).

3.3. Sphingolipid profile is differently characterized in ctr EVs and CF-EVs

In an attempt to gain insights in the potential mediators underlying the different anti-inflammatory behavior of ctr- and CF-EVs, we determined the composition of SPLs that play a well-known role in modulating inflammation. By means of LC–MS/MS analysis, we observed a significant rise in the content of total Cer and dhCer, its precursor along the neo synthesis pathway, in CF-EVs *vs* ctr EVs, with value ranging from 790.9 ± 76.3 to 991.1 ± 133.8 and from 18.17 ± 1.8 to 25.75 ± 3.7 pmoles/mg protein, respectively (Table 1).

When considering the single Cer species (Fig. 4, panel D), we found that the most representative fatty acid containing Cer is the C16:0 which accumulates in CF-EVs 15% more than in ctr EVs. Moreover, the ceramides bearing longer saturated and unsaturated fatty acid chains, namely C20:0, C22:0, C24:0, and C24:1, significantly increased in CF-EVs by 25%, 60%, 100%, and 25%, respectively. We observed the same trend in the corresponding dhCer species. As shown in panel E, dhC16-

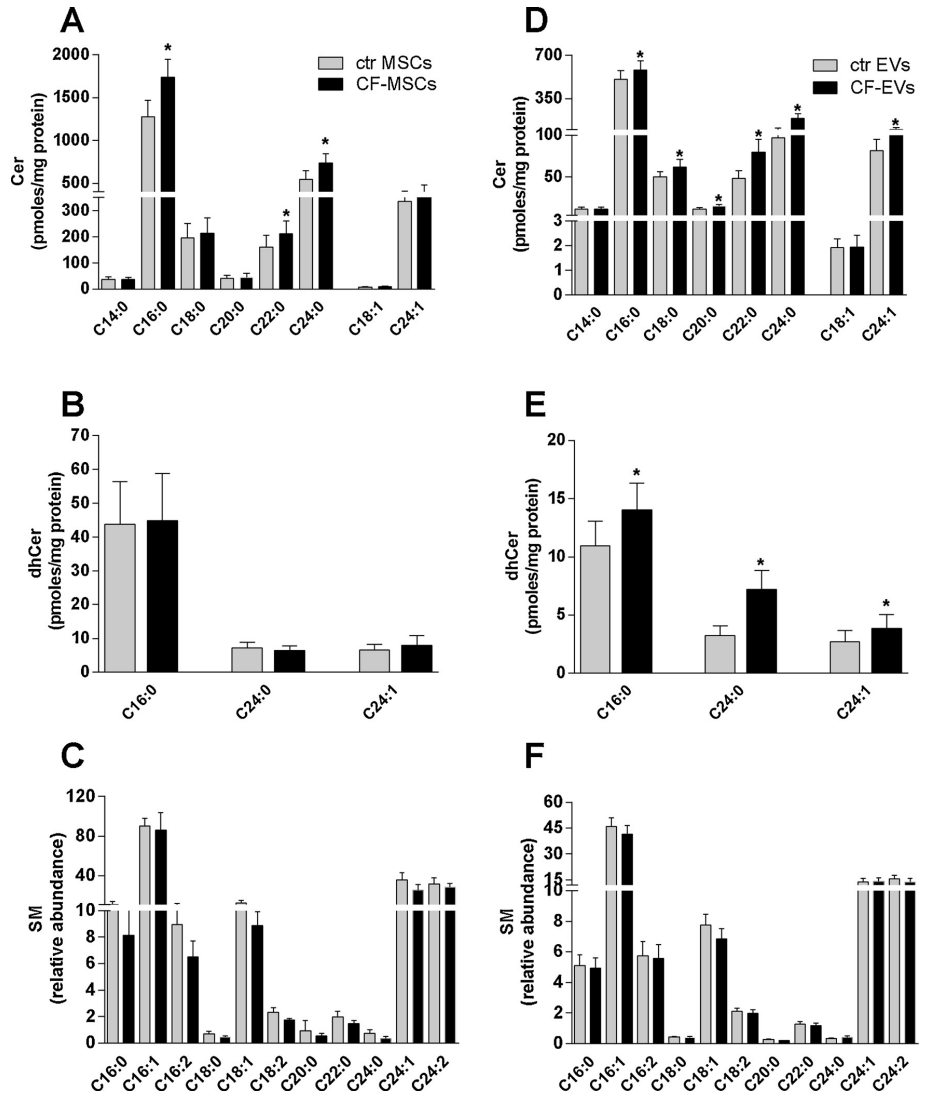

Fig. 4. Sphingolipid profile of ctr and CF-EVs and parental MSCs. Sphingolipid profile of EVs and parental MSCs was obtained by LC/MS analysis. Panel **A** and **D** represent single Cer species content, expressed as pmoles/mg protein, in MSCs and EVs populations, respectively. Panel **B** and **E** show single dhCer species content, reported as pmoles/mg protein, in MSCs and EVs populations, respectively. Panel **C** and **F** represent single SM species content, expressed as relative abundance, in MSCs and EVs populations, respectively. The gray bars correspond to ctr MSCs and ctr EVs while the black bars refer to CF-MSCs and CF-EVs. Data are expressed as mean ± SEM of five to seven independent experiments. The statistical significance was evaluated by two-tailed, paired, Student *t*-test (*, $P < 0.05$).

Cer rises by almost 30%, dhC24:0-Cer by more than twofold and dhC24:1-Cer by 40%. As for SM, we found no significant differences in the total (Table 1) and the single species expression (Fig. 4, panel F) but only a trend toward a decrease in their level was apparent. As compared to EVs, parental MSCs cells display a similar SPLs pattern. We observed a significant 30% increase in the total Cer content (from 2605 ± 461.4–3387 ± 496.8 pmoles/mg protein; Table 1) and about 35% accumulation of the most representative fatty acid containing Cer, namely C16:0, C22:0, and C24:0 (Fig. 4, panel A). On the contrary, total (Table 1) and single dhCer species (Fig. 4, panel B) were similarly expressed in both MSC populations. Finally, we found a reduction in the relative abundance of total and single SM species (Table 1; Fig. 4, panel C).

Next, we checked whether the ctr and the CF-MSCs, could differently express the Serine palmitoyl transferase (SPT), the rate limiting enzyme of the *de novo* ceramide biosynthesis pathway, and the neutral sphingomyelinase 2 (n-SMase 2), highly involved in the biogenesis of EVs. SPTLC-2 mRNA (panel A), one of the two catalytic subunits of SPT, as well as n-SMase 2 (panel B) were significantly upregulated (*, $p = 0.04$ and *, $p = 0.02$, respectively) in CF-MSCs as compared to ctr MSCs (Fig. 5).

Table 1
Total sphingolipid content in ctr and CF-EVs and parental MSCs. Total Cer and dhCer content was assessed by LC–MS/MS. The results are expressed as pmoles/mg protein. For total SM content, relative quantification was achieved by the ratio of the analyte/area IS (200 pmol SM C12). Data, reported as mean ± SEM, are obtained from five to seven independent experiments. The statistical significance was evaluated by two-tailed, paired, Student *t*-test.

Total	Cer pmoles/mg protein	dhCer pmoles/mg protein	SM relative abundance
Ctr MSCs	2605 ± 461.4 (n = 5)	55.68 ± 13.1 (n = 5)	195.1 ± 30.7 (n = 5)
CF-MSCs	3387 ± 496.8 (n = 5) P = 0.02	57.36 ± 15.9 (n = 5) P = ns	168 ± 30.2 (n = 5) P = 0.03
Ctr EVs	790.9 ± 76.3 (n = 7)	18.17 ± 1.8 (n = 7)	98.24 ± 11.7 (n = 7)
CF-EVs	991.1 ± 133.8 (n = 7) P = 0.04	25.75 ± 3.7 (n = 7) P = 0.01	90.87 ± 11.5 (n = 7) P = ns

4. Discussion

Our study focuses on determining whether MSCs could impact the inflammatory chronic condition that characterizes Cystic Fibrosis. We took advantage of an *in vitro* cellular model of CF-MSC by treating control human lung MSCs with a specific CFTR inhibitor (I-172) in order to obtain CF-EVs that mimic those particles physiologically released in the lung of CF patient. We used IB3-1, a transformed human bronchial epithelial cell line from a CF patient (ΔF508/W1282X), to gain the basal inflammatory CF phenotype (Armstrong et al., 1997; Tirouvanziam et al., 2000) and we compared the anti-inflammatory potential of CF-EVs with control EVs. As we previously published (Zulueta et al., 2018), here we show that EVs from control MSCs attenuate the pro-inflammatory profile of IB3-1 cell by reducing the cytokines expression and rescuing the transcription of PPARγ, highly involved in anti-inflammatory mechanisms. On the contrary, CF-EVs treatment is less effective on cytokines and PPARγ expression, providing an explanation for the basal physiological inflammatory phenotype. Accordingly, Sutton and colleagues (Sutton et al., 2017) recently showed that deficient CFTR function, achieved by the same CFTR inhibitor (I-172), alters human MSCs ability to control the inflammatory response to pathogenic organisms. They indicate that CF-MSCs do not behave similarly to control MSCs, due to the expression of different amounts of IL-6, CCL2 and IL-8. Moreover, they observed that by blocking CFTR activity in wild type bone marrow derived macrophages, PPARγ levels decrease.

Our results suggest that the two EVs populations released by the parental MSCs, exhibit quite different features. CF-EVs are more abundant and smaller than the ctr EVs and they are more efficiently uptaken by the recipient IB3-1 cells. Growing evidence indicates that inflammatory conditions might trigger the release of EVs that in turn maintain such condition. As reviewed by Cypryk and colleagues (Cypryk et al., 2018), inflammasome activity correlates with enhanced secretion of EVs and modulation of their mediators content. Murine microglial cell line challenged with LPS, acquires an activated pro-inflammatory status that greatly increases the release of EVs. In contrast, EV secretion was completely attenuated to control levels using a TNFα inhibitor (Yang et al., 2018). In our experimental model, we did not directly challenge MSCs with pro-inflammatory stimuli, but CF-MSCs seem to be immunological impaired since CFTR activity inhibition is *per se* correlated to inflammation (Sutton et al., 2017), thus enhancing EVs secretion. Though the ESCRT machinery represents the general process of exosomes release, in 2008 a Cer-mediated mechanism has been first described (Trajkovic et al., 2008). The authors proposed SM hydrolysis by n-SMase 2, the enzyme which mostly resides in the Golgi and ER, and the consequent Cer generation as important players in exosomes biogenesis. In fact, the cone-shaped structure of Cer spontaneously drives the negative curvature of the membrane, favouring vesicles formation. Consistently, the block of n-SMase reduces exosomes release in various cell lines (Kosaka et al., 2010; Asai et al., 2015; Xu et al., 2016). However, the same enzyme differentially controls the secretion of larger EV population, such as MVs (Menck et al., 2017). We found a significant decrease in the relative abundance of total SM in CF-MSCs *versus* ctr MSCs, together with a transcriptional activation of n-SMase 2, suggesting that this pathway could be involved in EVs production.

Therefore, the accumulation of Cer observed in both CF-EVs and parental MSCs, could contribute to the abundancy of CF-EVs as compared to ctr EVs. Ceramide formation upon SM hydrolysis, allows those membrane changes required for the release of exosomes that are on average smaller than MVs, thus accounting for the majority of CF-EVs distributed within 150 nm in size, as compared to ctr EVs. In our model, the significant accumulation of both Cer and dhCer species in CF-EVs points to the involvement of the *de novo* Cer synthesis in the parental CF-MSCs. This finding is further supported by the transcriptional upregulation of SPLTC-2, one of the two catalytic subunits of the SPT that regulates the rate limiting step of the *de novo* pathway. Though CF-MSCs exhibit unchanged dhCer levels, specific mechanisms of lipid sorting into EVs that export out of the cells the SPLs generated could occur (Podbielska et al., 2016). The higher content in dihydroceramides of EVs in comparison to MSCs, suggests that the Cer biosynthesis upregulation is tightly linked to the extrusion of signaling lipids, deriving from ER and including Cer precursor. Whereas this latter is rapidly

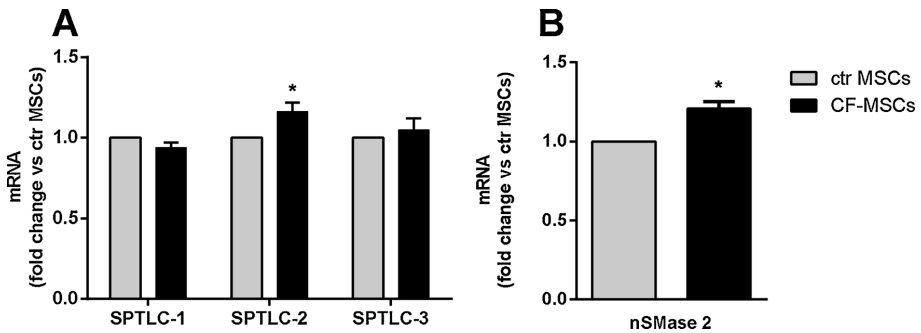

Fig. 5. mRNA expression of Serine palmitoyl transferase (SPT) and neutral sphingomyelinase 2 (n-SMase 2) in ctr and CF-MSCs. Control MSCs (ctr MSCs, gray bar) refer to untreated MSCs while CF-MSCs (black bar), refer to control MSCs treated for 48 h with 10 μg/ml of CFTR inhibitor, I-172. The results are expressed as fold change over the control MSCs. Data, reported as mean ± SEM, are obtained from five independent experiments. For each treatment, the samples were run in triplicate. The statistical significance was evaluated by two-tailed, paired, Student *t*-test.

dehydrogenated along with ER reactions, its early compartmentalization in multi-vesicular bodies may fuel extracellular lipid signaling in the effort of controlling lipid cellular homeostasis. Our results indicate that the inflammation activated Cer *de novo* synthesis and accumulation (Caretti et al., 2014; Caretti et al., 2016) trigger a transcriptionally driven response that requires higher sphingomyelinase activity to sustain the release of new formed ceramide throughout the exocytosis of vesicles that spread their originating inflammatory-alarm signal.

It has been reported that Cer-enriched exosomes mediate cytotoxic effects in recipient cells. Podbielska and colleagues (Podbielska et al., 2016) demonstrated that HOG, an oligodendroglioma cell line, responds to cytotoxic cytokines by eliciting the release of Cer-enriched exosomes. They support the idea that vesicular Cer contributes *per se* to the toxic effects elicited by the cytokines. This is consistent with previous studies illustrating that many dangerous effects of TNFα on different subsets of cells are mediated by Cer generation (Osawa et al., 2005; White-Gilbertson et al., 2009). Similarly, we have previously published that Cer from *de novo* biosynthesis pathway contributes to lung inflammation in CF murine models, upon infection with *P. aeruginosa* and *A. fumigatus* (Caretti et al., 2014; Caretti et al., 2016). Our present results corroborate these data since we found an inverse correlation between the anti-inflammatory efficacy of EVs and their Cer content.

5. Conclusion

In conclusion, our findings support the hypothesis that CFTR dysfunction, obtained by treating control MSCs with a specific CFTR inhibitor, associates with an enhanced sphingolipid metabolism leading to an increase in the content of ceramide. This in turn promotes the release of CF-EVs that export the excess of pro-inflammatory ceramide to the recipient cells, thus contributing to maintain the chronic, unresolved inflammatory status of Cystic Fibrosis. These results contribute to better elucidate the role of Cer-enriched EVs in Cystic Fibrosis, providing the rationale for novel therapeutic approaches.

Declaration of Competing Interest

The authors declare no conflict of interest.

Acknowledgments

A. Zulueta post doc position was funded by the University of Milan, Italy. V. Peli was granted by the University of Milan, Italy, “Borse Giovani promettenti laureati”. M. Dei Cas was supported by the PhD program in “Molecular and Translational Medicine” of the University of Milan, Italy. M. Colombo was granted by Fondazione Italiana per la Ricerca sul Cancro (post-doctoral fellowship 18013). EDF thanks BIOMETRA Dept. for in house support. AC thanks Dr. Andrea Brizzolari for FRAP assay. This work was supported by the University of Milan, Italy, Piano di Sostegno alla Ricerca 2015/2017, finanziamento LINEA 2″Dotazione annuale per attività istituzionale"

Appendix A. Supplementary data

Supplementary material related to this article can be found, in the online version, at doi:https://doi.org/10.1016/j.biocel.2019.105622.

References

Armstrong, D.S., et al., 1997. Lower airway inflammation in infants and young children with cystic fibrosis. Am. J. Respir. Crit. Care Med. 156 (4 Pt 1), 1197–1204.
Arocho, A., et al., 2006. Validation of the 2-DeltaDeltaCt calculation as an alternate method of data analysis for quantitative PCR of BCR-ABL P210 transcripts. Diagn. Mol. Pathol. 15 (1), 56–61.
Asai, H., et al., 2015. Depletion of microglia and inhibition of exosome synthesis halt tau propagation. Nat. Neurosci. 18 (11), 1584–1593.
Becker, K.A., et al., 2010. Accumulation of ceramide in the trachea and intestine of cystic fibrosis mice causes inflammation and cell death. Biochem. Biophys. Res. Commun. 403 (3–4), 368–374.
Benzie, I.F., Strain, J.J., 1999. Ferric reducing/antioxidant power assay: direct measure of total antioxidant activity of biological fluids and modified version for simultaneous measurement of total antioxidant power and ascorbic acid concentration. Methods Enzymol. 299, 15–27.
Bianco, F., et al., 2009. Acid sphingomyelinase activity triggers microparticle release from glial cells. EMBO J. 28 (8), 1043–1054.
Bonzini, M., et al., 2017. Short-term particulate matter exposure induces extracellular vesicle release in overweight subjects. Environ. Res. 155, 228–234.
Caretti, A., et al., 2014. Anti-inflammatory action of lipid nanocarrier-delivered myriocin: therapeutic potential in cystic fibrosis. Biochim. Biophys. Acta 1840 (1), 586–594.
Caretti, A., et al., 2016. Inhibition of ceramide de novo synthesis by myriocin produces the double effect of reducing pathological inflammation and exerting antifungal activity against A. fumigatus airways infection. Biochim. Biophys. Acta 1860 (6), 1089–1097.
Chiricozzi, E., et al., 2018. Sphingolipids role in the regulation of inflammatory response: from leukocyte biology to bacterial infection. J. Leukoc. Biol. 103 (3), 445–456.
Cypryk, W., Nyman, T.A., Matikainen, S., 2018. From inflammasome to exosome-does extracellular vesicle secretion constitute an inflammasome-dependent immune response? Front. Immunol. 9, 2188.
Dechecchi, M.C., et al., 2011. Modulators of sphingolipid metabolism reduce lung inflammation. Am. J. Respir. Cell Mol. Biol. 45 (4), 825–833.
Dinkins, M.B., et al., 2014. Exosome reduction in vivo is associated with lower amyloid plaque load in the 5XFAD mouse model of Alzheimer's disease. Neurobiol. Aging 35 (8), 1792–1800.
Dostert, G., et al., 2017. How do mesenchymal stem cells influence or are influenced by microenvironment through extracellular vesicles communication? Front. Cell Dev. Biol. 5, 6.
Fabiani, C., et al., 2017. 2-Acetyl-5-tetrahydroxybutyl imidazole (THI) protects 661W cells against oxidative stress. Naunyn Schmiedebergs Arch. Pharmacol. 390 (7), 741–751.
Fatima, F., et al., 2017. Non-coding RNAs in mesenchymal stem cell-derived extracellular vesicles: deciphering regulatory roles in stem cell potency, inflammatory resolve, and tissue regeneration. Front. Genet. 8, 161.
Gault, C.R., Obeid, L.M., Hannun, Y.A., 2010. An overview of sphingolipid metabolism: from synthesis to breakdown. Adv. Exp. Med. Biol. 688, 1–23.
Grassme, H., Riethmuller, J., Gulbins, E., 2013. Ceramide in cystic fibrosis. Handb. Exp. Pharmacol. (216), 265–274.
Hannun, Y.A., Obeid, L.M., 2008. Principles of bioactive lipid signalling: lessons from sphingolipids. Nat. Rev. Mol. Cell Biol. 9 (2), 139–150.
Hornemann, T., et al., 2006. Cloning and initial characterization of a new subunit for mammalian serine-palmitoyltransferase. J. Biol. Chem. 281 (49), 37275–37281.
Kosaka, N., et al., 2010. Secretory mechanisms and intercellular transfer of microRNAs in living cells. J. Biol. Chem. 285 (23), 17442–17452.
Kubota, S., et al., 2015. Secretion of small/microRNAs including miR-638 into extracellular spaces by sphingomyelin phosphodiesterase 3. Oncol. Rep. 33 (1), 67–73.
Lago, P., Rovati, L., 1993. A quasielastic light scattering detector for chromatographic analysis. Rev. Sci. Instrum. 64 (7), 1797–1802.
Lawson, C.L., Hanson, R.J., 1995. Solving Least Squares Problems. SIAM, Philadelphia.
Marchesini, N., Hannun, Y.A., 2004. Acid and neutral sphingomyelinases: roles and mechanisms of regulation. Biochem. Cell Biol. 82 (1), 27–44.
Mattoscio, D., et al., 2010. Cystic fibrosis transmembrane conductance regulator (CFTR) expression in human platelets: impact on mediators and mechanisms of the inflammatory response. FASEB J. 24 (10), 3970–3980.
Menck, K., et al., 2017. Neutral sphingomyelinases control extracellular vesicles budding from the plasma membrane. J. Extracell. Vesicles 6 (1) p. 1378056.
Osawa, Y., et al., 2005. Roles for C16-ceramide and sphingosine 1-phosphate in regulating hepatocyte apoptosis in response to tumor necrosis factor-alpha. J. Biol. Chem. 280 (30), 27879–27887.
Pergoli, L., et al., 2017. Extracellular vesicle-packaged miRNA release after short-term exposure to particulate matter is associated with increased coagulation. Part. Fibre Toxicol. 14 (1), 32.
Petrache, I., Petrusca, D.N., 2013. The involvement of sphingolipids in chronic obstructive pulmonary diseases. Handb. Exp. Pharmacol. (216), 247–264.
Platania, C.B.M., et al., 2019. Novel ophthalmic formulation of myriocin: implications in retinitis pigmentosa. Drug Deliv. 26 (1), 237–243.
Podbielska, M., et al., 2016. Cytokine-induced release of ceramide-enriched exosomes as a mediator of cell death signaling in an oligodendroglioma cell line. J. Lipid Res. 57 (11), 2028–2039.
Riethmuller, J., et al., 2009. Therapeutic efficacy and safety of amitriptyline in patients with cystic fibrosis. Cell. Physiol. Biochem. 24 (1–2), 65–72.
Subra, C., et al., 2007. Exosome lipidomics unravels lipid sorting at the level of multivesicular bodies. Biochimie 89 (2), 205–212.
Sutton, M.T., et al., 2017. Mesenchymal stem cell soluble mediators and cystic fibrosis. J. Stem Cell Res. Ther. 7 (9).
Teichgraber, V., et al., 2008. Ceramide accumulation mediates inflammation, cell death and infection susceptibility in cystic fibrosis. Nat. Med. 14 (4), 382–391.
Tirouvanziam, R., et al., 2000. Inflammation and infection in naive human cystic fibrosis airway grafts. Am. J. Respir. Cell Mol. Biol. 23 (2), 121–127.
Trajkovic, K., et al., 2008. Ceramide triggers budding of exosome vesicles into multivesicular endosomes. Science 319 (5867), 1244–1247.
Verderio, C., Gabrielli, M., Giussani, P., 2018. Role of sphingolipids in the biogenesis and biological activity of extracellular vesicles. J. Lipid Res. 59 (8), 1325–1340.
Wang, G., et al., 2012. Astrocytes secrete exosomes enriched with proapoptotic ceramide

and prostate apoptosis response 4 (PAR-4): potential mechanism of apoptosis induction in Alzheimer disease (AD). J. Biol. Chem. 287 (25), 21384–21395.
White-Gilbertson, S., et al., 2009. Ceramide synthase 6 modulates TRAIL sensitivity and nuclear translocation of active caspase-3 in colon cancer cells. Oncogene 28 (8), 1132–1141.
Xu, Y., et al., 2016. Macrophages transfer antigens to dendritic cells by releasing exosomes containing dead-cell-associated antigens partially through a ceramide-dependent pathway to enhance CD4(+) T-cell responses. Immunology 149 (2), 157–171.
Yang, Y., et al., 2018. Inflammation leads to distinct populations of extracellular vesicles from microglia. J. Neuroinflammation 15 (1), 168.
Yuyama, K., et al., 2012. Sphingolipid-modulated exosome secretion promotes clearance of amyloid-beta by microglia. J. Biol. Chem. 287 (14), 10977–10989.
Zulueta, A., et al., 2018. Lung mesenchymal stem cells-derived extracellular vesicles attenuate the inflammatory profile of Cystic Fibrosis epithelial cells. Cell. Signal. 51, 110–118.
Zulueta, A., et al., 2017. Inhibitors of ceramide de novo biosynthesis rescue damages induced by cigarette smoke in airways epithelia. Naunyn Schmiedebergs Arch. Pharmacol. 390 (7), 753–759.

APPENDIX

cells

MDPI

Article

An Innovative Lipidomic Workflow to Investigate the Lipid Profile in a Cystic Fibrosis Cell Line

Michele Dei Cas [1,2,*], Aida Zulueta [2], Alessandra Mingione [2,3], Anna Caretti [2], Riccardo Ghidoni [2,3], Paola Signorelli [2] and Rita Paroni [1]

1 Laboratory of Clinical Biochemistry and Mass Spectrometry, Department of Health Sciences, Università degli Studi di Milano, 20142 Milan, Italy; rita.paroni@unimi.it
2 Laboratory of Biochemistry and Molecular Biology, Department of Health Sciences, Università degli Studi di Milano, 20142 Milan, Italy; aidazulueta@gmail.com (A.Z.); alessandra.mingione@unimi.it (A.M.); anna.caretti@unimi.it (A.C.); riccardo.ghidoni@unimi.it (R.G.); paola.signorelli@unimi.it (P.S.)
3 Aldo Ravelli Center for Neurotechnology and Experimental Brain Therapeutics, Department of Health Sciences, Università degli Studi di Milano, 20142 Milan, Italy
* Correspondence: michele.deicas@unimi.it; Tel.: +39-025-0323-272/4

Received: 6 April 2020; Accepted: 8 May 2020; Published: 12 May 2020

Abstract: Altered lipid metabolism has been associated to cystic fibrosis disease, which is characterized by chronic lung inflammation and various organs dysfunction. Here, we present the validation of an untargeted lipidomics approach based on high-resolution mass spectrometry aimed at identifying those lipid species that unequivocally sign CF pathophysiology. Of n.13375 mass spectra recorded on cystic fibrosis bronchial epithelial airways epithelial cells IB3, n.7787 presented the MS/MS data, and, after software and manual validation, the final number of annotated lipids was restricted to n.1159. On these lipids, univariate and multivariate statistical approaches were employed in order to select relevant lipids for cellular phenotype discrimination between cystic fibrosis and HBE healthy cells. In cystic fibrosis IB3 cells, a pervasive alteration in the lipid metabolism revealed changes in the classes of ether-linked phospholipids, cholesterol esters, and glycosylated sphingolipids. Through functions association, it was evidenced that lipids variation involves the moiety implicated in membrane composition, endoplasmic reticulum, mitochondria compartments, and chemical and biophysical lipids properties. This study provides a new perspective in understanding the pathogenesis of cystic fibrosis and strengthens the need to use a validated mass spectrometry-based lipidomics approach for the discovery of potential biomarkers and perturbed metabolism.

Keywords: lipidomics; OMICS; untargeted analysis; cystic fibrosis; biomarker; sphingolipid; membrane composition; cell structure

1. Introduction

Lipids are a fundamental component of cellular membranes and signaling molecules regulating cellular functions that include energy storage, cell proliferation and death, stress response, and inflammation. Alterations in lipids metabolism are associated and suggested as causative for the pathophysiology of inflammation-related diseases such as neurodegenerative diseases (i.e., Alzheimer's and Parkinson's), diabetes, obesity, atherosclerosis and cardiovascular diseases, non-alcoholic fatty liver disease, cancer, obstructive sleep apnea, and respiratory diseases [1,2]. Thus, lipids are not only modulated by diseases but also recognized as therapeutic targets. Lipidomics is the most powerful tool to approach the study of lipids-related diseases. The increasing popularity of the lipidomics approach is strictly connected to the progress in the related analytical techniques, especially mass

spectrometry. This large-scale technique can cover the whole human lipidome, comprising from 10 to 100-thousand different chemical entities in a complex biological system. Lipids can be studied by two approaches: targeted or untargeted lipidomics. Targeted methods are a high-sensitive analysis dedicated to the identification and quantification of known classes of lipids, whereas nontargeted methods, usually employing high-resolution mass spectrometry, aim to identify and semi-quantify every likely lipid species contained in the samples [3–5]. Employing this technique, different tasks can be performed: (1) characterization, identification, and quantification of specific lipid species known to be related to pathological events, and (2) identification of new prognostic or diagnostic biomarkers able to discriminate with higher specificity and sensitivity the healthy phenotype from the pathological ones. The strength of lipidomic is to identify single species that stand for significant changes and offers broad-spectrum information on the inherently dynamic process. In this process, metabolites and, thus, their concentrations are continuously exposed to synthesis or degradation. By clustering metabolites that are simultaneously interested in changes, it is possible to identify pathways and cell functions involved in the studied stimulus or dysfunction [6]. Among chronic inflammatory and lipids-related diseases, cystic fibrosis (CF) is a significant and well-characterized fatal illness. CF is a pulmonary disease caused by different mutations in the gene for the chloride/carbonate channel CFTR. These mutations are responsible for dysregulation in the electrolytic equilibrium within the protective mucus of respiratory airways, leading to lung chronic inflammation and infections, together with pancreatic insufficiency and multiple organs dysfunction [7]. Pharmacological treatment aimed at CFTR function recovery failed in the clinical practice, and CF has no effective cure at present [8]. Lipid alterations in CF patients have been extensively reported. In particular, abnormalities in blood fatty acid (FA) composition have been described, showing a high level of saturated (SFA) and monounsaturated (MUFA) together with low levels of omega-3 and omega-6 polyunsaturated fatty acids (PUFA) in respect to a healthy control [9,10]. Alteration in the human CF plasma lipid profile comprises a modification in the levels of phospholipids and lysophospholipids (e.g., PC and LPC), cholesterol, cholesterol esters, and hypertriglyceridemia [11–13]. In addition, peripheral cholesterol accumulation was evidenced in the respiratory airways [14]. The cause of lipids altered homeostasis in CF is still debated, and it has been attributed to enhanced lipid synthesis that can derive from intestinal malabsorption [12], as well as from peripheral and systemic inflammation [15]. At a cellular level, it was demonstrated that CF cells exhibit increased lipid synthesis, possibly due to altered proteostasis [16,17], which can be counteracted by the sphingolipid synthesis inhibitor myriocin [18,19].

In this manuscript, we present a novel lipidomics approach aimed at identifying those lipid species that unequivocally sign CF pathophysiology. We evaluated the lipid tract of the CF broncho epithelial cell line, being the airways of the first body district involved in chronic inflammation and infection in these patients. Our data strengthen and specify previous reports, demonstrating that CF broncho epithelial cells exhibit a significant increase of all lipid species analyzed in comparison to the normal broncho epithelial cell line. Most importantly, we unequivocally indicate the ether-glycerophospholipids, cholesterol esters, and glycosylated sphingolipids as classes of molecules accurately representative of CF and not well-characterized yet as pathological markers. Our findings open a new bursting and crucial research field for the development of innovative CF therapeutic approaches.

2. Materials and Methods

2.1. Reagent and Chemicals

Lipids standard were purchased from Avanti Polar Lipids (Alabaster, AL, USA). The chemicals acetonitrile, 2-propanol, methanol, chloroform, formic acid, ammonium acetate, and ammonium formate were purchased by Sigma-Aldrich (St. Louis, MO, USA). All aqueous solutions were prepared using purified water at a Milli-Q grade (Burlington, MA, USA).

2.2. Cell Culture

Human bronchial epithelial cell line (IB3), derived from a CF patient (ΔF508/W1282X) provided by LGC Promochem (Teddington, UK), were grown in LHC-8 medium supplemented with 5% FBS, 1% penicillin/streptomycin at 37 °C, and 5% CO_2. Healthy (H) human lung bronchial epithelial cell line (16HBE14O, initially developed by Dieter C. Gruenert) were provided by Luis J. Galietta (Telethon Institute of Genetics and Medicine—TIGEM, Napoli, Italy). Originally HBE primary cells were grown in LHC-8, although in the present study they were cultured as recommended (Merck Millipore SCC150 datasheet) in MEM Earle's salt supplemented with 5% FBS, 1% penicillin/streptomycin at 37 °C, and 5% CO_2. For cell lipidomics, 1×10^5 cells/100-mm plate in 5 mL medium were plated, harvested when confluence has reached 90%, washed in PBS, and pelleted.

2.3. Lipids Extraction

Lipid extraction was completed by a modified version of the Folch method [18]. Cells (about 1×10^6) were reconstituted in 100 µL of water + 0.1% proteases inhibitor cocktail, and a small aliquot was used for total protein quantification by the Bradford dye-binding method. For lipid extraction, 100 µL of aqueous samples were added with 850 µL of a methanol/chloroform mixture (2:1, *v*/*v*), then sonicated for 30 min. The organic phase was evaporated under a stream of nitrogen. The residues were dissolved in 100 µL of isopropanol/acetonitrile (2:1, *v*/*v*), centrifuged for 10 min at 13,400 RPM, and withdrawn in a glass vial.

For a targeted sphingolipids analysis, after the addition of the methanol/chloroform mixture (2:1 *v*/*v*), samples were incubated overnight in an oscillator bath at 48 °C. Then, to enhance their recovery, alkaline methanolysis was performed by incubation at 37 °C for 2 h with 75 µL of potassium hydroxide 1 M in methanol. After neutralization with 75 µL of acetic acid 1 M in methanol, samples were evaporated. The residues were dissolved in 100 µL of methanol, centrifuged for 10 min at 13,400 RPM, and withdrawn in a glass vial.

2.4. LC-MS/MS Untargeted Method

The LC-MS/MS consisted of a Shimadzu UPLC coupled with a Triple TOF 6600 Sciex (Concord, ON, CA) equipped with Turbo Spray IonDrive. All samples were analyzed in duplicate in both positive and negative mode with electrospray ionization. The instrument parameters were: CUR 35, GS1 55, GS2 65, capillary voltage 5.5 kV, and source temperature 350 °C. Spectra were contemporarily acquired by both full-mass scan from 200–1500 m/z (100 ms accumulation time) and data-dependent acquisition from 50–1500 m/z (40 ms accumulation time, top 18 spectra per cycle 0.8 s). Declustering potential was fixed to 50 eV, and the collision energy was 35 eV, with a collision energy spread of 15 eV.

The chromatographic separation on an Acquity BEH C18 column 1.7 µm 2.1 × 50 mm (Waters, Franklin, MA, USA), equipped with a precolumn [20], was achieved using, as mobile phase A, water/acetonitrile (60:40) and, as mobile phase B, 2-propanol/acetonitrile (90:10), both containing 10-mM ammonium acetate and 0.1% of formic acid. The flow rate was 0.4 mL/min, and the column temperature was 45 °C. The elution gradient was set as below: 0–2 min (45% B), 2–12 min (45–97% B), 12–17 min (97% B), 17–17.10 min (97–45% B), and 17.10–21 min (45% B).

Additionally, another chromatographic separation was reached on an Acquity CSH C18 column 1.7 µm 2.1 × 100 mm (Waters, Franklin, MA, USA) equipped with a precolumn by using, as mobile phase A, water/acetonitrile (60:40) and, as mobile phase B, 2-propanol/acetonitrile (90:10), both containing 10-mM ammonium acetate and 0.1% of formic acid. The flow rate was 0.4 mL/min, and the column temperature was 45 °C. The elution gradient (%B) was set as below: 0–2.0 min (40%), 2.0–2.5 min (40–50%), 2.5–12.5 min (50–55%), 12.5–13.0 min (55–70%), 13.0–19.0 min (70–99%), 19.0–24.0 min (99%), and 24.0–24.2 (99–40%) and kept constant until 30 min. Five microliters of clear supernatant were directly injected in the LC-MS/MS.

2.5. Lipidomic Data Processing

The correct identification and relative quantification were attained using MS-DIAL (version 4.0) software [21–23]. Data raw files (.wiff) were converted into .abf format in order to perform retention time correction, peak alignment, and identification. The latter was achieved by comparison of experimental spectra with those in the LipidBlast library [24], using both accurate mass and MS/MS fragmentation (Table S1) data (total identification score >70%). Prevalent adducts were previously investigated in our experimental conditions, and thus, the identification was restricted only on them. MS and MS/MS tolerance for peak profile were set to 0.01 and 0.05 Da, respectively. Data were then filtered for blank samples signals with a fold change >10. A quality control pooled sample (QC, a mix of all samples in the batch) was prepared and injected several times (every four samples) during the batch analysis to test the instrumental variability. Lipids that presented a coefficient of variation (CV%) ≥30% in the QC were excluded for further investigation [25]. Then, to restrict biological and analytical variances, normalization was completed by correcting the peak intensities (Equation (1)) of each lipid for both (1) the amount of protein in the extract injected (μg) measured by the Bradford method and (2) the variation in the response of QCs dispersed evenly throughout the batch (by the Lowess algorithm). Lipids containing either a high number of unsaturations or odd-chain fatty acids were manually excluded. An overview of the entire lipid metabolism was represented as the summed amounts, after normalization, of the individual lipids per subclass (an example is shown in Equation (2)).

$$\text{Amount}_X = \frac{\text{Peak intensity} \times \text{after normalization}}{\mu\text{g protein injected}} \quad (1)$$

$$\text{Amount}_{\text{Cer}} = \text{Amount}_{\text{Cer1}} + \text{Amount}_{\text{Cer2}} + \text{Amount}_{\text{Cer n}} \quad (2)$$

2.6. Statistical and Data Analysis

As a first approach to evidence differences in lipid metabolisms between healthy and CF, the different classes (sum of the concentrations of the species) were compared by *t*-test with GraphPad Prism 7.0 (GraphPad Software, Inc, La Jolla, CA, USA). Then, for biomarker discovery, data tables with the lipids identified under both healthy and pathological conditions were formatted as .csv files and uploaded to the MetaboAnalyst server (version 4.0) [26,27]. Data were checked for integrity, filtered by interquartile range, log-transformed (generalized logarithmic transformation), and auto-scaled. If multiple isomeric lipid species were detected, the sum of their abundances would be further considered. This operation is driven by the fact that the exact position and stereochemistry of the unsaturations could not be deduced from this kind of experiment. The comparison between CF and healthy cells was performed by both univariate and multivariate methods. The volcano plot showed the statistical significance and the fold change of each lipid identified by selecting only those with a p-value < 0.05 (corrected for false discovery rate) and a fold change (FC) >2. Partial least squares discriminant analysis (PLS-DA) was performed in order to increase the group separation and investigate the variables with a Variance Importance in Projection (VIP) score >1. These features could be considered as a potential biomarker of CF [28]. The quality of the PLS-DA models was assessed by cross-validation: R^2 and Q^2 (i.e., cross-validated R^2) should be >0.8 in order to avoid overfitting or unreliable estimations [29]. The potential lipids biomarkers were finally determined, combining uni- and multivariate analysis by the combination of the VIP score in the PLS-DA model together with corrected p-value and fold change both derived from the Volcano plot. Specifically, it was taken into consideration the products of the VIP score (>1), $-\log_{10}$ p-value (>1.3), and $|\log_2 FC|$ (>1), here named as the impact factor (IF; Equation (3)). Enrichment analysis was performed, on normalized data from MetaboAnalyst, using LION/web by the ranking mode, with a one-tailed Welch 2-sample t-test as the local statistics [6]. Changes in lipid patterns between CF and healthy phenotypes were connected to the main branches of LION ontology and, especially, lipid function, cellular component, and physical-chemical properties. The chi-square or binomial tests were used to compare observed with expected data distributions.

3. Results

3.1. Pre-Analytical Optimization

Folch extraction followed by alkaline methanolysis is the gold-standard for sphingolipids quantification [30,31]. This specific extraction protocol warrants a higher extraction rate of sphingolipids species by suppressing the interferences of preeminent phospholipids [32,33]. Hereby, as expected, it was confirmed that the samples treated with alkaline methanolysis displayed a higher intensity of sphingolipids (Figure S1). Curiously, the procedure used for total lipid analysis yielded a higher number of sphingolipids species correctly identified (84 vs. 104, considering the main subclasses: ceramides, hexosylceramides, and sphingomyelins). The sphingolipids profile, measured as fold changes between the two cell lines, fairly differed when using the two extraction protocols (Figure S1). Taking these results altogether, we decided to avoid the methanolysis in the untargeted lipidomics approach, limiting this specific treatment to the target sphingolipids analysis.

3.2. Optimization of the Analytical Conditions for Lipidomics Analysis

Using a mixture of 14 chemically pure lipids (differential ion mobility system suitability kit, synthetic lipid mix, Avanti Polar, Alabaster, AL, USA) covering all the subclasses, two distinct mobile-phase modifiers, and two different columns were tested. Ammonium acetate and an Acquity CSH column gave the maximum peak intensities (Tables S2 and S3) and the best lipidome coverage (Figure S2). CSH column was verified in +34% in lipids identified correctly (995 vs. 741, Figure S2). This was probably related to a better separation of different lipid classes. The number of IDA experiments in a cycle-time was also taken into consideration: using the configuration with 20 spectra/cycle, not surprisingly, the number of total spectra acquired was about two-fold in respect to the top 10 (Figure S3).

3.3. Performances of the Untargeted Lipidomics Analysis

MS-DIAL performances were evaluated by running standard samples containing a mixture of chemically pure lipids with a concentration of 1 μg/mL (10 ng injected): 10/14 (65%) lipids were identified correctly matching for both MS and MS/MS data, 3/14 (21%) were identified only by accurate mass, and 1/14 (7%) was not recognized at all (Table S4). The normalization method is critical to balance variations and eliminate experimental or biological biases. Internal standard-based normalization is the gold standard for targeted analysis of metabolites, but for untargeted analysis, it has been demonstrated that the method is out-performed by other approaches. The use of a few selected internal standards is not reasonable for the untargeted analysis of complex biological mixtures, since lipids, also comprising in the same class, displayed different chemical structures (e.g., fatty acid chains) and chromatographic behaviors. The choice of internal standards normalization was for the above reasons avoided.

An alternative approach to reduce the analytical and biological variabilities could be the use of the total ion count (TIC) [34,35]. The TIC was tested in our experiment (ochre curve in Figure 1) and gave satisfactory results with both cell lines, but we noted a limited linearity range in dependence on the amount of proteins in each sample (data not shown).

QC sample (see Methods) was used to calibrate the symmetric biases using weighted scatterplot smoothing (Lowess algorithm on MS-DIAL) for analytical signal correction [21,36,37]. The choice of normalization should be executed with the aim of decreasing variation not only in QC but also in experimental groups [38,39]. Therefore, we lessen the biological variability by normalizing data on the total protein content of the sample. Lowess coupled with biological normalization is presented as a single curve (green) in Figure 1. The latter showed the same performance of TIC, with about 70%–90% acceptable features (CV% < 30%) and, thus, was finally selected for our purpose. These normalization techniques were compared to the raw, not normalized data (red curve in Figure 1). In this limited context, specifically in the comparison between two phenotypes, the different normalization methods demonstrated minimal experimental variations among them, and so we proposed to choose the Lowess

coupled with biological normalization (green in Figure 1). Lack of normalization significantly affected the results on the HBE cell line (Figure 1B).

The intra-batch variability, which is the coefficient of variation (CV%) of the QC sample dispersed throughout the batch, was about 16%.

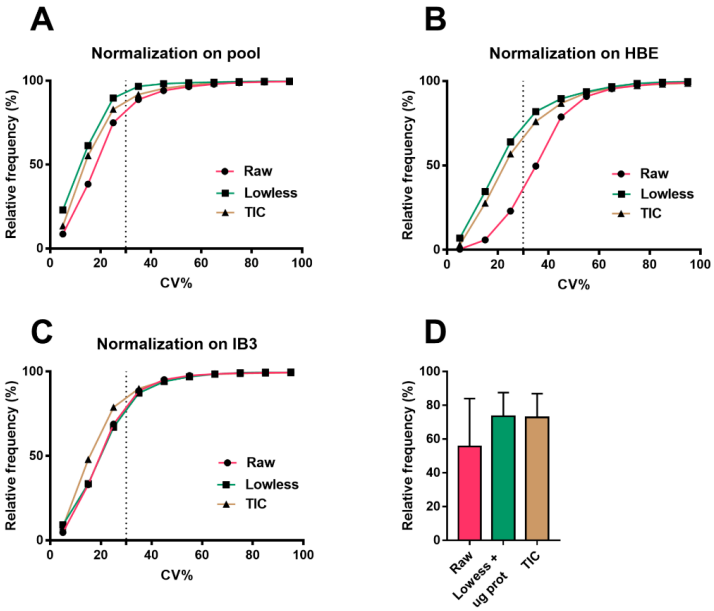

Figure 1. Cumulative frequency distribution of the coefficient of variations (CVs) (%) in (**A**) pool samples, (**B**) healthy HBE, and (**C**) cystic fibrosis (CF) cell extracts obtained for the precision evaluation of different normalization protocols comprehensive of results from both polarities. The dotted line indicates the separation between features within 30% of the CV, which is intended as the maximum permitted for the validation. The graphs showed the better performance of Lowess coupled to μg proteins as the normalization technique, reaching (**A**) 89%, (**B**) 64%, and (**C**) 68% in acceptable features (with a CV% inferior to 30%). (**D**) Graphs show the mean ± SD of the percentage of acceptable features (with a CV% inferior to 30%) between the different normalization techniques.

3.4. Untargeted Lipidomics of Cystic Fibrosis

MS-DIAL recorded, considering data from both polarities and after blank filtration, n.13375 mass spectra in the whole set of samples, of which, n. 7787 (58%) presented the MS/MS data. The software revealed n.1863-annotated lipids (MS^2-matched, 14%), and, after a manual validation, the final number was restricted to n.1159 (8.4%), which were grouped in the different classes and subclasses (Figure S4).

The distribution profile of lipid classes in healthy (H, HBE) and cystic fibrosis cells (CF, IB3) was achieved by summing all the normalized intensities of the lipids identified within the single classes (an example is shown in Equation (2)). As expected, in CF, we found a significant general accumulation of all lipid species, in particular ceramides, hexosylceramides, lactosylceramides, GM3, and cholesterol esters (Figure 2). In addition, ether-linked phospholipids (etherPL) were found to be highly modulated by the disease. Specifically, ether-linked phosphatidylcholine (fold change CF/H: 14.56) are the most abundant class recognized in our cell model, followed by ether-linked phosphatidylethanolamine (fold change CF/H: 4.75). No statistical differences were found in the concentrations of free fatty acids, dihydroceramides, sphingomyelins, phosphatidylcholines, phosphatidylinositols, sphingosine, free cholesterol, acylglycerols, cardiolipins (data not shown), and acylcarnitines (data not shown).

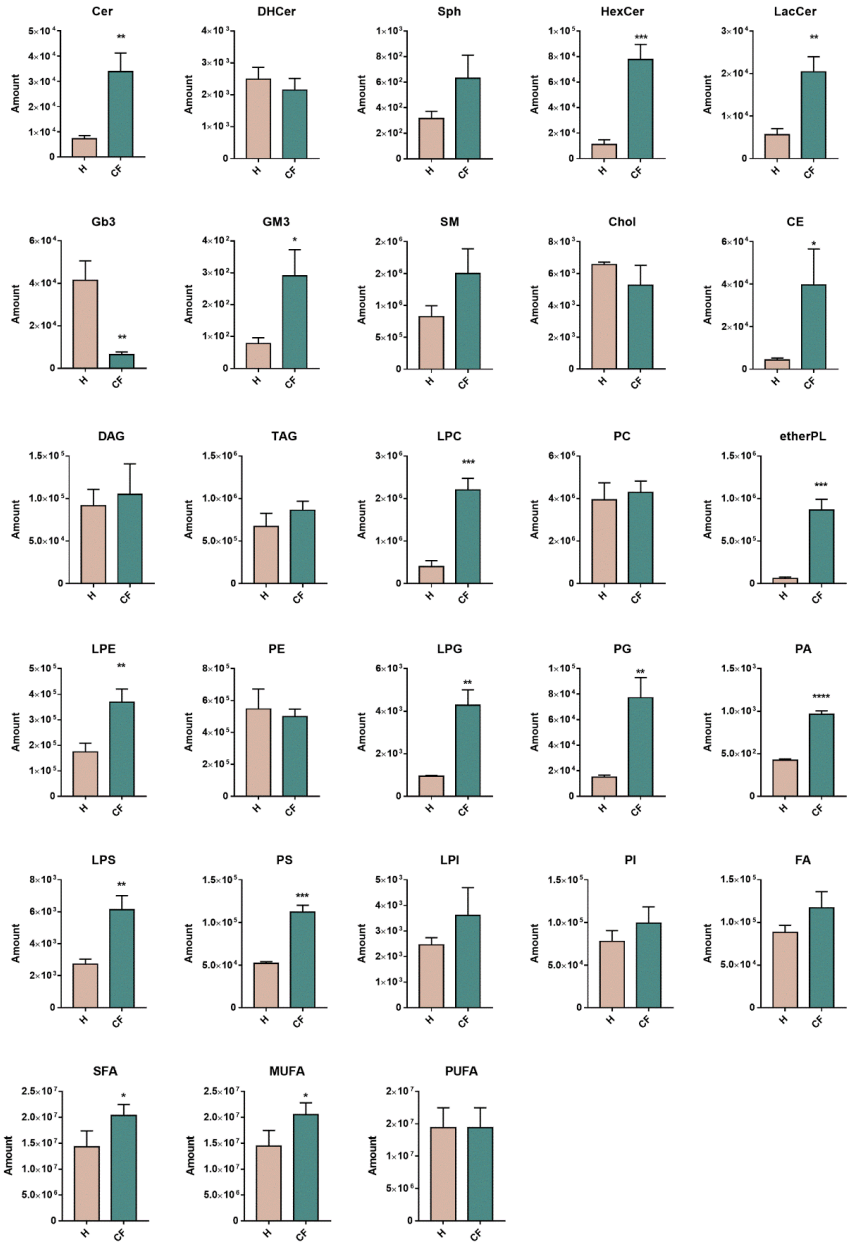

Figure 2. Lipid content comparison between healthy epithelial (H, n = 3 independent biological replicates) vs. cystic fibrosis (CF, n = 3 independent biological replicates) cells. Graphs represent the lipid amount (Amount, mean ± SD), which indicates the sum of the metabolites intensities within a class after normalization (see Equation (1)). Two-tailed unpaired t-tests were performed in each lipid class to establish a statistical difference (* $p \leq 0.05$; ** $p \leq 0.01$; *** $p \leq 0.001$; **** $p \leq 0.0001$).

Univariate and multivariate statistical approaches were employed in order to select relevant lipids for cellular phenotype discrimination. Volcano plot analysis selected n. 632 lipids (81.3% elevated and 18.7% reduced in CF vs. healthy), which contemporarily presented a fold change > 2 and a corrected p-value < 0.05 (Figure 3).

Chemometric analysis by supervised PLS-DA (Figure 4A) was then used to maximize the separation between groups and to determine important features of CF by VIP value >1, which were n. 709. Since PLS-DA tends to overfit data, the model was validated [40] by the Leave-one-out cross-validation method, displaying an R2 and Q2 of 0.96 and 0.94, respectively.

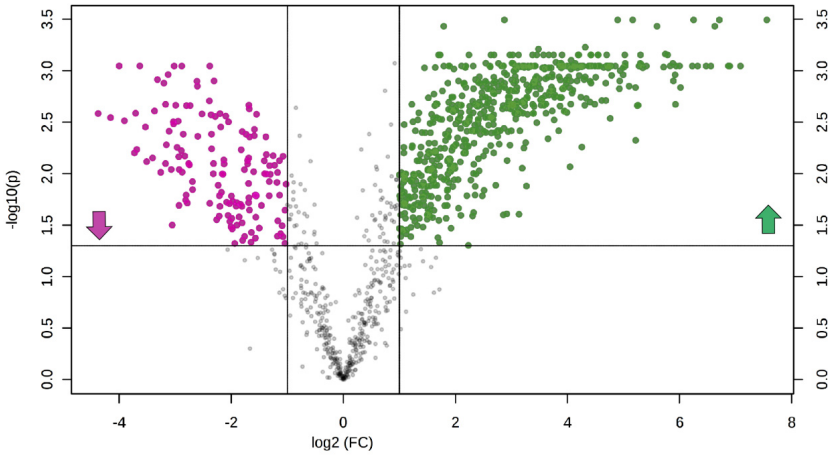

Figure 3. The volcano plot is a combination of fold change and t-tests: X-axis is $\log_2$(fold change, FC), and Y-axis is $-\log_{10}$ (adjusted for false discovery rate). Dots indicate features that presented both a FC >2 and p-value < 0.05. Lipids in pink and green are reduced (n.118) and augmented (n.514) in CF vs. H, respectively.

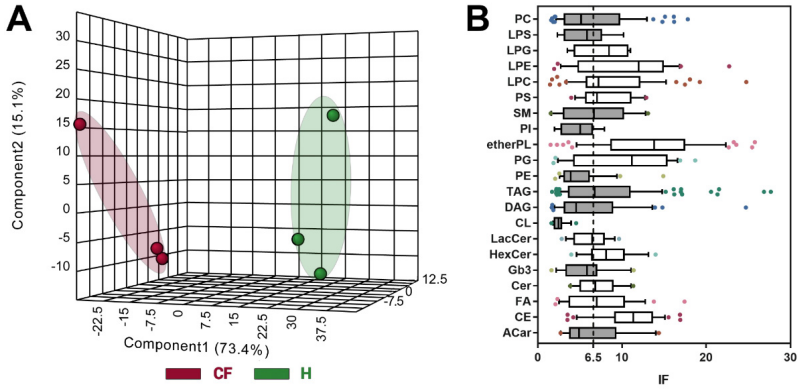

Figure 4. (**A**) Partial least squares discriminant analysis (PLS-DA) chemometric analysis. (**B**) Box and whiskers plots (line at median, and box stretched from the 25–75th percentiles; whiskers indicated the 10–90th, whereas outliers were plotted as single points) of the discriminant lipids (n = 624) subdivided for lipid classes and evaluated by their IF scores (see Equation (3)). Grey boxes designated lipid classes that displayed an IF< cut-off (visualized as a dotted line and calculated as the lower confidence limit of the median of the features considered).

Biomarker selection was finally performed combining the data obtained with the different scores from the Volcano plot and PLS-DA. The uni- and multivariate analyses were combined, by restricting features to n.624, in order to increase the discrimination power between the two phenotypes. To achieve this goal, for each identified feature, the IF score (data not shown) was calculated using the VIP score, *p*-value, and FC (see Equation (3)). From the n. 624 lipids, the top 100 discriminant lipids, which distinguished the pathological phenotype of CF from healthy bronchial cells significantly, are listed in Table S5.

$$\text{IF} = |\log_2 \text{FC}| \cdot (-\log_{10} p \text{ value}) \cdot \text{VIP score} \quad (3)$$

The high presence of lipids bringing an ether-linked acyl chain is shown within this group. In order to have an overview of the main alterations of the lipid CF phenotype, we added a further discriminating analysis that increases the screening of the feature and focuses the attention only on the most significant changes between CF vs. healthy. We proposed the use of the median IF for each lipid class (Table S6), which was graphed as box and whiskers plot (Figure 4B). All the classes were then compared with an arbitrary cut-off (6.5), that we chose to be the lower confidence limit of the median calculated from all the features (n.624). The classes represented by white boxes demonstrated an IF median superior to the cut-off, and therefore, were considered as the most significantly modulated: etherPL, cholesterol esters, and sphingolipids (especially hexosyl- and lactosylceramides).

Future validations on the identified biomarkers are highly suggested, possibly on patient-derived primary cells, since this preliminary study analyzed an immortalized cell line. Altered lipid composition, showed in Figure 2, was reflected in different lipid ontologies, indicating lipid function, cellular component, and chemical and physical properties (Figure 5A). The enrichment analysis showed a highly significant modification in the lipids implicated in cell membrane compositions (lipid function ontology). When looking at lipid components, the endoplasmic reticulum and mitochondria compartments are significantly modified in CF vs. healthy cells. Finally, these lipid alterations are also reflected in modifications on chemical and biophysical properties: specifically, affecting chain lengths, saturation, and ether-bound composition of glycerol- and sphingolipids. We noted a quantitative increase in the levels of saturated and monounsaturated fatty acids (SFAs and MUFAs) in CF vs. healthy, whereas the polyunsaturated (PUFAs) species resulted unchanged (Figure 2). Otherwise, in the subgroup of the top 100 discriminant lipids, we observed a prevalence % of PUFAs (Figure 5B). In the same way, we noted a prevalence % of ether-PL over ester-bound phospholipids (Figure 5C).

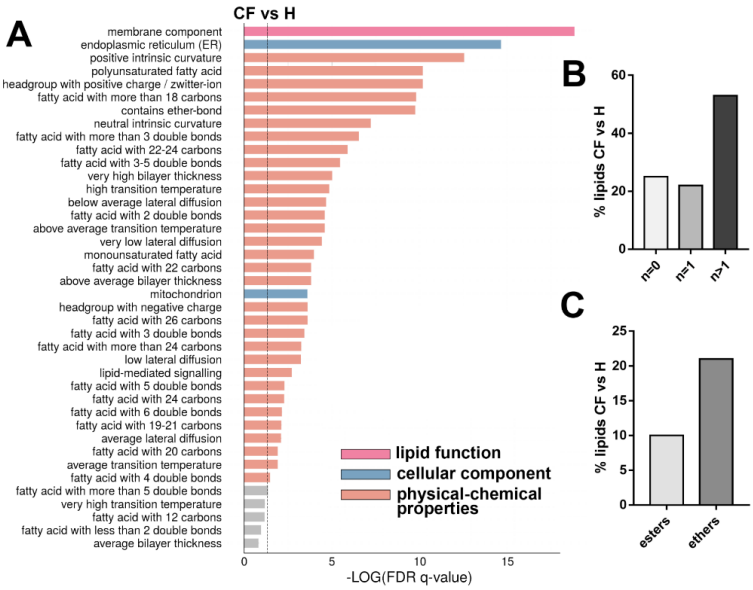

Figure 5. (A) Enrichment analysis (top 40) of CF vs. H phenotypes. The dotted line indicates the cut-off value of significant enrichments ($q < 0.05$). Bar length is related with the enrichment (−log q-values corrected for false discovery rate, FDR), whereas colors are dependent to the type of the enrichment: lipid function, cellular component, and physical-chemical properties. (**B**) Distribution of the acyl chain unsaturation from all lipid fraction (%) in CF vs. H discriminant lipid group (top 100). (**C**) Distribution of the ester and ether linkages in phospholipids (%) in CF vs. H in the discriminant lipid group (top 100). In (**B**) the chi-square test and in (**C**) binomial test, revealed a p-value < 0.05.

4. Discussion

In this study, we investigated the unusual lipid composition in CF epithelial bronchial cells using an untargeted LC-MS/MS approach. Before each experiment, to ensure that our study produced clinically valid results, we felt the need to carry out a comprehensive optimization study of each step of the method used. We tested two different modified Folch extraction protocols, and we chose the one with the higher number of species identified. We have also highlighted that the use of longer column (10 vs. 5 cm) and with peculiar silica charged surface allows improving the separation between phosphor- and sphingolipids compared to inert silica (BEH). Furthermore, we highlighted the strength of a conservative data-dependent approach in untargeted lipidomics to uncover pathophysiological mechanisms implicated in a disease and, in particular, in CF. It took dedicated time and attention to find the most suitable method for normalizing data before statistical processing, highlighting how this step is particularly critical in biological samples. We propose the use of an innovative statistical index (impact factor) able to combine data from different tests, augmenting the robustness of the discovery results and the consequent biological implications.

CFTR misfunction in CF is associated with altered lipid homeostasis, consisting in inflammatory ceramide accumulation in the lung, sterol accumulation in the airways, hepatic steatosis, and plasma dyslipidemia [11,12,17,41–43].

In this preliminary study, we aimed to validate the untargeted lipidomics by the application on the IB3 immortalized CF cell line. Secondly, we accrue to confirm the described lipid alterations and identify the potentially related signatures of the disease (in Figure 6). We strongly feel that our findings on CF lipidomic deregulation need additional confirmation, possibly using patient-derived primary cells or lung biopsies. These data do not attempt to give conclusive findings on the lipid profile in CF

but rather to show the importance of a reliable, large-scale analytical method to shed light on biological mechanisms. Despite the use of a single cell line, our results confirm many of the literature findings and disclose interesting topics that deserve further investigations.

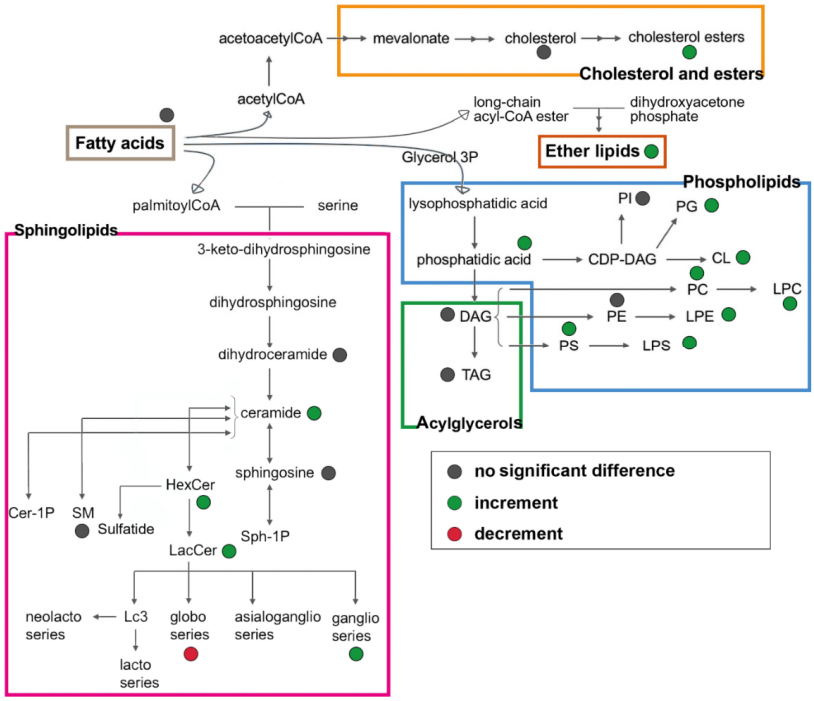

Figure 6. Overview of the lipid biosynthetic and metabolic pathways. Colored dots represented the lipid changes in CF bronchial epithelial cells.

The first observation is that, in CF epithelial cells, ceramide and glycosylated sphingolipids accumulate (Figure 2), such as hexosylceramides, lactosylceramides, and GM3 (monosialogangliosides). Ceramides are implicated in inflammation [44,45], and their accumulation, in CF cells, was previously demonstrated by us and others [15,46–48]. Studies from our group already demonstrated, through in vivo and in vitro CF models, the therapeutic role of reducing ceramide synthesis [46,49].

Besides, a reduced pool of luminal surface sphingosine, derived from apical membrane ceramide hydrolysis, has been previously reported in CF airways from Grassmé et al. [48], but when looking at the total bulk of cellular sphingosine, we did not observe any significant reduction.

Notably, in this study, using the untargeted lipidomics approach, we observed a significant increase in hexosylceramides (Figure 2). Although poorly characterized up to now, the accumulation of hexosylceramides was demonstrated to exacerbate the inflammation [50,51]; moreover, its synthesis was increased in damaged tissues [52]. In addition, hexosylceramides, which may link either glucose or galactose to ceramide, and lactosylceramides have been associated with oxidative stress and promotion of the inflammatory pathway [53]. The gangliosides (see GM3 in Figure 2) at the membrane were significantly increased. However, the high-ranked discrimination score (IF) found in hexosylceramides (Figure 4B) was not paralleled by polyglycosylated species such as GM3. We speculate that CF cells can enhance ceramide glycosylation to reduce its accrual and related inflammatory stress. The process of glycosylation is also enhanced in tumor metabolism [54]. This hypothesis opens new questions

on the physiologic role of this lipid metabolism, and it requires further investigations at the aim of identifying innovative biomarkers in inflammatory diseases and potential therapeutic targets.

Furthermore, we observed an increase in lysophospholipids (Figure 2), specifically in LPC, which was shown to increase during chronic inflammation [55,56]. Mainly, it was found to be incremented in CF bronco epithelial cells, and, for that reason, it can be considered as a possible marker for the chronic inflammatory status [57].

We measured a significant increase in storage lipids, such as cholesterol esters (Figure 2). As previously mentioned, this might be related to the inflammatory status associated with lipid accumulation and to altered lipid intracellular traffic. These data are in-line with reported evidence of cholesterol accumulation in CF bronchi [14,16,58] and, most importantly, with increased concentration of cholesterol esters in pediatric CF patients with bronchoalveolar lavage fluid vs. control subjects [59,60]. Mutated CFTR cells may display an altered lipid synthesis, along with lipid-defective storage, mobilization, and structural usage. These biochemical alterations could sustain chronic inflammation and an inadequate response to infection [19,61].

To note, we also observed a significant increase in etherPL (Figure 2). This finding was also supported by the increased presence of ether-linked fatty acids in lipids extracted from CF bronchoalveolar lavage [56]. Ether lipids, characterized by an ether bond between glycerol and the fatty acid in the *sn-1* position, are essential membrane regulators of fluidity and fusion. Our results suggest that CFTR alteration and disturbance of the membrane composition are somehow linked [62,63]. The increase in ether-link-bearing lipids may be a response to enhanced membrane stability [64]. In addition, it was suggested that ether lipids are involved in regulating cell differentiation, cellular signaling, and reducing oxidative stress by acting as endogenous antioxidants [65].

High levels of SFAs and MUFAs, along with low levels of omega-3 and omega-6 PUFAs, have been reported in CF plasma [9,10,66]. In our CF cell model, we confirmed the quantitative increase of SFAs and MUFAs as compared to control cells (Figure 2). Looking at the top 100 discriminant lipids, however, PUFA species are more represented (Figure 5B) with respect to healthy cells. The observed lipid modifications could impact the biophysical properties of cell membranes, mainly modulating the membrane stability and membrane protein's function [67,68]. Considering that, in the literature, plasma levels of PUFAs in CF were found to be reduced [9,10,66], however, the link between CF pathophysiology and this abnormality remains unclear [69].

5. Conclusions

In this study, we developed an untargeted high-throughput lipidomics workflow and applied it to the study of the unusual lipid composition in a CF epithelial bronchial cell line. We propose the innovative use of the impact factor statistical index to augment the robustness of the discovery, along with the biological and clinical significance. The tested model of the CF bronchial cell line (IB3) displayed a pervasive alteration in the lipid metabolism that, in turn, modified the lipid storage, cell membrane composition, and proinflammatory lipids. Future studies, possibly on patients' primary cell lines, are required to elucidate our experimental findings further and uncover the pathophysiological mechanisms implicated in CF.

Supplementary Materials: The following are available online at http://www.mdpi.com/2073-4409/9/5/1197/s1, Figure S1. Sphingolipidomics: comparison between the dedicated extraction of sphingolipid with alkaline methanolysis and total lipid extraction, Figure S2. Comparison between the number of lipids evidenced using two different LC analytical columns, Figure S3. Total number of MS/MS spectra acquired using different data-dependent settings, Figure S4. Distribution of the lipids recognized by lipidomics analysis on the whole set of samples divided by sub-class, Table S1. Lipids identification according to MS/MS fragmentation, Table S2. Performance comparison between mobile phases buffer, Table S3. Performance comparison between analytical columns, Table S4. MS-DIAL performances in the lipid identification, Table S5. Top-100 lipids selected as potential biomarkers associated with CF phenotype, Table S6. Descriptive statistic of the discriminant features divided for lipid classes.

Author Contributions: Conceptualization: M.D.C., P.S., and R.P. Investigation: M.D.C., A.M., A.Z., and A.C. Formal analysis: M.D.C. Drafting of the manuscript: M.D.C. Supervision: R.G., P.S., and R.P. Writing—review and editing: R.P. and P.S. All authors have read and agreed to the published version of the manuscript.

Funding: This research was funded by the Italian Cystic Fibrosis Foundation, Grant FFC#11-2016.

Acknowledgments: We thank the Italian Cystic Fibrosis Foundation for the financial support of this work. M.D.C. was supported by the PhD program in Molecular and Translational Medicine of the Università degli Studi di Milano, Milan. Part of this work was carried out in OMICs, an advanced mass spectrometry platform established by the Università degli Studi di Milano. The authors acknowledge Fiorenza Farè, Giulia Garrone, and Manuela Fontana from OMICs for their technical contributions. A particular thanks to my aunt, Laura Carla Tosi, who contributed to managing the data by Excel.

Conflicts of Interest: The authors declare no conflicts of interest.

Abbreviations

H	healthy phenotype
CF	cystic fibrosis
Cer	ceramides
DHCer	dihydroceramides
HexCer	glucosylceramides
LacCer	lactosylceramides
GM3	gangliosides
Gb3	globotriaosylceramide
SM	sphingomyelins
Chol	free cholesterol
CE	cholesterol esters
LPE	lysophosphatidyletanolamines
PC	phosphatidylcholines
PG	phosphatidylglicerols
PI	phosphatidylinositoles
LPI	lysophosphatidylinositoles
PG	phosphatidylglicerols
LPG	lysophosphatidylglicerols
FA	free fatty acids
ACar	acylcarnitines
CL	cardiolipins
etherPL	ether-linked phospholipids
SFA	saturated fatty acids
MUFA	monounsaturated fatty acids
PUFA	polyunsaturated fatty acids

References

1. Tang, Q.Q. Lipid metabolism and diseases. *Sci. Bull.* **2016**, *61*, 1471–1472. [CrossRef]
2. Yan, F.; Wen, Z.; Wang, R.; Luo, W.; Du, Y.; Wang, W.; Chen, X. Identification of the lipid biomarkers from plasma in idiopathic pulmonary fibrosis by Lipidomics. *BMC Pulm. Med.* **2017**, *17*, 174. [CrossRef] [PubMed]
3. Wenk, M.R. Lipidomics: New tools and applications. *Cell* **2010**, *143*, 888–895. [CrossRef]
4. Wenk, M.R. The emerging field of lipidomics. *Nat. Rev. Drug Discov.* **2005**, *4*, 594–610. [CrossRef] [PubMed]
5. Sethi, S.; Brietzke, E. Recent advances in lipidomics: Analytical and clinical perspectives. *Prostaglandins Other. Lipid. Mediat.* **2017**, *128*, 8–16. [CrossRef] [PubMed]
6. Molenaar, M.R.; Jeucken, A.; Wassenaar, T.A.; Van De Lest, C.H.A.; Brouwers, J.F.; Helms, J.B. LION/web: A web-based ontology enrichment tool for lipidomic data analysis. *Gigascience* **2019**, *8*, giz061. [CrossRef] [PubMed]
7. Elborn, J.S. Cystic fibrosis. *Lancet* **2016**, *388*, 2519–2531. [CrossRef]
8. De Boeck, K.; Amaral, M.D. Progress in therapies for cystic fibrosis. *Lancet Respir. Med.* **2016**, *4*, 662–674. [CrossRef]
9. Risé, P.; Volpi, S.; Colombo, C.; Padoan, R.F.; D'Orazio, C.; Ghezzi, S.; Melotti, P.; Bennato, V.; Agostoni, C.; Assael, B.M.; et al. Whole blood fatty acid analysis with micromethod in cystic fibrosis and pulmonary disease. *J. Cyst. Fibros.* **2010**, *9*, 228–233. [CrossRef]

10. Freedman, S.D.; Blanco, P.G.; Shea, J.C.; Alvarez, J.G. Analysis of lipid abnormalities in CF mice. *Methods Mol. Med.* **2002**, *70*, 517–524.
11. Ollero, M.; Astarita, G.; Guerrera, I.C.; Sermet-Gaudelus, I.; Trudel, S.; Piomelli, D.; Edelman, A. Plasma lipidomics reveals potential prognostic signatures within a cohort of cystic fibrosis patients. *J. Lipid Res.* **2011**, *52*, 1011–1022. [CrossRef] [PubMed]
12. Gelzo, M.; Sica, C.; Elce, A.; Dello Russo, A.; Iacotucci, P.; Carnovale, V.; Raia, V.; Salvatore, D.; Corso, G.; Castaldo, G. Reduced absorption and enhanced synthesis of cholesterol in patients with cystic fibrosis: A preliminary study of plasma sterols. *Clin. Chem. Lab. Med.* **2016**, *54*, 1461–1466. [CrossRef] [PubMed]
13. Figueroa, V.; Milla, C.; Parks, E.J.; Schwarzenberg, S.J.; Moran, A. Abnormal lipid concentrations in cystic fibrosis. *Am. J. Clin. Nutr.* **2002**, *75*, 1005–1011. [CrossRef] [PubMed]
14. White, N.M.; Jiang, D.; Burgess, J.D.; Bederman, I.R.; Previs, S.F.; Kelley, T.J. Altered cholesterol homeostasis in cultured and in vivo models of cystic fibrosis. *Am. J. Physiol.-Lung Cell. Mol. Physiol.* **2007**, *292*, 476–486. [CrossRef]
15. Teichgräber, V.; Ulrich, M.; Endlich, N.; Riethmüller, J.; Wilker, B.; De Oliveira-Munding, C.C.; Van Heeckeren, A.M.; Barr, M.L.; Von Kürthy, G.; Schmid, K.W.; et al. Ceramide accumulation mediates inflammation, cell death and infection susceptibility in cystic fibrosis. *Nat. Med.* **2008**, *14*, 382–391. [CrossRef]
16. Ernst, W.L.; Shome, K.; Wu, C.C.; Gong, X.; Frizzell, R.A.; Aridor, M. VAMP-associated proteins (VAP) as receptors that couple cystic fibrosis transmembrane conductance regulator (CFTR) proteostasis with lipid homeostasis. *J. Biol. Chem.* **2016**, *291*, 5206–5220. [CrossRef]
17. Fang, D.; West, R.H.; Manson, M.E.; Ruddy, J.; Jiang, D.; Previs, S.F.; Sonawane, N.D.; Burgess, J.D.; Kelley, T.J. Increased plasma membrane cholesterol in cystic fibrosis cells correlates with CFTR genotype and depends on de novo cholesterol synthesis. *Respir. Res.* **2010**, *11*, 61. [CrossRef]
18. Mingione, A.; Dei Cas, M.; Bonezzi, F.; Caretti, A.; Piccoli, M.; Anastasia, L.; Ghidoni, R.; Paroni, R.; Signorelli, P. Inhibition of Sphingolipid Synthesis as a Phenotype-Modifying Therapy in Cystic Fibrosis. *Cell. Physiol. Biochem.* **2020**, *50323257*, 110–125.
19. Caretti, A.; Torelli, R.; Perdoni, F.; Falleni, M.; Tosi, D.; Zulueta, A.; Casas, J.; Sanguinetti, M.; Ghidoni, R.; Borghi, E.; et al. Inhibition of ceramide de novo synthesis by myriocin produces the double effect of reducing pathological inflammation and exerting antifungal activity against A. fumigatus airways infection. *Biochim. Biophys. Acta-Gen. Subj.* **2016**, *1860*, 1089–1097. [CrossRef]
20. Della Corte, A.; Chitarrini, G.; Di Gangi, I.M.; Masuero, D.; Soini, E.; Mattivi, F.; Vrhovsek, U. A rapid LC-MS/MS method for quantitative profiling of fatty acids, sterols, glycerolipids, glycerophospholipids and sphingolipids in grapes. *Talanta* **2015**, *140*, 52–61. [CrossRef]
21. Cajka, T.; Smilowitz, J.T.; Fiehn, O. Validating Quantitative Untargeted Lipidomics Across Nine Liquid Chromatography-High-Resolution Mass Spectrometry Platforms. *Anal. Chem.* **2017**, *89*, 12360–12368. [CrossRef] [PubMed]
22. Huan, T.; Forsberg, E.M.; Rinehart, D.; Johnson, C.H.; Ivanisevic, J.; Benton, H.P.; Fang, M.; Aisporna, A.; Hilmers, B.; Poole, F.L.; et al. Systems biology guided by XCMS Online metabolomics. *Nat. Methods* **2017**, *14*, 461–462. [CrossRef] [PubMed]
23. Tsugawa, H.; Cajka, T.; Kind, T.; Ma, Y.; Higgins, B.; Ikeda, K.; Kanazawa, M.; Vandergheynst, J.; Fiehn, O.; Arita, M. MS-DIAL: Data-independent MS/MS deconvolution for comprehensive metabolome analysis. *Nat. Methods* **2015**, *12*, 523–526. [CrossRef] [PubMed]
24. Shan, J.; Qian, W.; Shen, C.; Lin, L.; Xie, T.; Peng, L.; Xu, J.; Yang, R.; Ji, J.; Zhao, X. High-resolution lipidomics reveals dysregulation of lipid metabolism in respiratory syncytial virus pneumonia mice. *RSC Adv.* **2018**, *8*, 29368–29377. [CrossRef]
25. Hu, C.; Zhou, Y.; Feng, J.; Zhou, S.; Li, C.; Zhao, S.; Shen, Y.; Hong, L.; Xuan, Q.; Liu, X.; et al. Untargeted Lipidomics Reveals Specific Lipid Abnormalities in Nonfunctioning Human Pituitary Adenomas. *J. Proteome Res.* **2019**, *19*, 455–463. [CrossRef] [PubMed]
26. Xia, J.; Wishart, D.S. Using metaboanalyst 3.0 for comprehensive metabolomics data analysis. *Curr. Protoc. Bioinforma.* **2016**, *55*, 14.10.1–14.10.91. [CrossRef]
27. Chong, J.; Soufan, O.; Li, C.; Caraus, I.; Li, S.; Bourque, G.; Wishart, D.S.; Xia, J. MetaboAnalyst 4.0: Towards more transparent and integrative metabolomics analysis. *Nucleic Acids Res.* **2018**, *46*, 486–494. [CrossRef]

28. Rahman, M.A.; Akond, M.; Babar, M.A.; Beecher, C.; Erickson, J.; Thomason, K.; De Jong, F.A.; Mason, R.E. LC-HRMS Based Non-Targeted Metabolomic Profiling of Wheat (Triticum aestivum; L.) under Post-Anthesis Drought Stress. *Am. J. Plant Sci.* **2017**, *8*, 3024–3061. [CrossRef]
29. Jiang, W.; Gao, L.; Li, P.; Kan, H.; Qu, J.; Men, L.; Liu, Z.; Liu, Z. Metabonomics study of the therapeutic mechanism of fenugreek galactomannan on diabetic hyperglycemia in rats, by ultra-performance liquid chromatography coupled with quadrupole time-of-flight mass spectrometry. *J. Chromatogr. B Anal. Technol. Biomed. Life Sci.* **2017**, *1044*, 8–16. [CrossRef]
30. Platania, C.B.M.; Dei Cas, M.; Cianciolo, S.; Fidilio, A.; Lazzara, F.; Paroni, R.; Pignatello, R.; Strettoi, E.; Ghidoni, R.; Drago, F.; et al. Novel ophthalmic formulation of myriocin: implications in retinitis pigmentosa. *Drug Deliv.* **2019**, *26*, 237–243. [CrossRef]
31. La Corte, E.; Cas, M.D.; Raggi, A.; Patan, M.; Broggi, M.; Schiavolin, S.; Calatozzolo, C.; Pollo, B.; Pipolo, C.; Bruzzone, M.G.; et al. Long and Very-Long-Chain Ceramides Correlate with A More Aggressive Behavior in Skull Base Chordoma Patients. *Int. J. Mol. Sci.* **2019**, *20*, 4480. [CrossRef] [PubMed]
32. Jiang, X.; Cheng, H.; Yang, K.; Gross, R.W.; Han, X. Alkaline methanolysis of lipid extracts extends shotgun lipidomics analyses to the low-abundance regime of cellular sphingolipids. *Anal. Biochem.* **2007**, *371*, 135–145. [CrossRef] [PubMed]
33. Merrill, A.H.; Sullards, M.C.; Allegood, J.C.; Kelly, S.; Wang, E. Sphingolipidomics: High-throughput, structure-specific, and quantitative analysis of sphingolipids by liquid chromatography tandem mass spectrometry. *Methods* **2005**, *36*, 207–224. [CrossRef] [PubMed]
34. Liu, X.; Ser, Z.; Locasale, J.W. Development and quantitative evaluation of a high-resolution metabolomics technology. *Anal. Chem.* **2014**, *86*, 2175–2184. [CrossRef] [PubMed]
35. Rombouts, C.; De Spiegeleer, M.; Van Meulebroek, L.; De Vos, W.H.; Vanhaecke, L. Validated comprehensive metabolomics and lipidomics analysis of colon tissue and cell lines. *Anal. Chim. Acta* **2019**, *1066*, 79–92. [CrossRef] [PubMed]
36. Han, T.-L.; Yang, Y.; Zhang, H.; Law, K.P. Analytical challenges of untargeted GC-MS-based metabolomics and the critical issues in selecting the data processing strategy. *F1000Research* **2017**, *6*, 967. [CrossRef]
37. Van Der Kloet, F.M.; Bobeldijk, I.; Verheij, E.R.; Jellema, R.H. Analytical error reduction using single point calibration for accurate and precise metabolomic phenotyping. *J. Proteome Res.* **2009**, *8*, 5132–5141. [CrossRef]
38. Drotleff, B.; Lämmerhofer, M. Guidelines for Selection of Internal Standard-based Normalization Strategies in Untargeted Lipidomic Profiling by LC-HR-MS/MS. *Anal. Chem.* **2019**, *91*, 9836–9843. [CrossRef]
39. Barupal, D.K.; Fan, S.; Wancewicz, B.; Cajka, T.; Sa, M.; Showalter, M.R.; Baillie, R.; Tenenbaum, J.D.; Louie, G.; Kaddurah-Daouk, R.; et al. Generation and quality control of lipidomics data for the alzheimer's disease neuroimaging initiative cohort. *Sci. Data* **2018**, *5*, 1–13. [CrossRef]
40. Chiu, C.-Y.; Yeh, K.-W.; Lin, G.; Chiang, M.-H.; Yang, S.-C.; Chao, W.-J.; Yao, T.-C.; Tsai, M.-H.; Hua, M.-C.; Liao, S.-L.; et al. Metabolomics Reveals Dynamic Metabolic Changes Associated with Age in Early Childhood. *PLoS ONE* **2016**, *11*, e0149823. [CrossRef]
41. Ollero, M. Methods for the study of lipid metabolites in cystic fibrosis. *J. Cyst. Fibros.* **2004**, *3*, 97–98. [CrossRef]
42. Del Ciampo, I.R.L.; Sawamura, R.; Machado Fernandes, M.I. Cystic fibrosis: From protein-energy malnutrition to obesity with dyslipidemia. *Iran. J. Pediatr.* **2013**, *23*, 605–606. [PubMed]
43. Ziobro, R.; Henry, B.; Edwards, M.J.; Lentsch, A.B.; Gulbins, E. Ceramide mediates lung fibrosis in cystic fibrosis. *Biochem. Biophys. Res. Commun.* **2013**, *434*, 705–709. [CrossRef] [PubMed]
44. Hannun, Y.A.; Obeid, L.M. The ceramide-centric universe of lipid-mediated cell regulation: Stress encounters of the lipid kind. *J. Biol. Chem.* **2002**, *277*, 25847–25850. [CrossRef] [PubMed]
45. Hannun, Y.A.; Obeid, L.M. Principles of bioactive lipid signalling: Lessons from sphingolipids. *Nat. Rev. Mol. Cell Biol.* **2008**, *9*, 139–150. [CrossRef]
46. Caretti, A.; Bragonzi, A.; Facchini, M.; De Fino, I.; Riva, C.; Gasco, P.; Musicanti, C.; Casas, J.; Fabriàs, G.; Ghidoni, R.; et al. Anti-inflammatory action of lipid nanocarrier-delivered myriocin: Therapeutic potential in cystic fibrosis. *Biochim. Biophys. Acta-Gen. Subj.* **2014**, *1840*, 586–594. [CrossRef]
47. Ramu, Y.; Xu, Y.; Lu, Z. Inhibition of CFTR Cl- channel function caused by enzymatic hydrolysis of sphingomyelin. *Proc. Natl. Acad. Sci. USA* **2007**, *104*, 6448–6453. [CrossRef]

48. Grassmé, H.; Henry, B.; Ziobro, R.; Becker, K.A.; Riethmüller, J.; Gardner, A.; Seitz, A.P.; Steinmann, J.; Lang, S.; Ward, C.; et al. β1-Integrin Accumulates in Cystic Fibrosis Luminal Airway Epithelial Membranes and Decreases Sphingosine, Promoting Bacterial Infections. *Cell Host Microbe* **2017**, *21*, 707–718.e8. [CrossRef]
49. Hamai, H.; Keyserman, F.; Quittell, L.M.; Worgall, T.S. Defective CFTR increases synthesis and mass of sphingolipids that modulate membrane composition and lipid signaling. *J. Lipid Res.* **2009**, *50*, 1101–1108. [CrossRef]
50. Hannun, Y.A.; Obeid, L.M. Sphingolipids and their metabolism in physiology and disease. *Nat. Rev. Mol. Cell Biol.* **2018**, *19*, 175–191. [CrossRef]
51. Astudillo, L.; Therville, N.; Colacios, C.; Ségui, B.; Andrieu-Abadie, N.; Levade, T. Glucosylceramidases and malignancies in mammals. *Biochimie* **2016**, *125*, 267–280. [CrossRef] [PubMed]
52. Nagata, M.; Izumi, Y.; Ishikawa, E.; Kiyotake, R.; Doi, R.; Iwai, S.; Omahdi, Z.; Yamaji, T.; Miyamoto, T.; Bamba, T.; et al. Intracellular metabolite β-glucosylceramide is an endogenous Mincle ligand possessing immunostimulatory activity. *Proc. Natl. Acad. Sci. USA* **2017**, *114*, e3285–e3294. [CrossRef] [PubMed]
53. Apostolopoulou, M.; Gordillo, R.; Koliaki, C.; Gancheva, S.; Jelenik, T.; De Filippo, E.; Herder, C.; Markgraf, D.; Jankowiak, F.; Esposito, I.; et al. Specific hepatic sphingolipids relate to insulin resistance, oxidative stress, and inflammation in nonalcoholic steato hepatitis. *Diabetes Care* **2018**, *41*, 1235–1243. [CrossRef] [PubMed]
54. Barth, B.M.; Shanmugavelandy, S.S.; Tacelosky, D.M.; Kester, M.; Morad, S.A.F.; Cabot, M.C. Gaucher's disease and cancer: A sphingolipid perspective. *Crit. Rev. Oncog.* **2013**, *18*, 221–234. [CrossRef]
55. Chiurchiù, V.; Leuti, A.; Maccarrone, M. Bioactive lipids and chronic inflammation: Managing the fire within. *Front. Immunol.* **2018**, *9*, 38. [CrossRef]
56. Seidl, E.; Kiermeier, H.; Liebisch, G.; Ballmann, M.; Hesse, S.; Paul-Buck, K.; Ratjen, F.; Rietschel, E.; Griese, M. Lavage lipidomics signatures in children with cystic fibrosis and protracted bacterial bronchitis. *J. Cyst. Fibros.* **2019**, *18*, 790–795. [CrossRef]
57. Tselepis, A.D.; Chapman, M.J. Inflammation, bioactive lipids and atherosclerosis: Potential roles of a lipoprotein-associated phospholipase A2, platelet activating factor-acetylhydrolase. *Atheroscler. Suppl.* **2002**, *3*, 57–68. [CrossRef]
58. Gentzsch, M.; Choudhury, A.; Chang, X.B.; Pagano, R.E.; Riordan, J.R. Misassembled mutant ΔF508 CFTR in the distal secretory pathway alters cellular lipid trafficking. *J. Cell Sci.* **2007**, *120*, 447–455. [CrossRef] [PubMed]
59. Ma, D.C.; Yoon, A.J.; Faull, K.F.; Desharnais, R.; Zemanick, E.T.; Porter, E. Cholesteryl esters are elevated in the lipid fraction of bronchoalveolar lavage fluid collected from pediatric cystic fibrosis patients. *PLoS ONE* **2015**, *10*, e0125326. [CrossRef]
60. Ma, D.; Yoon, A.; Bartlett, J.; Faull, K.F.; McCray, P.B., Jr.; Zemanick, E.T.; Porter, E. Antimicrobial cholesteryl esters in cystic fibrosis airway secretions. *Pediatr. Pulmonol.* **2013**, *10*, e0125326.
61. Ghidoni, R.; Caretti, A.; Signorelli, P. Role of sphingolipids in the pathobiology of lung inflammation. *Mediators Inflamm.* **2015**, *2015*, 487508. [CrossRef] [PubMed]
62. Arora, K.; Naren, A.P. Pharmacological Correction of Cystic Fibrosis: Molecular Mechanisms at the Plasma Membrane to Augment Mutant CFTR Function. *Curr. Drug Targets* **2016**, *17*, 1275–1281. [CrossRef] [PubMed]
63. Matos, A.M.; Pinto, F.R.; Barros, P.; Amaral, M.D.; Pepperkok, R.; Matos, P. Inhibition of calpain 1 restores plasma membrane stability to pharmacologically rescued Phe508del-CFTR variant. *J. Biol. Chem.* **2019**, *294*, 13396–13410. [CrossRef] [PubMed]
64. Wallner, S.; Orso, E.; Grandl, M.; Konovalova, T.; Liebisch, G.; Schmitz, G. Phosphatidylcholine and phosphatidylethanolamine plasmalogens in lipid loaded human macrophages. *PLoS ONE* **2018**, *13*, 1–21. [CrossRef]
65. Dean, J.M.; Lodhi, I.J. Structural and functional roles of ether lipids. *Protein Cell* **2018**, *9*, 196–206. [CrossRef]
66. Drzymała-Czyż, S.; Krzyżanowska, P.; Koletzko, B.; Nowak, J.; Miśkiewicz-Chotnicka, A.; Moczko, J.A.; Lisowska, A.; Walkowiak, J. Determinants of serum glycerophospholipid fatty acids in cystic fibrosis. *Int. J. Mol. Sci.* **2017**, *18*, 185. [CrossRef]
67. Zhou, J.J.; Linsdell, P. Molecular mechanism of arachidonic acid inhibition of the CFTR chloride channel. *Eur. J. Pharmacol.* **2007**, *563*, 88–91. [CrossRef]

68. Li, Y.; Wang, W.; Parker, W.; Clancy, J.P. Adenosine regulation of cystic fibrosis transmembrane conductance regulator through prostenoids in airway epithelia. *Am. J. Respir. Cell Mol. Biol.* **2006**, *34*, 600–608. [CrossRef]
69. Seegmiller, A.C. Abnormal unsaturated fatty acid metabolism in cystic fibrosis: Biochemical mechanisms and clinical implications. *Int. J. Mol. Sci.* **2014**, *15*, 16083–16099. [CrossRef]

APPENDIX

Cellular Physiology and Biochemistry

Cell Physiol Biochem 2020;54:110-125
DOI: 10.33594/000000208
Published online: 31 January 2020
Accepted: 7 January 2020

Original Paper

Inhibition of Sphingolipid Synthesis as a Phenotype-Modifying Therapy in Cystic Fibrosis

Alessandra Mingione[a] Michele Dei Cas[b] Fabiola Bonezzi[c] Anna Caretti[a] Marco Piccoli[c] Luigi Anastasia[d] Riccardo Ghidoni[a] Rita Paroni[b] Paola Signorelli[a]

[a]Biochemistry and Molecular Biology Laboratory, Health Sciences Department, University of Milan, Italy, [b]Clinical Biochemistry and Mass Spectrometry Laboratory, Health Sciences Department, University of Milan, Italy, [c]Stem Cells for Tissue Engineering Lab, IRCCS Policlinico San Donato, San Donato Milanese, Milan, Italy, [d]Università Vita-Salute San Raffaele, Milan, Italy

Key Words
Lipid metabolism • Ceramide • Proteinopathy • Autophagy • Cystic Fibrosis

Abstract
Background/Aims: Cystic Fibrosis (CF) is an inherited disease associated with a variety of mutations affecting the CFTR gene. A deletion of phenylalanine 508 (F508) affects more than 70% of patients and results in unfolded proteins accumulation, originating a proteinopathy responsible for inflammation, impaired trafficking, altered metabolism, cholesterol and lipids accumulation, impaired autophagy at the cellular level. Lung inflammation has been extensively related to the accumulation of the lipotoxin ceramide. We recently proved that inhibition of ceramide synthesis by Myriocin reduces inflammation and ameliorates the defence response against pathogens infection, which is downregulated in CF. Here, we aim at demonstrating the mechanisms of Myriocin therapeutic effects in Cystic Fibrosis broncho-epithelial cells. ***Methods:*** The effect of Myriocin treatment, on F508-CFTR bronchial epithelial cell line IB3-1 cells, was studied by evaluating the expression of key proteins and genes involved in autophagy and lipid metabolism, by western blotting and real time PCR. Moreover, the amount of glycerol-phospholipids, triglycerides, and cholesterols, sphingomyelins and ceramides were measured in treated and untreated cells by LC-MS. Finally, Sptlc1 was transiently silenced and the effect on ceramide content, autophagy and transcriptional activities was evaluated as above mentioned. ***Results:*** We demonstrate that Myriocin tightly regulates metabolic function and cell resilience to stress. Myriocin moves a transcriptional program that activates TFEB, major lipid metabolism and autophagy regulator, and FOXOs, central lipid metabolism and anti-inflammatory/anti-oxidant regulators. The activity of these transcriptional factors is associated with the induction of PPARs nuclear receptors activity, whose targets are genes involved in lipid

Paola Signorelli, PhD
Associate Professor of Biochemistry

University of Milan, Health Sciences Department
San Paolo Hospital Medical School, Via Antonio di Rudinì 8, 20142 Milan (Italy)
Tel. (++39)02 50323257(65), Fax (++39)02 50323245, E-Mail paola.signorelli@unimi.it

transport compartmentalization and oxidation. Transient silencing of SPTCL1 recapitulates the effects induced by Myriocin. ***Conclusion:*** Cystic Fibrosis bronchial epithelia accumulate lipids, exacerbating inflammation. Myriocin administration: i) activates the transcriptions of genes involved in enhancing autophagy-mediated stress clearance; ii) reduces the content of several lipid species and, at the same time, iii) enhances mitochondrial lipid oxidation. Silencing the expression of Sptlc1 reproduces Myriocin induced autophagy and transcriptional activities, demonstrating that the inhibition of sphingolipid synthesis drives a transcriptional program aimed at addressing cell metabolism towards lipid oxidation and at exploiting autophagy mediated clearance of stress. We speculate that regulating sphingolipid *de novo* synthesis can relieve from chronic inflammation, improving energy supply and anti-oxidant responses, indicating an innovative therapeutic strategy for CF.

Introduction

Cystic fibrosis (CF) is a hereditary disease related to six different classes of mutations, affecting the chloride/carbonate channel CFTR [1]. CFTR dysfunction has a devastating effect primarily on the lungs and pancreas physiology and function. Although CF causes life threat because of pulmonary inflammation and infections, the improved therapeutic management of the last decades significantly increased life expectancy up to late adulthood. The disease, along with aging, is characterized by chronic inflammation and progressive manifestation and deterioration of comorbidities. Among comorbidities, dyslipidemia with high triglycerides and low LDL and cholesterol levels were identified in plasma of CF patients [2, 3], together with peripheral tissue fat accumulation [2, 4-8]. CF-related malabsorption of cholesterol is thought to enhance its synthesis, thus contributing to cholesterol accumulation, in the liver but also in other tissues [9, 10]. The most common CF mutations belong to class II and include the 508-phenylalanine deletion, which is encoded in 70% of mutant alleles in Caucasian patients. This mutation originates a proteinopathy due to ΔF508-CFTR unfolded protein accumulation, which saturates the clearance ability of the ER-associated degradation (ERAD), even when enhanced by the UPR system [11, 12]. The UPR modulates the expression of a variety of genes, that are involved in ER-related activities such as proteasome-lysosomal degradation, protein synthesis, sphingo- and glycerol-lipids and cholesterols metabolism, efficaciously adapting cell activities to a survival response to stress [13, 14]. Aggregates accrual, formed by misfolded mutant CFTR and a miscellaneous of sequestered proteins within, induces inflammation and oxidative stress, impairing proteins and lipids transport [1, 15]. Autophagy is a major supportive harm evoked under stress conditions and aimed to the degradation of unnecessary or un-wanted materials. Due to such aggregate-formation prone phenotype of ΔF508-CFTR expressing cells, autophagy is impaired by the segregation and degradation of key autophagic proteins, thus exacerbating the proteinopathy induced stress [12]. Intracellular organized lipid storages are a source for autophagosome membrane formation [16]. Consequently, an upregulated lipid synthesis or deregulated transport and metabolism was demonstrated to impair autophagy and to trigger ER stress [16-18]. TFEB is a master regulator of stress response insuring energy refueling via autophagy induction and lipid oxidation [19]. Autophagy sustains the clearance of proteins, lipids (lipophagy) [20] and infective pathogens (xenophagy) [21, 22]. A TFEB target is p62-sequestosome, a key component of autophagy vesicles that connects TFEB activation to lipophagy, in support of mitochondrial β-oxidation of fatty acids; interestingly, p62-sequestosome loss is also associated with diabetes and obesity [23]. Moreover, TFEB activates a set of genes involved in lipid mobilization and oxidation, mostly by the induction of the transcriptional activities of PPARs, their co-activator PGC-1α and FOXOs [20, 24].

FOXOs and PPARs transcriptional activity regulates lipid metabolism and inflammatory reaction. CF epithelial cells have reduced the level of FOXO1 [25], and CF models have a profound deficiency in the function of the lipid-activated PPAR-γ [26], possibly due to its sequestration into aggregates [27]. Overall, these observations suggest that protein

misfolding in the ER leads to global effects on lipid homeostasis [28]. Importantly, such cellular deregulation of lipid homeostasis is somewhat mirrored in CF patients by altered plasma lipid profile [3, 8, 9, 29-33]. Cholesterol increased synthesis was associated to ΔF508-CFTR expression, independently from CFTR channel function, but caused by late endosomal/lipid vesicle traffic impairment, in response to the proteinopathy stress. Moreover, the accumulation of esterified cholesterol in endosomal vesicles is accompanied by defects in the traffic of glycosphingolipids [7, 10, 34, 35]. These outcomes recall the Niemann-Pick disease type C (NPC) deficiency of cholesterol transport [36], responsible for membrane equilibrium alteration and impaired lipid trafficking [7]. The altered cholesterol transport and metabolism are sensed by the ER leading to the activation of SREBP (sterol regulatory element-binding protein) and endogenous cholesterol synthesis, in CFTR deficient cells [7] and mice [37]. Accordingly, CF patients present increased cholesterol in the lung and trachea sections [38]. Sphingomyelin, phosphatidylcholine, and cholesterol are the major components of cellular membranes. Their synthesis occurs at ER and it requires the coordinated activity of all the involved enzymes insuring that the modulation of one lipid class is related to the modulation of the other two classes [39], following the overall design of feeding the membranes [40-43]. Thus, triggering cholesterol synthesis may cause an increased synthesis of sphingolipids [14, 44]. Sphingolipid and glycerolipid metabolisms overlap at the enzymatic step where ceramide competes with diacylglycerol for the phosphocholine (deriving from CDP-choline). The ratio between the key enzymes of the two pathways, Serine Palmitoyl Transferase over Glycerol 3-phosphate Acyl Transferase, is significantly higher in the microsomal lung (and pancreas) than in most other adult rat tissues; accordingly, the percentage of sphingomyelin is higher in the total phospholipid content in these fractions [45, 46]. Sphingomyelin is formed, at Golgi or plasma membrane, by the addition of phosphocholine to ceramide. Ceramide is the core molecule of all sphingolipids metabolites, synthesized in the ER and translocated by vesicles or protein-mediated transport to the Golgi apparatus. Ceramide accumulation is involved in a variety of proteinopathies, that share with CF an inflammatory and ER stress condition, due to altered proteostasis, such as Retinitis Pigmentosa, Parkinson's, Alzheimer's, and Hungtinton's diseases [47, 48]. We and others previously demonstrated that ceramide content is pathologically increased in CF lungs and pulmonary epithelia, and that pharmacological impairment of ceramide accumulation reduces chronic inflammation and bacterial/fungal infections in CF [49-54]. Gulbins and his research group demonstrated that ceramide increases in CF lungs via enhanced sphingomyelin hydrolysis and they evaluated, in a clinical trial, the therapeutic effect of the sphingomyelinase inhibitor amitriptyline, a tricyclic antidepressant, which is already known for its action on lipid membranes and related signaling in neuropharmacology [49]. We proved, in different models, that *de novo* sphingolipid synthesis is an inflammation responsive pathway. It is enhanced by inflammatory mediators, both at transcriptional and at enzyme activity level and the accumulation of its metabolite ceramide potentiates inflammation in a vicious circle [52, 53, 55]. In this manuscript, we provide evidences that Myriocin (Myr), by inhibiting the first and rate-limiting reaction in the sphingolipid *de novo* synthesis pathway, is able to promote lipid oxidation and overall reduction and to induce autophagy, thus driving energy fueling and stress removal in ΔF508-CFTR bronchial epithelial cells.

Materials and Methods

Reagents and antibodies

The following materials were purchased: LHC Basal, LHC-8 w/o gentamicin culture media from Gibco (US); Fetal Bovine Serum and Minimum Essential Medium Earle's salt from EuroClone Life Science Italy; penicillin/streptomycin and RIPA buffer were purchased from Sigma-Aldrich; OA/BSA cell colture mix (Sigma); protease inhibitors cocktail (Roche); Quick Start™ Bradford Dye Reagent and Clarity™ Western ECL Blotting Substrates, iScript™ cDNA synthesis, retro-transcription kit (BioRad); BODIPY 493/503 (4, 4-difluoro-1, 3,5, 7,8-pentamethyl-4-bora-3a,4a-diaza-s-indacene), catalogue number D3922, and BODIPY™

558/568 C_{12} (4, 4-Difluoro-5-(2-Thienyl)-4-Bora-3a,4a-Diaza-*s*-Indacene-3-Dodecanoic Acid), catalogue number D3835, Prolong® Gold antifade reagent, were purchased from ThermoFisher Scientific, Molecular Probes™; NE-PER™ Nuclear and Cytoplasmic Extraction Reagents from ThermoFisher Scientific; ReliaPrep™ Miniprep RNA extraction System and GoTaq qPCR Master Mix (Promega); SYBR Green system (Qiagen); synthetic oligonucleotides from M-Medical Italy. The chemicals acetonitrile (ACN), 2-propanol (IPA), methanol, chloroform, formic acid (FA) and ammonium formate were purchased by Sigma-Aldrich (Milan, Italy). Cholesterol d7 (cod. 700041P), C15 ceramide d7 (cod. 860681P), 15:0-18:1-d7-phosphatidylcholine (cod. 791637C) and 16:0-18:0-16:0 d5 triglyceride (cod. 860902P), used as internal standards were purchased by Avanti Polar Lipids (Alabaster, AL). All aqueous solutions were prepared using purified water at a Milli-Q grade (Millipore, Milan, Italy). Primary antibodies: anti- PPAR-γ, Foxo1A and anti-Laminin A/C (ElabScience, US), SQSTM1/p62 (D1Q5S), anti β-actin (Sigma, US), anti-TFEB (ab2636, Abcam), anti-LC3 (Cell Signaling, US). The secondary antibodies were purchased from Jackson Laboratories (Bar Harbor, ME, US).

Cell lines and treatments

IB3-1 cells (named CF cells), an adeno-associated virus-transformed human bronchial epithelial cell line derived from a CF patient (ΔF508/W1282X) and provided by LGC Promochem (US), were grown in LHC-8 medium supplemented with 10% FBS, 1% penicillin/streptomycin at 37°C and 5% CO_2. Human lung bronchial epithelial cells 16HBE14o- (named healthy), originally developed by Dieter C. Gruenert, were provided by Luis J. Galietta, (Telethon Institute of Genetics and Medicine - TIGEM, Napoli) and cultured, as recommended, in Minimum Essential Medium (MEM) Earle's salt, supplemented with 10% FBS, 1% penicillin/streptomycin at 37°C and 5% CO_2. Myriocin (Myr) treatments were performed at a concentration of 50 μM, for the indicated time lengths, in 100 mm dishes plated at $1x10^5$ cells/each.

Protein extraction and western blotting

For transcriptional factors western blottings, nuclear and cytoplasmic extracts from cells were obtained with the NE-PER Nuclear and Cytoplasmic Extraction Reagents kit (ThermoFisher Scientific) according to the manufacturer's instructions. Total cell proteins were extracted from cells in RIPA buffer. The concentration of proteins in lysates was measured by Quick Start™ Bradford Dye Reagent (595 nm OD read). 50μg of proteins *per* sample were separated on SDS-PAGE gel and electro-blotted onto an either PVDF membrane for LC3 protein detection or nitrocellulose membrane for other protein targets. After washing in Tris-buffered saline containing 0.1% Tween-20 (TBS-T) and blocking with 5% non-fat dry milk for 1 hour at room temperature, membranes were probed overnight at 4°C with the primary antibodies. After three washes in TBS-T, the blot was incubated with the horseradish peroxidase-conjugated secondary antibodies. After the final washings, proteins were detected using an enhanced chemo-luminescent horseradish peroxidase substrate and the relative bands were captured and quantified by Alliance UVITEC Cambridge.

qRT-PCR

Cells were harvested, washed in PBS and total RNA was isolated from cell pellet with the ReliaPrep™ Miniprep RNA extraction System, according to the manufacturer's instructions. 1 μg of purified RNA was reverse transcribed and the obtained cDNA was stored at -20°C. The amplification of target genes was performed for the following targets: TFEB (*TFEB*), LAMP 2a, 2b and 2c (*LAMP2a,2b,2c*), PGC-1α (*PPARGC1A*), PPAR-α (*PPARA*), PPAR-γ (*PPARG*), FOXO 1a and 3a (*FOXO 1a, 3a*), FATP1 (*SLC27A1*), CPT-1a (*CPT1A*), CPT-1b (*CPT1B*), SCAD *(ACADS)*, MCAD (*ACADM*), LCAD (*ACADL*). Relative mRNA expression of target genes was normalized to the endogenous GAPDH control gene and represented as fold change *versus* control, calculated by the comparative CT method (ΔΔCT Method). All the primer sequences are reported in the Supplementary Table 1 (for all supplemental material see www.cellphysiolbiochem.com).

Lipidomic analysis

Lipids extraction from cell pellets was performed using a monophasic extraction method with water: chloroform: methanol (1:3:6 v/v/v) [56]. Then a small aliquot (2 μl) of the extracts was analysed by LC-HRMS (Shimadzu UPLC coupled with a Triple Tof 6600 Sciex). All samples were analysed in duplicate in positive mode with electrospray ionization for the identification and semi-quantification of sphingolipids, cholesterol and its esters, phospholipids and triacylglycerols. MS/MS spectra were acquired by data

dependent acquisition. Separation was achieved by an Acquity BEH C18 column 1.7 μm 2.1x50 mm (Waters, MA, USA) using as mobile phase A water/acetonitrile (60:40) and as mobile phase B 2-propanol/acetonitrile (90:10) both containing 10 mM ammonium formate and 0.1% of formic acid. The identification and semi-quantification were attained using MS-DIAL (ver. 3.82) [57]. Peak intensities of each lipid were normalized (Intensity norm.) by correcting for both total amount of protein (mg) measured by Bradford method and total-ion count. Results were presented as the sum of the normalized intensity for each lipid within a class. Absolute sphingolipid determination was achieved using a targeted analysis by a LC-MS/MS system (Dionex 3000 UltiMate coupled to a tandem mass spectrometer AB Sciex 3200 QTRAP) as already described [58].

Sptlc1 silencing by siRNA

CF cells were seeded in 6 wells plates and grown for 24 hours (70% confluency). For each well, 20pmol of Sptlc1 siRNA (or Scrambled sequence as negative control, Thermofisher) were diluted into 250 μl of Opti-MEM (w/o FCS); 5ul of Lipofectamine RNAiMAX (Thermofisher) was diluted into 250 μl of Opti-MEM LHC8 (w/o FCS); diluted oligomers and lipofectamine were gently mixed and incubated at RT for 15 minutes, then added to each cell colture well in a total volume of 2ml/well of serum free medium (LHC8). Cells were incubated at 37°C in a CO2 incubator for 5 hours, than fresh medium, containing 10% FCS, was replaced, either with or without 30 μM of oleic acid/BSA. Cells were additionally incubated up to 24-48 hours before collecting for analytical procedures.

Statistical analysis

All the experiments were performed in a minimum of 3 separate experiments. In some cases, the reported data derive from 5 independent experiments. Data are expressed as mean ± SD, calculated from experimental replicates. For western blotting analysis, the images are the most representative whereas the quantification of protein signals is calculated on the average of all the experiments performed. Data significance was evaluated by two-tailed Student T-test or ANOVA test followed by Bonferroni post test ($p<0.05$), as indicated in figure legends. Statistical analysis was performed by GraphPad Instat software (La Jolla, CA, USA) and graph illustrations generated by GraphPad Prism software (La Jolla, CA, USA).

Results

Myriocin induces autophagy in CF epithelial cells

Proteinopathies, in particular, ΔF508CFTR induced CF, are characterized by impaired cellular transports, ER stress, and deficiency in proteasomal and autophagic clearance of accumulated material. Therefore, we evaluated the effect of Myr treatment on autophagy induction in ΔF508CFTR and in a healthy broncho epithelial cell line as control. CF cells exhibit a reduced basal amount of lipidated form of LC3 (LC3II) in respect to healthy broncho epithelial cells (Fig. 1 A and B), as previously shown [12]. We demonstrated that Myr (50 μM) was effectively inducing the accumulation of the lipidated form of LC3 (LC3II) within 5 hours of treatment (Fig. 1A). In addition, we observed that Myr (50 μM) induced a significant reduction of p62-sequestosome in CF cells (Fig. 1B). These observations indicate that the treatment with Myr induced an increase in autophagic flux in CF cells.

Myriocin induces TFEB, PPARγ and FOXO1A nuclear translocation in CF epithelial cells

In order to understand why Myr is able to enhance autophagy, we investigated the activation of TFEB, a key inducer of autophagy and a regulator of energy homeostasis. TFEB nuclear migration and activation is significantly increased in CF cells treated with Myr (50 μM) *versus* untreated cells, already after 5 hours of treatment (Fig. 2A). By promoting autophagy, TFEB enhances lipid catabolism at the aim of conveying cell resources to energy production and to organize a survival stress response. To do so, TFEB promotes the activation of PPARs and FOXOs family of transcriptional factors involved in lipid homeostasis and inflammatory responses. We demonstrated that a slightly longer treatment with Myr (50 μM, 12 hours) stimulates nuclear translocation of PPAR-γ and FOXO1A (Fig. 2A, 2B).

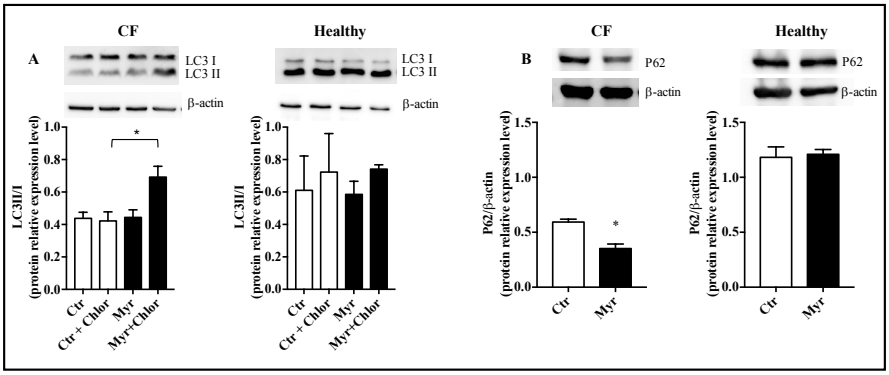

Fig. 1. Myriocin induces autophagy in CF cells. CF cells and healthy cells, treated with Myriocin for 12 hours. Detection of LC3 I and II protein expression by western blot in absence or in presence of 1 hour treatment with chloroquine and normalized on β-actin (A). Quantification of LC3II/I ratio obtained from triplicate samples and normalized onto β Actin and represented in the bars graph. Quantification of P62 protein expression by western blot analysis on whole lysates and normalized on β-actin (B); two-tailed unpaired Student's T-test.

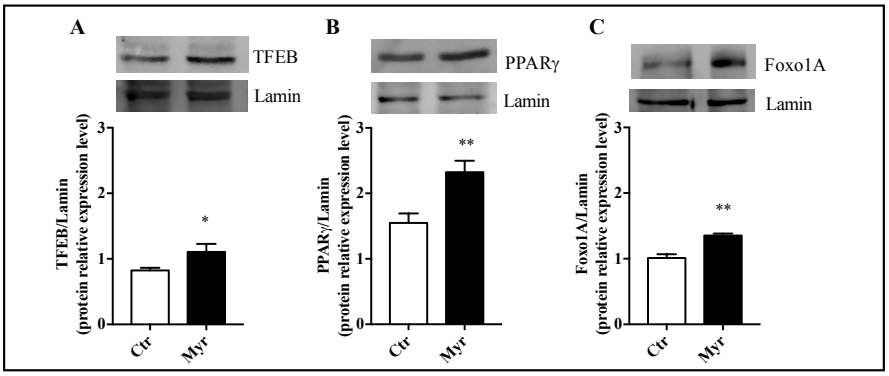

Fig. 2. Myriocin induces transcriptional factors activation. CF bronchoepithelial cells were treated or not with Myr (5 hours for TFEB evaluation and 12 hours for PPARγ; C, FOXO1A). Quantification of the transcriptional factor nuclear translocation by western blot on nuclear extracts and normalized on Lamin A/C: A, TFEB; B, PPARγ; C, FOXO1A. Protein signals were quantified by densitometry analysis and the normalized values reported in the graphs; two-tailed unpaired Student's T-test.

Myriocin activates a stress response transcriptional program

TFEB is a master regulator of the transcription of genes involved in autophagy and lysosome formation. First of all, the same TFEB expression resulted increased upon Myr treatment (50 μM, 12 hours; Fig. 3A) in CF cells *versus* healthy cells, indicating that initial activation of this critical regulatory factor is sustained, in the time, by the activation of a transcriptional program underlining TFEB induced effect. Next, we evaluated the expression of Myr nuclear translocation-activated transcriptional factors PPARγ and FOXO1A. We observed that their activation is sustained by their increased expression (Fig. 3B, 3E), together with the increased expression of PPAR-α, PGC1α and FOXO3A (Fig. 3C, 3D, 3F). Therefore, Myr drives the expression of a set of genes that are aimed at sustaining lipid catabolism and energy production inhibition. To note that Myr induced transcriptional activities is significantly regulated in CF cells but only to a minor extent in healthy cells.

Then, we evaluated the expression of TFEB targets, involved in sustain of autophagy flux, Lamp2a, Lamp2b, and Lamp2c. We observed that overnight (24 hours) treatment with Myr (50 μM) increased the expression of all these genes in CF cells *versus* healthy cells (Fig. 4A). In order to verify the effect of PPARs and FOXOs activation, we evaluated the expression of their target genes involved in lipid transport and catabolism. We proved that a 24 hours Myr treatment significantly increases the expression of the plasma membrane lipid transporter FATP1 (*Slcl27a1*), which mediates the uptake of long-chain FA, and the expression of the transporters Ctp1a and Cpt1b, which instead control the mitochondrial entry of FA for oxidation, as compared to untreated cells (Fig. 4B and 4C). In order to prove that fat entry and mobilization was finalized at oxidation and energy production, we evaluated the Myr-induced transcriptional response of enzymes involved in mitochondrial fatty acid oxidation (FAO). SCAD (*ACADS*), MCAD (*ACADM*) and LCAD (*ACADL*), which are the mitochondrial dehydrogenases primarily responsible for β-oxidation of small, medium and long chains of FAs respectively, are upregulated by 24 hours Myr treatment, reaching statistical significance for *ACADL* (Fig. 4C). To note that Myr significantly upregulated the transcription of the above mentioned genes in CF cells but only to a minor extent in healthy cells.

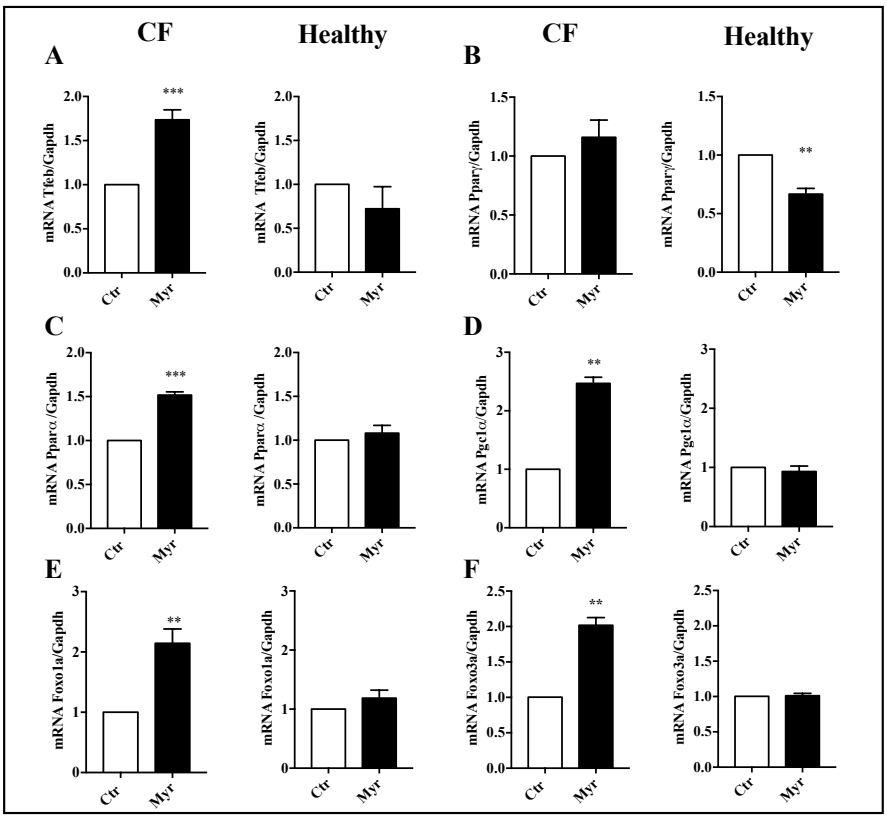

Fig. 3. Myriocin activates the transcription of TFEB-induced transcriptional factors. Quantification of the expression of genes encoding for transcriptional factors activated by TFEB: A, TFEB; B, Ppar-γ; C, Ppar-α;D, Pgc1α; E, Foxo1A; F, Foxo3A by qRT-PCR, in CF cells and healthy cells, treated and untreated with Myr (12 hours). All data are normalized on the housekeeping gene GAPDH and expressed as mean±SE (* $p<0.05$; ** $p<0.01$; *** $p<0.001$); two-tailed unpaired Student's T-test.

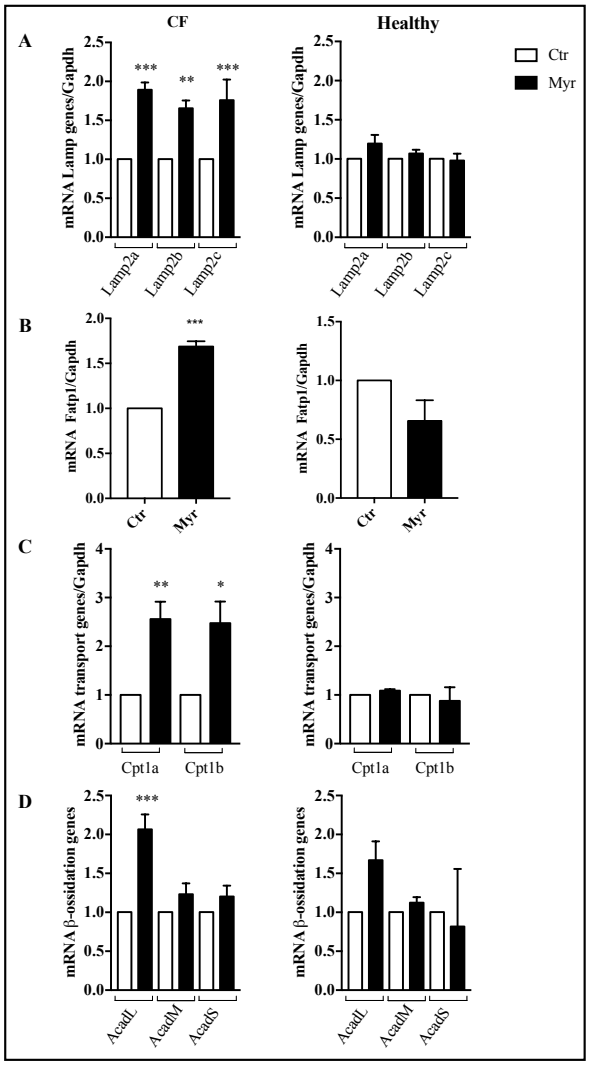

Fig. 4. Myriocin activates the transcription of TFEB-induced autophagy and lipid metabolism related genes in CF and healthy broncho epithelial cells. Quantification of the expression of genes involved in autophagy and cell lipid transport/metabolism: A, Lamp alternative splicing derived mRNA levels (Lamp2a, Lamp2b, Lamp2c);B, Fatp1; C, CPT1a, CPT1b and; D, AcadL, AcadM and AcadS by qRT-PCR in CF cells and healthy cells, treated and untreated with Myr (24 hours). All data are expressed as mean±SE (* $p<0.05$; ** $p<0.01$; *** $p<0.001$; **** $p<0.0001$); two-tailed unpaired Student's T-test for Fig. 4B and Anova followed by Bonferroni post-test for all other Figures.

Myriocin reduces lipid content in CF epithelial cells

Myr inhibits ceramide and related sphingolipids synthesis and, according to our results, it also promotes the expression of genes involved in lipid oxidation. We compared the amount of different lipid species in Myr treated healthy and CF cells, versus untreated ones. CF cells have a significantly higher content in sphingolipids (namely ceramides CER and sphingomyelins SM), glycerophospholipids (namely phosphatidylcholine PC and phosphatidylserine, PS), triacylglycerols (TAG) and cholesterol esters (CE) (Fig. 5 A, B, C, E, H, I). We observed that Myr not only reduces ceramide and sphingomyelin content (Fig. 5A-4C), but it also reduces glycerolipids (PC, PS and phosphatidylethanolamine, PE), Lyso-phosphatidylcholine (LPC), TAG, and cholesterol esters (CE), with a particular significance for the decrease of PC, PS, and CE (Fig. 5). Thus, the inhibition of sphingolipids biosynthesis causes an overall depletion of cellular lipids from different classes.

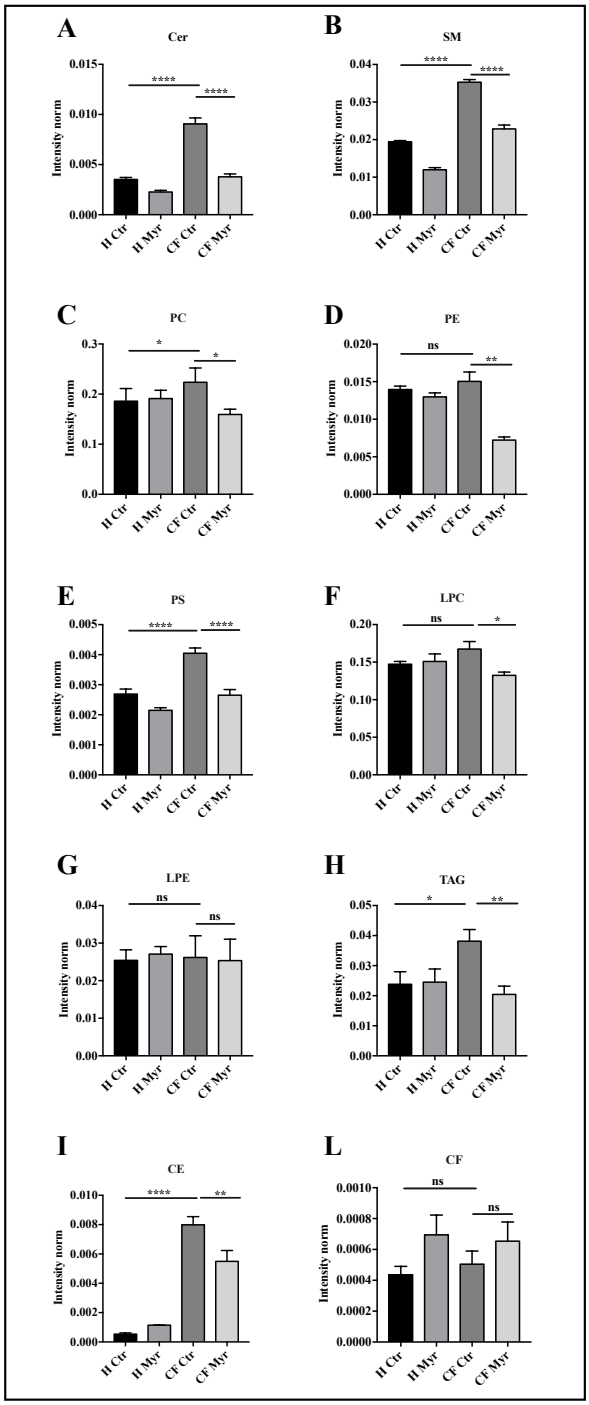

Fig. 5. LCMS measurement of different lipid species and Myriocin effects in CF cells and in healthy (H) broncho epithelial cells. The content of different lipid species was analyzed by LC-MS. CF cells lipid content is higher than healthy in all the observed species; 24 hours Myr reduced the content of all the evaluated lipid species in CF cells: A, Ceramide (Cer); B, Sphingomyelin (SM); C, phosphatidylcholine (PC); D, phosphatidylethanolamine (PE); E, phosphatidylserine (PS); F, Lysophosphatidylcholine (LPC); G, lysophosphatidylethanolamine (LPE); H, triacylglycerols (TE); I, cholesterol esters (CE); L, free cholesterols (CF). Data are expressed as mean ± SE (* $p<0.05$; ** $p<0.01$); Anova followed by Bonferroni post-test.

Reduced expression of SPT1 recapitulates Myr effects

To better prove that the control of sphingolipid synthesis is tightly linked to the overall cell metabolism and it can be used to switch on stress response and total lipid consume in CF model, we transiently silenced the expression of Sptlc1 gene, by specific targeting of its mRNA, siRNA, in CF cells. We observed a reduction of 83% gene expression within 24 hours, that was still stable at 48 hours (Fig. 6A), paralleled by a reduced protein expression of more than 50% (6B). After 48 hours, Cer and SM were significantly reduced, indicating the efficacy of gene expression silencing in counteracting sphingolipid *de novo* synthesis (Fig. 6C and D). In order to prove that Sptlc1 downregulation reproduces the effects of Myr treatment, we evaluated the induction of autophagy by LC3 lipidation analysis *via* western blotting. We observed that Sptlc1 silencing significantly enhances autophagic flux, either in the presence or in the absence of chloroquine for lysosomal activity inhibition (24 hours). Since nucleotide oligomers may activate autophagy, we added scrambled siRNA as a control, showing a slight and not significant increase of LC3II/LC3I ratio in respect to control (w/o scrambled siRNA) (Fig. 6E). Next, we compared the expression of the key genes activated by Myr in Sptlc1-silenced cells *versus* control. We investigated the expression of TFEB, master regulator of autophagy and energy metabolism, and we observed that 24 hours Sptlc1-silenced CF cells exhibit an increased expression of TFEB (Fig. 6F), and of one of its target genes involved in autophagic flux, LAMP2a (Fig. 6H). Similarly to Myr, Sptlc1 silencing increased the expression of PPARα (Fig. 6G), CPT1a (Fig. 6I), involved in fatty acids entry into mitochondria, and of ACADs (Fig. 6L), the dehydrogenases involved in fatty acids β oxidation (especially the enzyme which preferentially recognizes long chain fatty acids). From these data we conclude that the effects of Myr are entirely due to its inhibitory activity on SPT enzyme and that reducing the synthesis of sphingolipids triggers the TFEB mediated stress response of autophagy and lipid consume.

Discussion

We previously showed the therapeutic potential of Myr, a fungal-derived molecule known to be a specific inhibitor of the Serine Palmitoyl Transferase, rate-limiting enzyme of the sphingolipid synthesis. We proved that intra-trachea administration of this molecule reduces chronic inflammation and ameliorates endogenous rejection of bacterial and fungal infections in CF murine models [52, 53]. We also demonstrated that Myr corrects the defective ability of CF epithelial cells to kill internalized pathogens [53]. We here investigated the mechanisms underlying the therapeutic actions of Myr. CF proteinopathy is characterized by defective autophagy response to stress and altered lipid metabolism, as previously elucidated. In this manuscript, we demonstrate that Myr treatment of ΔF508CFTR broncho-epithelial cells is able to recover and stimulate autophagy, leading to LC3II accumulation and p62-sequestosome consume, thus counteracting the CF defective mechanism. In order to understand how an inhibitor of the sphingolipids' synthesis can be related to autophagy induction, we investigated the activation of TFEB, one of the master regulator of stress response. TFEB activation allows energy gain from the oxidation of lipid storage and the recycle of dispensable material via autophagy, inducing, at the same time, anti-oxidant response and sustaining mitochondrial activity [24, 59]. In doing so, TFEB stimulates the activation of other transcriptional factors such as PPARs and FOXOs, which regulate the lipid oxidation and the anti-inflammatory response [22, 24, 60, 61] We previously demonstrated that Myr induces TFEB transcriptional activation and its down stream pathway which is aimed at enhancing lipid oxidation and ATP production in myocardium [62]. We here observed that Myr promotes TFEB nuclear translocation and, subsequently, the nuclear translocation of PPAR-γ and Foxo1A, demonstrating that a transcriptional program is triggered by this molecule, aimed at enhancing cellular energy metabolism and reducing inflammation. In line with the activation of these transcriptional factors, we previously showed that Myr significantly reduces inflammatory cytokines transcription and release and favours the anti-

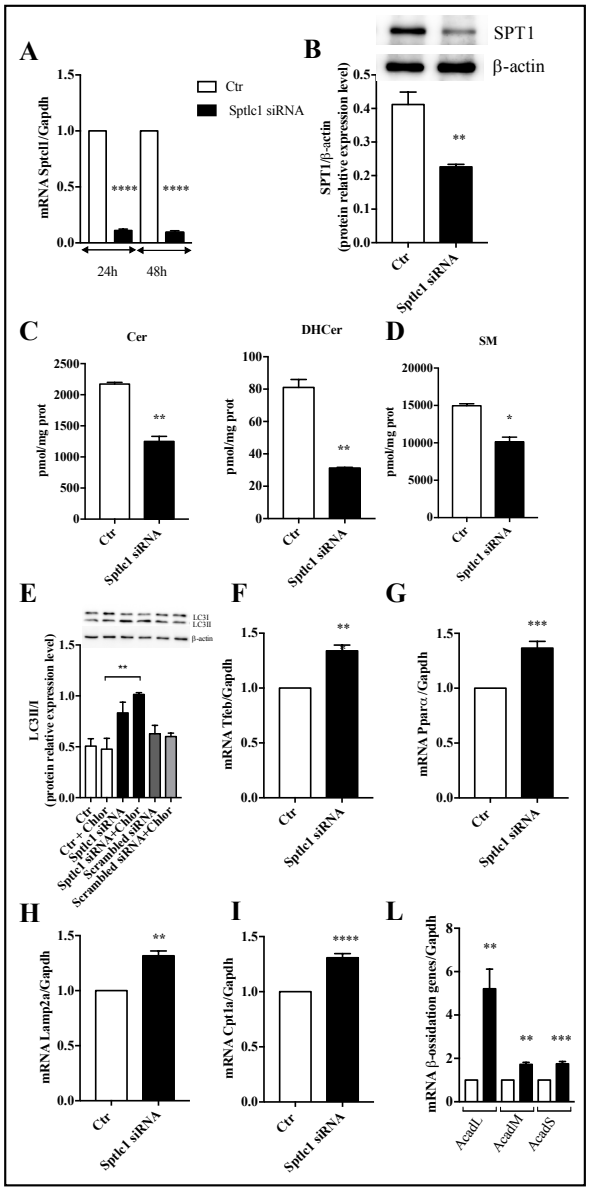

Fig. 6. Transient silencing of Sptlc1 expression recapitulates Myr effects in CF cells. A) Quantification of the expression of the gene encoding for Sptlc1 was obtained by qRT-PCR in CF cells treated with Sptlc1-directed siRNA for 24 and 48 hours. All data are normalized on the housekeeping gene GAPDH and expressed as mean±SE (* p<0.05; ** p<0.01; *** p<0.001); two-tailed unpaired Student's T-test. B). Detection of SPT1 protein expression by western blotting in cells treated with Sptlc1-directed siRNA for 24 hours. LCMS quantification of Ceramides (C) and Sphingomyelins (D) in cells treated with Sptlc1-directed siRNA for 48 hours. E) Detection of LC3 I and II protein expression by western blot, in absence or in presence of 1 hour treatment with chloroquine. Quantification of LC3II/I ratio obtained from triplicate samples of Sptlc1-siRNA or Scrambled-siRNa or vehicle was normalized onto β Actin and represented in the bars graph. Quantification by qRT-PCR of the expression of genes encoding for transcriptional factors activated by TFEB after 24 hours of Sptlc1 directed siRNA: F), TFEB; G), Ppar-α; quantification by qRT-PCR of the expression of genes encoding for TFEB- induced genes after 24 hours of Sptlc1 directed siRNA: H) Lamp2a; I) Cpt1a; L) AcadL, AcadM, AcadS. All data are normalized on the housekeeping gene GAPDH and expressed as mean±SE (* p<0.05; ** p<0.01; *** p<0.001); Anova followed by Bonferroni post-test for Fig. L and two-tailed unpaired Student's T-test for the other Figures.

oxidant response by inducing the HO-1 transcription in ΔF508CFTR CF epithelial cells [53]. We now demonstrate that the transcription of genes involved in lipid transport (cellular import and mitochondrial import of FA) and their mitochondrial oxidation (FA dehydrogenases), known to be stimulated by the TFEB/PPARs-axis, are significantly increased, indicating that, effectively, Myr enhances lipid consume. Consequently, we performed a lipidomic analysis of CF cells and healthy cells treated with Myr and observed an overall increased content of

glycerophospholipids, sphingolipids and cholesterols in CF cells *versus* healthy cells. To the best of our knowledge, this is the first report of increased lipids content in CF pulmonary epithelia and it is in line with reported cholesterol accumulation in peripheral tissues in CF patients. Lipids accumulation can derive from impaired membrane trafficking, and it is responsible for clogging the ER-Golgi network, exacerbating ROS and inflammation in CF. Lipids content was significantly reduced by Myr treatment in CF. The reduction is particularly evident for phosphatidylcholine and cholesterol esters. Moreover, lyso- glycerophospholipids, considered pro-inflammatory molecules [63, 64], were significantly reduced, indicating a decreased inflammation-driven metabolism of the lipid moiety. To note, healthy cells were poorly affected, indicating that Myr is acting on a CF specific defective mechanisms of lipid altered homeostasis.

Conclusion

Thus, lipids homeostasis is intrinsically deranged in ΔF508CFTR proteinopathy of CF, and lipid metabolism stands for an important therapeutic target that can be envisaged in sustain of pharmacological efficiency of correctors. Based on our results, we can envision that Myr treatment has the potential of partially restoring CF cellular dysmetabolism, releasing cells from the excessive stress which is deemed an important cause of correctors failure in CF patients. We can also speculate that this molecule may exert favourable systemic effects to reduce dyslipidemia occurring in CF patients. The limitation in this present study is the overall difference between a CF cell line and a patient's derived broncho epithelium. We are aware that molecular signaling might be affected by peculiarities of the specific cell line and this is the reason why we intend to investigate the mechanism of Myr induced autophagy and relief from proteinopathy stress, as well as lipid accumulation in CF primary cells. The comparison between primary broncho epithelial cells derived from CF patients and from control donors will furtherly shed light on lipid dysmetabolism in CF.

Acknowledgements

We thank the Italian Cystic Fibrosis Research Foundation for the financial support of this work and for a 4 months fellowship for a post-doctoral researcher working at the project. Part of this work was carried out in OMICs, an advanced mass spectrometry platform established by the Università degli Studi di Milano.

Financial Support

The presented data have been entirely obtained by the Italian Cystic Fibrosis Research Foundation for the financial support (Grant FFC#11-2016 adopted by: Gruppo di Sostegno FFC di Vercelli, Gruppo di Sostegno FFC di Genova "Mamme per la ricerca", Delegazione FFC Valle Scrivia Alessandria, Delegazione FFC di Olbia).

Author Contributions

Mingione A. contributed to design and execute the experimental work, with analysis and interpretation; Bonezzi F., Piccoli M., Caretti A. contributed to data collection analysis and interpretation; Dei Cas M. and Paroni R.C. contributed by lipidomic analysis; Ghidoni R. contributed with critical revision of the manuscript; Anastasia L. contributed with data analysis and interpretation and with critical revision of the manuscript; Signorelli P. is the PI and contributed to design the work, its analysis and interpretation.

Disclosure Statement

All the authors of this manuscript have no conflicts of interest to declare.

References

1 Elborn JS: Cystic fibrosis. Lancet 2016;388:2519-2531.
2 Tham RT, Heyerman HG, Falke TH, Zwinderman AH, Bloem JL, Bakker W, Lamers CB: Cystic fibrosis: MR imaging of the pancreas. Radiology 1991;179:183-186.
3 Figueroa V, Milla C, Parks EJ, Schwarzenberg SJ, Moran A: Abnormal lipid concentrations in cystic fibrosis. Am J Clin Nutr 2002;75:1005-1011.
4 Khoury T, Asombang AW, Berzin TM, Cohen J, Pleskow DK, Mizrahi M: The Clinical Implications of Fatty Pancreas: A Concise Review. Dig Dis Sci 2017;62:2658-2667.
5 Chryssostalis A, Hubert D, Coste J, Kanaan R, Burgel PR, Desmazes-Dufeu N, Soubrane O, Dusser D, Sogni P: Liver disease in adult patients with cystic fibrosis: a frequent and independent prognostic factor associated with death or lung transplantation. J Hepatol 2011;55:1377-1382.
6 Wilschanski M, Durie PR: Patterns of GI disease in adulthood associated with mutations in the CFTR gene. Gut 2007;56:1153-1163.
7 White NM, Jiang D, Burgess JD, Bederman IR, Previs SF, Kelley TJ: Altered cholesterol homeostasis in cultured and *in vivo* models of cystic fibrosis. Am J Physiol Lung Cell Mol Physiol 2007;292:L476-486.
8 Hardin DS, LeBlanc A, Para L, Seilheimer DK: Hepatic insulin resistance and defects in substrate utilization in cystic fibrosis. Diabetes 1999;48:1082-1087.
9 Gelzo M, Sica C, Elce A, Dello Russo A, Iacotucci P, Carnovale V, Raia V, Salvatore D, Corso G, Castaldo G: Reduced absorption and enhanced synthesis of cholesterol in patients with cystic fibrosis: a preliminary study of plasma sterols. Clin Chem Lab Med 2016;54:1461-1466.
10 Ernst WL, Shome K, Wu CC, Gong X, Frizzell RA, Aridor M: VAMP-associated Proteins (VAP) as Receptors That Couple Cystic Fibrosis Transmembrane Conductance Regulator (CFTR) Proteostasis with Lipid Homeostasis. J Biol Chem 2016;291:5206-5220.
11 Bartoszewski R, Rab A, Jurkuvenaite A, Mazur M, Wakefield J, Collawn JF, Bebok Z: Activation of the unfolded protein response by deltaF508 CFTR. Am J Respir Cell Mol Biol 2008;39:448-457.
12 Luciani A, Villella VR, Esposito S, Brunetti-Pierri N, Medina D, Settembre C, Gavina M, Pulze L, Giardino I, Pettoello-Mantovani M, D'Apolito M, Guido S, Masliah E, Spencer B, Quaratino S, Raia V, Ballabio A, Maiuri L: Defective CFTR induces aggresome formation and lung inflammation in cystic fibrosis through ROS-mediated autophagy inhibition. Nat Cell Biol 2010;12:863-875.
13 Stevenson J, Huang EY, Olzmann JA: Endoplasmic Reticulum-Associated Degradation and Lipid Homeostasis. Annu Rev Nutr 2016;36:511-542.
14 Ron D, Walter P: Signal integration in the endoplasmic reticulum unfolded protein response. Nat Rev Moll Cell Biol 2007;8:519-529.
15 Luciani A, Villella VR, Esposito S, Brunetti-Pierri N, Medina DL, Settembre C, Gavina M, Raia V, Ballabio A, Maiuri L: Cystic fibrosis: a disorder with defective autophagy. Autophagy 2011;7:104-106.
16 Velazquez AP, Tatsuta T, Ghillebert R, Drescher I, Graef M: Lipid droplet-mediated ER homeostasis regulates autophagy and cell survival during starvation. J Cell Biol 2016;212:621-631.
17 Selvam S, Ramaian Santhaseela A, Ganesan D, Rajasekaran S, Jayavelu T: Autophagy inhibition by biotin elicits endoplasmic reticulum stress to differentially regulate adipocyte lipid and protein synthesis. Cell Stress Chaperones 2019;24:343-350.
18 To M, Peterson CW, Roberts MA, Counihan JL, Wu TT, Forster MS, Nomura DK, Olzmann JA: Lipid disequilibrium disrupts ER proteostasis by impairing ERAD substrate glycan trimming and dislocation. Mol Biol Cell 2017;28:270-284.
19 Settembre C, Ballabio A: TFEB regulates autophagy: an integrated coordination of cellular degradation and recycling processes. Autophagy 2011;7:1379-1381.
20 Settembre C, Ballabio A: Lysosome: regulator of lipid degradation pathways. Trends Cell Biol 2014;24:743-750.

21 Pehote G, Bodas M, Brucia K, Vij N: Cigarette Smoke Exposure Inhibits Bacterial Killing via TFEB-Mediated Autophagy Impairment and Resulting Phagocytosis Defect. Mediators Inflamm 2017;2017:3028082.
22 Kim YS, Lee HM, Kim JK, Yang CS, Kim TS, Jung M, Jin HS, Kim S, Jang J, Oh GT, Kim JM, Jo EK: PPAR-alpha Activation Mediates Innate Host Defense through Induction of TFEB and Lipid Catabolism. J Immunol 2017;198:3283-3295.
23 Angelini C, Nascimbeni AC, Cenacchi G, Tasca E: Lipolysis and lipophagy in lipid storage myopathies. Biochim Biophys Acta 2016;1862:1367-1373.
24 Settembre C, De Cegli R, Mansueto G, Saha PK, Vetrini F, Visvikis O, Huynh T, Carissimo A, Palmer D, Klisch TJ, Wollenberg AC, Di Bernardo D, Chan L, Irazoqui JE, Ballabio A: TFEB controls cellular lipid metabolism through a starvation-induced autoregulatory loop. Nat Cell Biol 2013;15:647-658.
25 Smerieri A, Montanini L, Maiuri L, Bernasconi S, Street ME: FOXO1 content is reduced in cystic fibrosis and increases with IGF-I treatment. Int J Mol Sci 2014;15:18000-18022.
26 Andersson C, Zaman MM, Jones AB, Freedman SD: Alterations in immune response and PPAR/LXR regulation in cystic fibrosis macrophages. J Cyst Fibros 2008;7:68-78.
27 Maiuri L, Luciani A, Giardino I, Raia V, Villella VR, D'Apolito M, Pettoello-Mantovani M, Guido S, Ciacci C, Cimmino M, Cexus ON, Londei M, Quaratino S: Tissue transglutaminase activation modulates inflammation in cystic fibrosis via PPARgamma down-regulation. J Immunol 2008;180:7697-7705.
28 Ambler SK, Hodges YK, Jones GM, Long CS, Horwitz LD: Prolonged administration of a dithiol antioxidant protects against ventricular remodeling due to ischemia-reperfusion in mice. Am J Physiol Heart Circ Physiol 2008;295:H1303-H1310.
29 Rhodes B, Nash EF, Tullis E, Pencharz PB, Brotherwood M, Dupuis A, Stephenson A: Prevalence of dyslipidemia in adults with cystic fibrosis. J Cyst Fibros 2010;9:24-28.
30 Christophe AB, Warwick WJ, Holman RT: Serum fatty acid profiles in cystic fibrosis patients and their parents. Lipids 1994;29:569-575.
31 Ishimo MC, Belson L, Ziai S, Levy E, Berthiaume Y, Coderre L, Rabasa-Lhoret R: Hypertriglyceridemia is associated with insulin levels in adult cystic fibrosis patients. J Cyst Fibros 2013;12:271-276.
32 Del Ciampo IR, Sawamura R, Fernandes MI: Cystic fibrosis: from protein-energy malnutrition to obesity with dyslipidemia. Iran J Pediatr 2013;23:605-606.
33 Levy E, Gurbindo C, Lacaille F, Paradis K, Thibault L, Seidman E: Circulating tumor necrosis factor-alpha levels and lipid abnormalities in patients with cystic fibrosis. Pediatr Res 1993;34:162-166.
34 Fang D, West RH, Manson ME, Ruddy J, Jiang D, Previs SF, Sonawane ND, Burgess JD, Kelley TJ: Increased plasma membrane cholesterol in cystic fibrosis cells correlates with CFTR genotype and depends on de novo cholesterol synthesis. Respir Res 2010;11:61.
35 Gentzsch M, Choudhury A, Chang XB, Pagano RE, Riordan JR: Misassembled mutant DeltaF508 CFTR in the distal secretory pathway alters cellular lipid trafficking. J Cell Sci 2007;120:447-455.
36 Cianciola NL, Carlin CR, Kelley TJ: Molecular pathways for intracellular cholesterol accumulation: common pathogenic mechanisms in Niemann-Pick disease Type C and cystic fibrosis. Arch Biochem Biophys 2011;515:54-63.
37 Xu Y, Tertilt C, Krause A, Quadri LE, Crystal RG, Worgall S: Influence of the cystic fibrosis transmembrane conductance regulator on expression of lipid metabolism-related genes in dendritic cells. Respir Res 2009;10:26.
38 Worgall TS: Lipid metabolism in cystic fibrosis. Curr Opin Clin Nutr Metab Care 2009;12:105-109.
39 Fabiani C, Zulueta A, Bonezzi F, Casas J, Ghidoni R, Signorelli P, Caretti A: 2-Acetyl-5-tetrahydroxybutyl imidazole (THI) protects 661W cells against oxidative stress. Naunyn-Schmiedebergs Arch Pharmacol 2017;390:741-751.
40 Lagace TA: Phosphatidylcholine: Greasing the Cholesterol Transport Machinery. Lipid Insights 2015;8:65-73.
41 Snyder B, Freire E: Compositional domain structure in phosphatidylcholine--cholesterol and sphingomyelin--cholesterol bilayers. Proc Natl Acad Sci U S A 1980;77:4055-4059.
42 Yan N, Ding T, Dong J, Li Y, Wu M: Sphingomyelin synthase overexpression increases cholesterol accumulation and decreases cholesterol secretion in liver cells. Lipids Health Dis 2011;10:46.
43 Leppimaki P, Kronqvist R, Slotte JP: The rate of sphingomyelin synthesis de novo is influenced by the level of cholesterol in cultured human skin fibroblasts. Biochem J 1998;335:285-291.

44 Worgall TS, Juliano RA, Seo T, Deckelbaum RJ: Ceramide synthesis correlates with the posttranscriptional regulation of the sterol-regulatory element-binding protein. Arterioscler Thromb Vasc Biol 2004;24:943-948.
45 Merrill AH, Jr., Nixon DW, Williams RD: Activities of serine palmitoyltransferase (3-ketosphinganine synthase) in microsomes from different rat tissues. J Lipid Res 1985;26:617-622.
46 Nahrlich L, Mainz JG, Adams C, Engel C, Herrmann G, Icheva V, Lauer J, Deppisch C, Wirth A, Unger K, Graepler-Mainka U, Hector A, Heyder S, Stern M, Doring G, Gulbins E, Riethmuller J: Therapy of CF-patients with amitriptyline and placebo--a randomised, double-blind, placebo-controlled phase IIb multicenter, cohort-study. Cell Physiol Biochem 2013;31:505-512.
47 Czubowicz K, Jesko H, Wencel P, Lukiw WJ, Strosznajder RP: The Role of Ceramide and Sphingosine-1-Phosphate in Alzheimer's Disease and Other Neurodegenerative Disorders. Mol Neurobiol 2019;56:5436-5455.
48 Strettoi E, Gargini C, Novelli E, Sala G, Piano I, Gasco P, Ghidoni R: Inhibition of ceramide biosynthesis preserves photoreceptor structure and function in a mouse model of retinitis pigmentosa. Proc Natl Acad Sci U S A 2010;107:18706-18711.
49 Teichgraber V, Ulrich M, Endlich N, Riethmuller J, Wilker B, De Oliveira-Munding CC, van Heeckeren AM, Barr ML, von Kurthy G, Schmid KW, Weller M, Tummler B, Lang F, Grassme H, Doring G, Gulbins E: Ceramide accumulation mediates inflammation, cell death and infection susceptibility in cystic fibrosis. Nat Med 2008;14:382-391.
50 Hamai H, Keyserman F, Quittell LM, Worgall TS: Defective CFTR increases synthesis and mass of sphingolipids that modulate membrane composition and lipid signaling. J Lipid Res 2009;50:1101-1108.
51 Ulrich M, Worlitzsch D, Viglio S, Siegmann N, Iadarola P, Shute JK, Geiser M, Pier GB, Friedel G, Barr ML, Schuster A, Meyer KC, Ratjen F, Bjarnsholt T, Gulbins E, Doring G: Alveolar inflammation in cystic fibrosis. J Cyst Fibros 2010;9:217-227.
52 Caretti A, Bragonzi A, Facchini M, De Fino I, Riva C, Gasco P, Musicanti C, Casas J, Fabrias G, Ghidoni R, Signorelli P: Anti-inflammatory action of lipid nanocarrier-delivered myriocin: therapeutic potential in cystic fibrosis. Biochim Biophys Acta 2014;1840:586-594.
53 Caretti A, Torelli R, Perdoni F, Falleni M, Tosi D, Zulueta A, Casas J, Sanguinetti M, Ghidoni R, Borghi E, Signorelli P: Inhibition of ceramide de novo synthesis by myriocin produces the double effect of reducing pathological inflammation and exerting antifungal activity against A. fumigatus airways infection. Biochim Biophys Acta 2016;1860:1089-1097.
54 Caretti A, Vasso M, Bonezzi FT, Gallina A, Trinchera M, Rossi A, Adami R, Casas J, Falleni M, Tosi D, Bragonzi A, Ghidoni R, Gelfi C, Signorelli P: Myriocin treatment of CF lung infection and inflammation: complex analyses for enigmatic lipids. Naunyn-Schmiedebergs Arch Pharmacol 2017;390:775-790.
55 Reforgiato MR, Milano G, Fabrias G, Casas J, Gasco P, Paroni R, Samaja M, Ghidoni R, Caretti A, Signorelli P: Inhibition of ceramide de novo synthesis as a postischemic strategy to reduce myocardial reperfusion injury. Basic Res Cardiol 2016;111:12.
56 Lydic TA, Busik JV, Reid GE: A monophasic extraction strategy for the simultaneous lipidome analysis of polar and nonpolar retina lipids. J Lipid Res 2014;55:1797-1809.
57 Tsugawa H, Cajka T, Kind T, Ma Y, Higgins B, Ikeda K, Kanazawa M, VanderGheynst J, Fiehn O, Arita M: MS-DIAL: data-independent MS/MS deconvolution for comprehensive metabolome analysis. Nat Methods 2015;12:523-526.
58 La Corte E, Dei Cas M, Raggi A, Patane M, Broggi M, Schiavolin S, Calatozzolo C, Pollo B, Pipolo C, Bruzzone MG, Campisi G, Paroni R, Ghidoni R, Ferroli P: Long and Very-Long-Chain Ceramides Correlate with A More Aggressive Behavior in Skull Base Chordoma Patients. Int J Mol Sci 2019;20:pii:E4480.
59 Settembre C, Fraldi A, Medina DL, Ballabio A: Signals from the lysosome: a control centre for cellular clearance and energy metabolism. Nat Rev Mol Cell Biol 2013;14:283-296.
60 Ouimet M, Koster S, Sakowski E, Ramkhelawon B, van Solingen C, Oldebeken S, Karunakaran D, Portal-Celhay C, Sheedy FJ, Ray TD, Cecchini K, Zamore PD, Rayner KJ, Marcel YL, Philips JA, Moore KJ: Mycobacterium tuberculosis induces the miR-33 locus to reprogram autophagy and host lipid metabolism. Nat Immunol 2016;17:677-686.
61 Liu L, Tao Z, Zheng LD, Brooke JP, Smith CM, Liu D, Long YC, Cheng Z: FoxO1 interacts with transcription factor EB and differentially regulates mitochondrial uncoupling proteins via autophagy in adipocytes. Cell Death Discov 2016;2:16066.

62 Bonezzi F, Piccoli M, Dei Cas M, Paroni R, Mingione A, Monasky MM, Caretti A, Riganti C, Ghidoni R, Pappone C, Anastasia L, Signorelli P: Sphingolipid Synthesis Inhibition by Myriocin Administration Enhances Lipid Consumption and Ameliorates Lipid Response to Myocardial Ischemia Reperfusion Injury. Front Physiol 2019;10:986.
63 Chiurchiu V, Leuti A, Maccarrone M: Bioactive Lipids and Chronic Inflammation: Managing the Fire Within. Front Immunol 2018;9:38.
64 Sevastou I, Kaffe E, Mouratis MA, Aidinis V: Lysoglycerophospholipids in chronic inflammatory disorders: the PLA(2)/LPC and ATX/LPA axes. Biochim Biophys acta 2013;1831:42-60.